Modeling and Operation of Ground Source Heat Pumps in Electricity Markets Considering Uncertainty

by

Dario Peralta Moarry

A thesis
presented to the University of Waterloo
in fulfillment of the
thesis requirement for the degree of
Doctor of Philosophy
in
Electrical and Computer Engineering

Waterloo, Ontario, Canada, 2022

Examining Committee Membership

The following served on the Examining Committee for this thesis. The decision of the Examining Committee is by majority vote.

Supervisor:	Claudio A. Cañizares University Professor, Department of Electrical and Computing Engineering University of Waterloo
Supervisor:	Kankar Bhattacharya Professor, Department of Electrical and Computing Engineering University of Waterloo
Internal Member:	Sahar Azad Assistant Professor, Department of Electrical and Computing Engineering University of Waterloo
Internal Member:	Mehrdad Pirnia Lecturer, Department of Management Sciences University of Waterloo

Internal-External Member: Maurice Dusseault
Professor,
Department of Earth Sciences
University of Waterloo

External Examiner: Francois Bouffard
Associate Professor,
Department of Electrical and Computer Engineering
University of McGill

Author's Declaration

I hereby declare that I am the sole author of this thesis. This is a true copy of the thesis, including any required final revisions, as accepted by my examiners.

I understand that my thesis may be made electronically available to the public.

Abstract

Ground Source Heat Pump (GSHP) systems have grown in popularity and acceptance worldwide as an attractive option to replace conventional Heating Ventilation and Air Conditioning (HVAC) technologies due to their capacity to provide space heating and cooling in buildings and houses. Such GSHP systems may participate as a price-taker in electricity markets through a load aggregator to optimize their load demand, being able to provide grid services, such as load shifting. Therefore, aggregated GSHP systems have the potential, if properly designed, integrated, and applied, to yield energy and carbon savings in the energy market. However, the integration of such aggregated GSHP systems brings new challenges to operators, as it involves uncertainties on ambient temperature and electricity price forecasts, which can be highly volatile and thus impact the GSHP system operation and its participation in electricity markets. From a detailed literature review of GSHP applications for load management for residential users, it can be concluded that there are no works that discuss the operational performance of large-scale GSHP systems, modeled in detail, and their integration in electricity markets; additionally, none of the existing works have considered uncertainties in terms of ambient temperature and electricity price forecasts for the optimal operation of aggregated GSHP systems.

After a comprehensive review of the relevant background related to GSHP systems, aggregator strategies in the electricity market, and optimization in the presence of uncertainties, in this thesis, a detailed mathematical model is presented of a GSHP with a vertical U-pipe Ground Heat eXchanger (GHX) configuration to provide residential space heating/cooling, integrating them into a load aggregator model. Based on this model, a two-stage operational strategy for the GSHP price-taker aggregator participating in Day-Ahead Market (DAM) and Real-Time Market (RTM) is proposed, to determine the optimal annual heating/cooling load dispatch to control the temperatures for a community of houses that minimizes the aggregator's cost. Simulations are presented then of an aggregator's optimal load dispatch with a conventional HVAC and the proposed GSHP alternative, considering comfort maximization vis-a-vis minimization of electricity costs, and showing the impact of each objective with respect to the dispatch of controllable loads, in-house temperature, and total procurement costs.

Finally, a novel model based on Robust Optimization (RO) is proposed and developed, considering uncertainties in terms of the DAM and RTM electricity prices and hourly ambient temperature forecasts, which yields an optimum schedule that protects against the

worst-case scenario for a given level of conservatism. The RO model is compared and validated in a realistic test system with respect to Model Predictive Control (MPC) and Monte Carlo Simulations (MCS) approaches that are traditionally used to manage uncertainty. It is shown that the proposed RO approach is computationally efficient compared to the MPC and MCS approaches, and properly accounts for the considered uncertainties, demonstrating the advantage of the presented RO technique for GSHP dispatch by aggregators.

Acknowledgements

First of all, First, I want to thank God for giving me strength in the moments I felt weak and alone, and for all the wonderful people I met during these years.

I would also like to acknowledge and thank all the invaluable support of my supervisors, Professor Kankar Bhattacharya and Professor Claudio Cañizares, I offer my deepest gratitude for their guidance during my graduate studies at the University of Waterloo. During these past years, I had the opportunity to learn from such amazing researchers and human beings who are an example for our generation. It has been an honour to work under their supervision.

I want to thank my Ph.D. Examining Committee for their valuable comments and observations: Waterloo's Professors Sahar Azad from the Department of Electrical and Computer Engineering, Mehrdad Pirnia from the Department of Management Sciences, and Maurice Dusseault from the Department of Earth Sciences, and Prof. François Bouffard from the Department of Electrical and Computer Engineering at McGill. I also sincerely acknowledge all the professors who guided my studies by sharing their invaluable knowledge through outstanding lectures, in particular Prof. Jatin Nathawani, and Prof. Ramadan El-Shatshat at the University of Waterloo.

My deepest gratitude to all friends and colleagues who helped me throughout my studies: Andres Arias, Anshul Goyal, Baheej Alghamdi, Behnam Tamimi, Bharat Solanki, Carlos Ceja, Chioma Anierobi, Diego Ortiz, Emin Mammadov, Enrique Vera, Fabian Calero, Fulong Li, Hanwen Gu, Ivan Calero, Jean-Michell Clairand, Katharina Wieninger, Mariano Arriaga, Abolfazl (Amir) Mosaddegh, Matheus Zambroni de Souza, Mauricio Restrepo, Mikaela Lewis, Mostafa Farrokhabadi, Muhammad Mahmoud, Nitin Padmanabhan, Pablo Verdugo, Samuel Cordova, Santiago Bustamante, Sofía Guzman, Talal Alharbi, Walter Violante, and William Mendieta. I am thankful for all their help and the friendly environment provided during this journey.

I would like to specially acknowledge my sister Nicole Peralta, in Ecuador, for assisting me with her expertise by helping me to prepare some of the high quality and detailed illustrations shown in this work.

Dedication

This work is dedicated to my parents, Dario and Patricia; my sisters, Pierina and Nicole; my niece, Angélica; and all my family, who have always given me their unconditional support.

I would like to dedicate this thesis especially to my son, Alexander, who gave me the special motivation to continue working tirelessly. Everything I do and everything I am is for you.

Finally, I dedicate this work to my grandma, my mami Yula. You were the proudest person of everything I have accomplished in a different country. I will try to do my best so you can still be proud of me. I miss you.

Table of Contents

List of Figures

List of Tables

List of Acronyms

AC	Air Conditioning
AGC	Automatic Generation Control
ASHP	Air Source Heat Pump
CDF	Cumulative Distribution Function
CHP	Combined Heat and Power
COP	Coefficient of Performance
DAM	Day-Ahead Market
DER	Distributed Energy Resources
DR	Demand Response
DTC	Direct Thermostat Control
EER	Energy Efficiency Ratio
EMS	Energy Management System
ESS	Energy Storage System
EV	Electric Vehicle
GHG	Green House Gas
GHX	Ground Heat eXchanger
GSHP	Ground Source Heat Pump
HEMS	Home Energy Management System
HVAC	Heating Ventilation and Air Conditioning

IESO	Independent Electric System Operator
LP	linear programming
LES	Local Energy Systems
MCP	Market Clearing Price
MCS	Monte Carlo Simulation
MILP	Mixed Integer Linear Programming
MPC	Model Predictive Control
HOEP	Hourly Ontario Energy Price
PDF	Probability Density Function
PEV	Plug-In Electric Vehicle
PFC	Primary Frequency Control
PV	Photovoltaic
RES	Renewable Energy Sources
RTM	Real-Time Market
RMSE	Root Mean Square Error
RO	Robust Optimization
SO	Stochastic Optimization
TCL	Thermostatically Controlled Loads
TES	Thermal Energy Storage
UTES	Underground Thermal Energy Storage

Nomenclature

Indices

i	Index for number of houses, $i \epsilon \mathcal{I}$.
j	Index for the borehole section, $j \epsilon \mathcal{J}$.
t	Index for hours of the day, $t \epsilon \mathcal{T}$.

Sub- and Super-scripts

$*$	Variable converted to a parameter
0	Center value
A	External glazed surfaces
E	Building envelope
F	Forecasted
r	room
up/dn	Up/down
Y	DAM/RTM

Parameters

$\tilde{\alpha}$	Heating/Cooling capability of the HVAC unit and secondary resistances at house i [°C/kWh]
$\overline{\Delta\lambda}$	Max. price mismatch
$\overline{\Delta T^F_{amb}}$	Max. ambient temperature mismatch
Δt	Time interval in which fluid temperature passes through segment j in U-pipe borehole , [h]
ϵ^{λ}_t	Electricity price forecasting error
ϵ^{T}_t	Ambient temperature forecasting error
Γ	Budget of uncertainty
$\xi^{\lambda^Y}_t$	Electricity price random scalar deviation
$\xi^{T^F_{amb}}_t$	Ambient temperature random scalar deviation
Δz	Height of each segment of the borehole j [m]
$\lambda^{DAM/RTM}_t$	Energy price in DAM/RTM at hour t [$/kWh]
$\widehat{\lambda}^{DAM/RTM}$	Maximum energy price in DAM/RTM [$/kWh]
ϕ_t	Solar radiation power [kW]
ψ	Solar radiation incidence factor
$A - C$	linear data-fitting coefficients from the GSHP data-sheets
c_f	Specific heat of the underground fluid [kJ/kg°C]
COP^{HP}_{ref}	Rated Coefficient of Performance (COP) of GSHP
$D_{i,GHX}$	Internal diameter of the GHX unit [mm]
$D_{o,GHX}$	External diameter of the GHX unit [mm]
d_b	Borehole diameter [mm]

d_g	Ground node position [mm]
d_{pe}	External U-pipe diameter [mm]
d_x	Grout node position [mm]
EER_{ref}^{HP}	Rated Energy Efficiency Ratio (EER) of GSHP
H_P	Thermal capacitance [kJ/°C]
h_1 - h_4	Enthalpy of the GSHP [J]
k_b	Grout thermal conductivity [W/m °C]
k_g	Ground thermal conductivity [W/m °C]
L_t^{DAM}	Aggregated uncontrolled load at hour t [kW]
l_{GHX}	Vertical length of the GHX unit [m]
$\dot{m}_f$	Mass flow rate of the underground fluid [kg/s]
$\dot{m}_{Re}$	Mass flow rate of GSHP refrigerant [kg/s]
$\overline{P_i}$	Power capacity of a heating/cooling device in house i [kW]
Q_G	House internal heat gain [kW or kJ/s]
R_{pp}	Pipe-to-pipe thermal resistance [°C/kW]
R_b	Borehole conductive thermal resistance [°C/kW]
R_{bb}	Grout-to-grout thermal resistance [°C/kW]
R_g	Grout-to-ground thermal resistance [°C/kW]
S	Shank spacing [mm]
SD_t^{λ}	Electricity price hourly standard deviation
SD_t^T	Ambient temperature hourly standard deviation
$\overline{T_i}/\underline{T_i}$	Maximum/Minimum limits of comfortable temperature in house i [°C]

T_{amb_t}	Ambient temperature at hour t [°C]
T^{Ref}	Reference in-house temperature [°C]
T^{HP}_{ref}	GSHP's reference temperature of operation [°K]
U	Heat transfer coefficient [kW/m^2°C]
v	Velocity of the underground fluid [m/s]
W_{com}	Compressor power consumption [kW]
$Z_{a_{i,t}}$	GSHP operation mode (1 for heating, and 0 for cooling)

Variables

β^Y	Dual variable in Y
$\Delta\lambda^Y$	Price deviation in Y [%]
$\Delta\lambda^{Y+/-}$	Upward/Downward Price deviation in Y [%]
ΔP_t	Aggregated demand deviation [kW]
$\Delta T_{i,t}$	In-house temperature deviation [°C]
ΔT^F_{amb}	Ambient temperature deviation [%]
$\Delta T^{F+/-}_{amb}$	Upward/Downward Ambient temperature deviation [%]
C_t	Energy procurement cost at hour t [$]
$COP^{HP}_{i,t}$	COP of GSHP in heating mode
$EER^{HP}_{i,t}$	EER of GSHP in cooling mode
J_1-J_3	Objective functions of the aggregator model
$p^{h/c}_{i,t}$	Electric load of house i during heating/cooling operation at hour t (decision variable) [kW]

$p_{i,t}^{res}$	Electric load of house i from secondary thermal resistance (decision variable) [kW]
P_t	Total aggregated demand at hour t (decision variable) [kW]
$Q_{in/out}$	House heat transfer and GHX contribution [kW]
$Q_{i,t}^{h/c}$	Heat transfer heat injected to/extracted from each house i at hour t in heating/cooling mode [kW]
$Q_{i,t}^{abs/rej}$	Heat transfer contribution of the GHX unit in each house i at hour t in heating/cooling mode [kW]
$T_{i,t,j}^{b}$	Borehole grout temperature of house i at hour t in segment j [°C]
$T_{i,t,j}^{f}$	Borehole fluid temperature of house i at hour t in segment j [°C]
$T_{i,t,j}^{g}$	Borehole ground temperature of house i at hour t in segment j [°C]
$T_{i,t}$	In-house temperature of house i at hour t [°C]
$T_{in/out_{i,t}}$	Inlet/outlet temperature at the GHX terminal of house i at hour t [°C]
$W_{i,t}^{h/c}$	COP^{HP}/EER^{HP} of GSHP in heating/cooling mode

Chapter 1

Introduction

1.1 Motivation

Canada has set a target of 30% reduction in Green House Gas (GHG) emissions by 2030, from its 2005 levels, which is expected to be achieved by implementing different strategies determined from a high-level analysis. In this context, the total residential energy use in 2016 in Canada was 1458 PJ, of which 60% was accounted for by space heating and cooling [1]. The main source of energy for space heating and cooling varies by province; for example, in Ontario, the majority of residences are heated with natural gas, whereas in Quebec, the use of electric-based heaters is preponderant [2]. Therefore, there is a need for alternative low-cost and more efficient energy sources for residential and commercial heating and cooling, in which the development and application of Ground Source Heat Pump (GSHP) systems could play a role.

GSHP is a viable energy-efficient alternative to traditional furnaces and air conditioners, and can help existing electrically heated homes reduce their energy consumption for heating, by up to 60% [3]. It has been reported in [4] that, when gas heated homes are transformed to GSHP heating, there are significant reductions in GHG emissions; however, the economic benefits are only realized over a long-term time horizon after recovery of the capital costs. On the other hand, transformation of electrical heated homes to GSHP heating has significant economic benefits, with relatively low impact on GHG reductions in power systems with low emission, such as Ontario and Quebec, but higher impact on systems with high GHG emissions as in some regions in USA, Canada and Europe.

GSHP systems are generally preferred over other types of heat pump systems, because the ground temperature remains almost constant throughout the year and is usually higher than the ambient temperature in winter and lower than the ambient in summer [5, 6]. The application of GSHP systems to provide in-house air comfort has been studied for over 60 years, such as in Philadelphia, USA, in 1947 [7], when the city's electric utility undertook a project on the heat transfer features of the earth and its use as a heat source for heat pumps. In Canada, a number of operational and pilot projects have been implemented to satisfy the inter-seasonal cooling and heating demand with the application of Underground Thermal Energy Storage (UTES) facilities [8], in conjunction with the implementation of GSHP units, for the development of an efficient Energy Management System (EMS). Studies in different cities and provinces of Canada have demonstrated that the use of GSHP systems can reduce the heating energy cost by up to 50%, compared to furnace based heating systems [9].

The evolution of wholesale electricity markets has predominantly focused on the development of a competitive supply (generation) system. Residential customers are usually not eligible to purchase electricity directly from the wholesale energy market [10], and hence GSHP systems cannot participate in the demand bidding process individually. To capture the benefits of demand elasticity of individual GSHP loads, they can be represented as a group, typically referred to as a *load aggregator*. For example, in Ontario, Canada, the Independent Electric System Operator (IESO) launched the Demand Response (DR) auction program in 2016 to develop an operating reserve provision that is available, at lower cost than the capacity installation cost, and almost 50% of the participants were load aggregators [11].

Even though GSHP is a well known technology in Canada, few projects have been built [12]. As a result, only limited data, information, and research has been reported on the viability of this technology for reducing end-user electricity consumption. This imposes further challenges to system operators, utilities, and new investors to understand the benefits that can be obtained from GSHPs in reducing building space heating and cooling energy demand, their potential to provide additional services to the utility, such as load shifting, and to properly assess the economics of new developments. Therefore, the development of new load aggregator models to study the application of GSHPs connected to the grid should help provide sufficient insights into their impact on the rest of the system. This is specially important for Ontario, not only because of the interest of the province to promote installation of GSHPs at their end-use customers [9], but also to exploit the

favorable geological features of the region.

Therefore, the main objectives of this thesis are to propose appropriate load aggregator models and frameworks for optimal dispatch and market participation of GSHPs for energy, heating, and DR provisions, with the inclusion of a novel mathematical model of a GSHP system with vertical U-pipe Ground Heat eXchanger (GHX) configuration, considering its thermal and geometric characteristics. In this context, the deployment of these GSHP systems in practical settings, introduces new challenges to operators and especially for aggregators participating in competitive electricity markets, because it involves uncertainties in ambient temperatures and electricity prices, which can be highly volatile and thus impact the GSHP operation considerably [13, 14]. There is a need to consider these uncertainties are considered here to optimally schedule the power dispatch of GSHP loads in electricity markets by aggregators as price-taker participants.

1.2 Literature Review

The literature review presented in this section concentrates on the modeling and operation of GSHP systems, discussing the thermodynamic models of the GHX. This is followed by a summary on the participation of load aggregators in electricity markets, and the application of Robust Optimization (RO), Model Predictive Control (MPC), and Monte Carlo Simulation (MCS) approaches to consider uncertainties in power system operation.

1.2.1 GSHP Modeling and Operation

This section discusses research works focusing on GSHP system modeling and operation in the context of electricity markets. The provision of Primary Frequency Control (PFC) in isolated microgrids has been considered in [15], with the application of GSHP units using a DR strategy for Thermostatically Controlled Loads (TCL). The thermodynamic characteristics of the house are represented with a thermal-electrical equivalent circuit, which considers parameters such as outdoor temperature, solar irradiance, internal heat loads, house thermal properties, among others. The model of the GSHP unit comprises the thermo-electrical equivalent circuit model of the house, the equation fit model of the reversible water-to-air based GSHP, and the thermodynamic model of the borehole-based

GHX. The performance of the thermo-electrical models for the provision of PFC with the proposed DR strategy is then evaluated, using a model of an actual hybrid PV-diesel microgrid. Different tests are conducted to analyze the system frequency response under different controls, and including GSHP, Air Conditioning (AC), and electric water heating, demonstrating the advantages of using GSHP for PFC. Some of the models developed in this thesis are based on the work in [15], but for long-term GSHP operations rather than dynamic analyses, to evaluate its advantage of GSHP over conventional HVAC systems.

An MPC approach for residential heating is presented in [16], wherein the thermal mathematical model of a building is developed with a GSHP system used to supply thermal energy to a water-based floor heating system. An MPC controller is implemented to manage the GSHP compressor performance, in order to minimize the overall electricity cost while maintaining the indoor temperature within a comfortable range. The thermal model of the house is expressed as a continuous-time state space model to include the GSHP dynamics, which are faster than the thermal characteristics of the building. The results demonstrate that the MPC based approach is able to shift the on-peak loads to periods of low electricity prices. However, this work [16] does not consider it detailed modeling of the GHX system to represent the thermodynamics of the borehole component of the GSHP systems, but instead assuming that the Coefficient of Performance (COP) is a constant that is not affected by the heat contribution from the terminals of the GHX system. Furthermore, the MPC approach uses perfect forecasts for the thermal characteristics of the GSHP units.

The annual analysis of energy consumption for space heating and cooling in a residence in Greece is presented in [17], wherein a conventional HVAC system comprising a fan-coil, chiller/boiler 2-pipe system is compared to a water-to-water based GSHP with a horizontal ground array. The study is performed on the dynamic performance of both systems during 10 days in the winter for heating operation, and 10 days in the summer for cooling operation, considering different control strategies. The simulation results demonstrated that in southern Europe climates, for residential space heating and cooling services, GSHP systems yield a 50% lower operation cost as compared to the standard chiller/boiler based HVAC system. Although the study brings out advantages of GSHPs over conventional HVAC systems, it lacks a detailed representation of the GSHP thermodynamic model.

A study for different GSHP systems in [18] presents a comparison with other heating systems, such as Air Source Heat Pumps (ASHPs), electric baseboard heaters, and natural

gas furnaces, with the objective of improving the understanding of GSHP systems and promote their use in several applications. A detailed description of the heating systems is provided, and the characteristics of each system is analyzed, highlighting the different configurations, global status, and their advantages and limitations. A brief overview of recent developments in GSHP systems for different applications is also included. A detailed comparison with respect to efficiency, economy, and carbon dioxide emissions is carried out as well, concluding that for Canadian climate conditions, GSHP systems possess the most efficient COP, and from the economic point of view, these systems are the most economic option in two of the three provinces considered, although it has a slightly higher cost compared to ASHP systems in the third province. Finally, it is demonstrated that GSHP systems are the largest emissions reductions option as compared to conventional electrical heating devices or natural gas fired systems. This work [18] however, does not consider large-scale aggregated GSHP systems, nor their optimal operation to minimize the annual cost of heat provision.

A method is presented in [19] for the optimal design of GSHPs systems, combining financial and thermodynamic characteristics to obtain estimates of the total costs and optimal COP. The objective of this work is to determine the optimal technical configuration of specific GSHP components, especially heat pumps, bore well size, number of bore wells, and mass flow rate, satisfying the physical and technical system needs while minimizing the total annual investment and operational costs. However, the proposed optimal design model of the GSHP system does not consider detailed GHX system models that represent the thermodynamic characteristics of the borehole performance. Furthermore, no large-scale analysis of aggregated GSHP systems is included in the study.

Three different numerical models are reported in [20] to estimate the long-term thermal behavior and operation of GSHP systems, focusing on the physical configuration and geometrical characteristics of different GHX boreholes, two real GSHP facilities in Italy are considered in the analysis; first, the performance of both facilities is monitored over a year, to obtain enough data; then, computational simulations are carried out over a 10-year period to analyze the behaviour of the u-pipe borehole based GHX configuration in both facilities. The proposed numerical models are not suitable for optimal operation studies due to the complexity of these models, that would result in considerable computational costs.

1.2.2 Electricity Market Load Aggregator

The authors in [21] propose a method to determine Day-Ahead Market (DAM) bidding strategies of an aggregator of flexible loads seeking to maximize its profit, considering different risk factors. The aggregator load profile is forecasted considering the aggregate power demand of residential customers responding to dynamic tariffs. Uncertainties related to consumers' behaviour and their willingness to participate in the aggregation are considered. The studies show that risk-averse aggregators tend to adopt the bidding strategies with larger power demand imbalances. Washing machines, dryers, dishwashers, and Electric Vehicle (EV) charging stations are included in the study as source of flexible loads, but thermal loads such as conventional HVAC or GSHP systems are not considered.

In [22], a retail electricity market is proposed that includes AC loads as DR providers, managed using an agent-based approach. The framework comprises two optimization problems, the first seeks to maximize the retailer's profit from the sale of energy, subject to the price-sensitivity of loads. In the lower level problem, the AC agent seeks to minimize the AC load consumption, implementing local controls, such as temperature set-point variations, considering the given retail prices and the consumers' comfort levels. However, the proposed agent-based approach focuses on the DAM only, with no consideration for the Real-Time Market (RTM) operations.

The optimal operation of a DR aggregator participating in the wholesale electricity market is presented in [23], where the aggregator manages a portfolio of different DR programs to participate in the DAM and RTM as a price-taker participant. The optimization problem, formulated as a bi-level optimization, determines the optimal schedule of the different DR resources available, in dispatching ACs, with the upper-level objective of maximizing the aggregator's profit, whereas the lower level problem minimizes the cost of providing energy balance to the system. The proposed model does not include GSHP systems and does not consider the users' satisfaction such as comfort constraints, which are important in aggregator modeling.

The optimal schedule of aggregated flexible loads of commercial and residential buildings, such as HVAC and smart appliances, participating in a DAM is studied in [24]. The demand profile considers two types of flexible loads: residential loads such as washers, dryers and ACs; and commercial loads, mainly water heaters and HVAC systems. The optimization model however, does not consider participation in the RTM, and no thermodynamic constraints are included to calculate the indoor temperature of the buildings

and thus the effect of thermal controllable loads, such as conventional HVAC and GSHP systems cannot be measured.

An optimal bidding strategy of an aggregator of Distributed Energy Resourcess (DERs) and flexible demand in the DAM is proposed in [25]. The aggregator seeks to maximize its expected profit considering the participation of multiple Local Energy Systems (LES), such as Combined Heat and Power (CHP), Photovoltaics (PVs), chillers, conventional HVAC, and Thermal Energy Storage (TES). The optimization problem considers the technical and physical constraints from each energy system, along with the novel power dispatch constraints. The Mixed Integer Linear Programming (MILP) optimization problem, however, is deterministic, and has a considerable computational cost since the model is rather complex and not purely linear.

An optimization framework for the participation of DR aggregators in wholesale electricity markets is proposed in [26] that maximizes their profit in a DAM, considering different DR strategies such as load curtailment and load shifting, and energy storage units. The proposed MILP optimization problem maximizes the difference between the revenue for selling the aggregated total load reduction from all four strategies, and the cost of paying the contracted customers for the load reductions, subject to the specific constraints for each strategy. Results show that the use of energy storage units provides a more flexible alternative and thus are a more profitable solution. However, the proposed model is deterministic and does not include the potential DR contribution of thermal controllable loads, especially GSHP systems.

1.2.3 Modeling uncertainties in load aggregator operation

Various works present load aggregator operation strategies considering uncertainties. For example, a stochastic-based decision-making framework for the efficient management of smart energy hubs is proposed in [27], where an optimal self-scheduling model is developed for DAM and RTM to minimize the procurement cost of electricity, considering uncertainties on electricity prices, renewable energy generation, and load demand. The energy hub includes a boiler, a CHP unit, a battery storage system, a diesel generator, a wind turbine, and an EV fleet. The model provides acceptable results with significant uncertainty in the parameters, for a reasonable computational burden. On the other hand, a stochastic operation strategy is presented in [28] for a Plug-In Electric Vehicle (PEV) load aggregator

in the DAM, considering uncertainties based on customer's driving patterns and market prices, where the load aggregator determines the optimal PEV fleet charging schedule to minimize its total energy cost. The bidding strategy of the aggregator is formulated as a bilevel problem, which is implemented as a MILP optimization. The upper level problem represents the charging cost minimization of the aggregator, whereas the lower level problem represents the market clearing. The stochastic model in both the works assume a probability distribution function to represent the uncertainties, which could be a challenge depending on data availability.

In [29] a schedule for an Energy Storage System (ESS) aggregator is proposed using an RO approach to represent the uncertainties in the power output of Renewable Energy Sources (RES), loads, and real-time thermal ratings of transmission lines. The problem is first formulated as a deterministic scenario where the objective is to minimize the operational cost of the ESSs. The RO problem is solved for the worst-case scenario considering a specific value of budget of uncertainty. The model provides robust results against significant uncertainty with a reasonable computational burden. An MPC-based scheduling and operation approach is proposed in [30] for a load aggregator, with the inclusion of generic ESSs participating in DAM and RTM, and in the presence of price and load uncertainties. With increasing uncertainty in price and load, the MPC-based strategy yields significantly improved performance with respect to the other strategies, reducing the total electricity costs of the load aggregator. However, none of the aforementioned works consider inclusion of thermal based loads in the load aggregator framework, such as GSHP systems.

A strategic bidding and financial compensation mechanism for a load aggregator is proposed in [31], which involves a Direct Thermostat Control (DTC) program implemented for space heating and cooling services. The load control model is implemented in a two-stage market framework, i.e., DAM and RTM. Uncertainties in DAM prices, non-controllable loads, ambient temperature, and thermal characteristics of the house are considered in a MCS based approach. However, only limited historical data was considered for the MCS approach, which does not allow an accurate representation of the uncertainties, while resulting in high computational costs.

A hybrid stochastic RO approach is proposed in [32] to develop an optimal bidding strategy in the DAM for a microgrid, minimizing the total electricity cost. Uncertainties in distributed generation output and DAM prices are modeled as stochastic optimization problem using forecasted data. The results of the DAM settlement using the RO approach

are used to model the uncertainty in RTM price, and hence limit the power unbalance in real-time. It is noted that microgrids can benefit significantly from bidding in the DAM, and the budget of uncertainty can be used to set different risk levels for the agent. However, there is no consideration of thermal loads in the reported work, such as GSHP systems.

A novel stochastic-based optimization model for a residential energy hub is presented in [33] for an optimal schedule of RES units that minimizes the total cost of electricity, considering uncertainties in RES output power and electricity market prices, simultaneously, as well as the seasonal heat and power demands. The residential hub considers different energy sources, such as EVs, PV, CHP and AC. The results show the advantages of the proposed scenario-based model considering different uncertainties, compared with deterministic methods. However, the RES device models included in the system [33], are generic and do not capture their specific characteristics, nor there is representation of seasonal heat and power demand uncertainties.

In [34], an optimal bidding strategy is proposed for a residential load aggregator to maximize its total profit considering uncertainties, based on their willingness to participate in the DR program to control residential flexible loads. The optimization problem considers average models for HVAC, water heater and EV systems, which are treated as flexible loads; uncertainties on the level of the consumer's willingness to participate in the DR program are modeled by implementing fuzzy logic inference rules. However, there is no consideration for uncertainties in the house thermal characteristics, and the thermal/technical characteristics of the flexible loads are not modeled.

1.2.4 Discussion

From the literature review, it can be observed that some works examine the different applications of GSHP systems for space heating and cooling, such as frequency regulation services, strategies to reduce costs, and GSHP integration into the grid. However, load aggregator models presented in the literature, in general, do not consider GSHP modeling and load management, with the majority of research papers focusing on optimal load dispatch of existing thermostatically controllable loads, such as ACs, electric water heaters and other flexible loads. Furthermore, most of the reported research that consider GSHP systems focus on their modeling and overall efficiency, but do not consider their participation in electricity markets. Finally, there are no works dealing with the application of

GSHP systems for optimal heating and cooling load dispatch by aggregators.

The load aggregator models and their participation in electricity markets discussed in the literature review are based on low fidelity and incomplete models of household thermal characteristics, since these do not consider a number of key components such as internal heat gains, solar radiance and household building heat transfer. No load aggregator models have yet been reported in the literature for optimal power dispatch of heating/cooling loads of GSHP systems. Performance comparisons between GSHP and other TCLs for power consumption reduction in heating mode have not been reported so far either.

To represent uncertainties in power systems studies, techniques based on range arithmetic such as RO have been shown to perform well, compared to MCS and MPC approaches. However, only a few papers have focused on studying conservative solutions against worst-case scenarios in the context of load aggregation. Furthermore, uncertainties related to the thermal characteristics of households and the GSHP units have not been considered in the aggregator framework for flexible load dispatch. Finally, works that consider uncertainties on thermodynamic characteristics of thermal loads are generic and do not capture their specific characteristics.

Based on the aforementioned discussion, the main objective of the research presented in this thesis is to develop a two-stage operational strategy for the GSHP price-taker aggregator participating in DAM and RTM, and hence determine the optimal annual heating/cooling load dispatch to control the temperatures for a community of houses that minimizes the aggregator's cost, considering uncertainties by means of an RO approach. The detailed objectives of the thesis are discussed next.

1.3 Research Objectives

The main objectives and expected contributions of this thesis are the following:

- Develop a novel mathematical model of a GSHP system with vertical U-pipe GHX configuration, integrated with the thermal model of households in closed-loop and accounting for the thermal and geometric characteristics of residential space heating/cooling, with the capacity to switch between heating and cooling operation modes based on the ambient temperature.

- Propose a GSHP/HVAC load aggregator model for its participation in wholesale electricity markets as a price-taker participant, to provide peak load reduction and load shifting by optimally dispatching the aggregated GSHP loads with the following different operating strategies: a) maximize the house comfort, and b) two-stage operation in DAM and RTM to minimize the aggregator's total electricity cost.
- Carry out simulations for a year considering the integration of several GSHPs/HVACs by a load aggregator for comparative optimal operation strategies in the DAM and RTM, with mathematical models augmented with a set of coordination equations to manage the switching between heating and cooling operations of the GSHP/HVAC systems when operating over the yearly cycle.
- Carry out a techno-economic analysis, to examine the feasibility and long-term profitability for the load aggregator to invest in GSHP systems operating with the proposed strategy, compared to HVAC systems.
- Propose an RO mathematical model that considers uncertainties in electricity prices and ambient temperature to optimize the aggregated GSHP load dispatch, controlling their in-house temperatures to minimize overall costs under the worst-case scenario.

To realize the aforementioned objectives, a realistic test system that includes a community of 800 houses is used, with different house thermal and geometric characteristics, along with different HVAC and GSHP unit characteristics. This allows to realistically compare and analyze the results of the proposed models and operation methodology, and evaluate the RO approach performance with respect to MPC and MCS techniques.

1.4 Outline of the Thesis

The rest of the thesis is organized as follows:

- Chapter 2 discusses the relevant background on GSHP systems and modeling. A general overview on the Ontario electricity market model, the services provided and the role of load aggregators is also presented. Finally, a brief background on optimization techniques based on MPC, MCS, and RO approaches to represent uncertainties, are discussed.

- Chapter 3 presents a deterministic GSHP model for a price-taker load aggregator participating in electricity markets. First, a linear formulation to represent the thermodynamic characteristics of the GSHP and HVAC system are presented. Thereafter, a linear load aggregator model is developed for the proposed two-stage and base case strategies, followed by the results and comparisons of the simulation studies based on the long-term performance of the deterministic GSHP model, compared with the HVAC system and for both the proposed two-stage and base case strategies.

- Chapter 4 presents the GSHP mathematical models considering uncertainties in electricity prices and ambient temperatures, using an RO technique and MPC and MCS approaches. Results obtained when uncertainties are modeled, presented and compared among the three approaches used, to account for uncertainties.

- Chapter 5 summarizes the thesis content, and highlights the main conclusions and contributions of the presented work. The scope for future work is also discussed.

Chapter 2

Background

In this Chapter, a general overview, modeling and operation of GSHP systems are discussed, considering all the thermodynamic characteristics associated with the system. A general overview of the Ontario electricity market is presented next, followed by a description of the role of aggregators participating in electricity markets. Finally, a general description is provided of optimization techniques that consider uncertainties, together with their mathematical formulation.

2.1 Ground Source Heat Pump

2.1.1 Overview

GSHP systems utilize the earth or ground water to provide space heating and cooling for residential houses and commercial buildings. The system takes advantage of the earth as a source of heat in the winter, and as a reservoir/sink for heat that is extracted from the house or building in the summer [15, 35].

GSHP systems are categorized based on the GHX configuration used, i.e., open loop, closed loop, or hybrid. In open loop GHX systems, the underground water can be drawn up to the heat pump, where the heat is extracted before re-injection. On the other hand, in closed loop GHX systems, heat exchanger pipes are installed underground to extract/inject

the heat via an antifreeze solution, which is then transferred to the heat pump's refrigeration system [36]. In extreme cold areas, or in areas with poor water quality, closed loop GHX based GSHP systems are preferable for space heating and cooling applications.

Two types of closed loop GSHP systems are available in the market, based on the physical orientation of their GHX, namely, vertical and horizontal GHX arrangements [3]. Systems with vertical GHX do not require large areas, rendering then suitable for urban areas, they are immersed in the boreholes of 0.1-0.2 m in diameter at a depth of 40-200 m (see Figure 2.1) [18]. These systems operate efficiently in all types of geological areas, except soils with low thermal conductivity, such as dry sand or gravel (as in deserts). The horizontal GHX arrangement is more common in rural areas, where properties are larger, and these pipes are placed in trenches normally 1.0 to 1.8 m deep. These systems are generally cheaper to install than vertical loops, but require large amount of land area.

The main components of a GSHP unit, shown in Figure 2.2, are the following [15, 35]:

- Refrigerant: It is the liquid or gaseous substance that circulates within the heat pump.
- Reversing Valve: It controls the direction of flow of the refrigerant in the heat pump to operate either in heating or cooling mode.
- Evaporator: It is a device in which the refrigerant absorbs heat from its surroundings and reaches its boiling point to become a low-temperature vapour.
- Compressor: It compresses the molecules of the refrigerant vapour, thus increasing its temperature.
- Condenser: It is the device wherein the refrigerant vapour transfers the heat to its surroundings and becomes a liquid refrigerant.
- Expansion Valve: It lowers the pressure created by the compressor, which causes the temperature to drop, and the refrigerant becomes a low-temperature liquid.

The principle of operation of a GSHP unit is characterized by its ability to provide space heating and cooling, as shown in Figure 2.3. In the heating cycle, the heat transferred from the ground to the water in the borehole is transferred to the antifreeze or refrigerant solution in the heat pump unit inside the house (see Figure 2.3a). The cooling cycle is

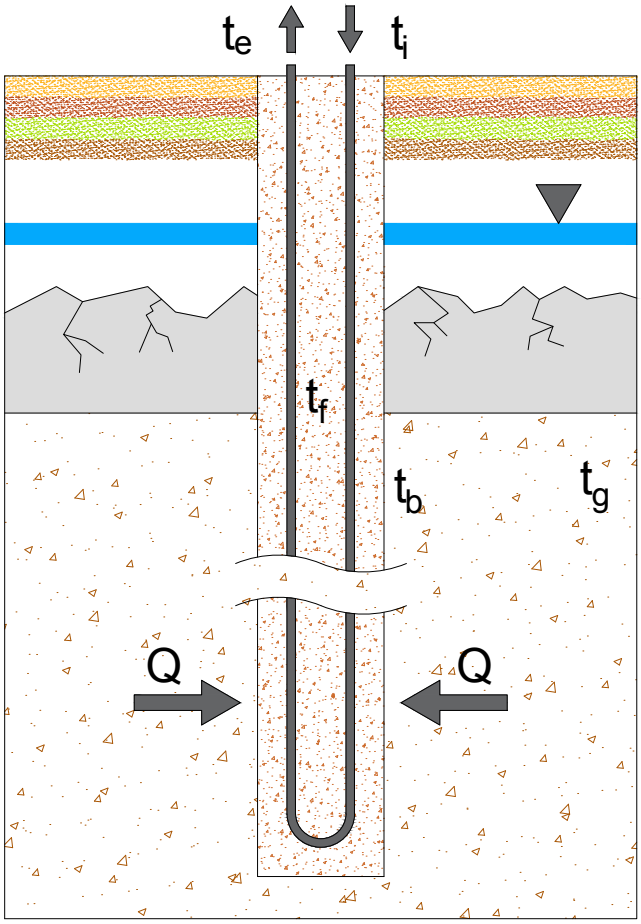

Figure 2.1: Vertical Ground Heat Exchanger (GHX) [36].

basically the reverse of the heating cycle, as shown in Figure 2.3b. The direction of the refrigerant flow is changed by the reversing valve. The refrigerant absorbs heat from the house air and transfers it directly to the ground through the GHX [35].

Based on past experiences, a summary of the major challenges associated with GSHP systems are the following [37, 38]:

- Large initial investment: The installation cost of GSHP systems are high in ur-

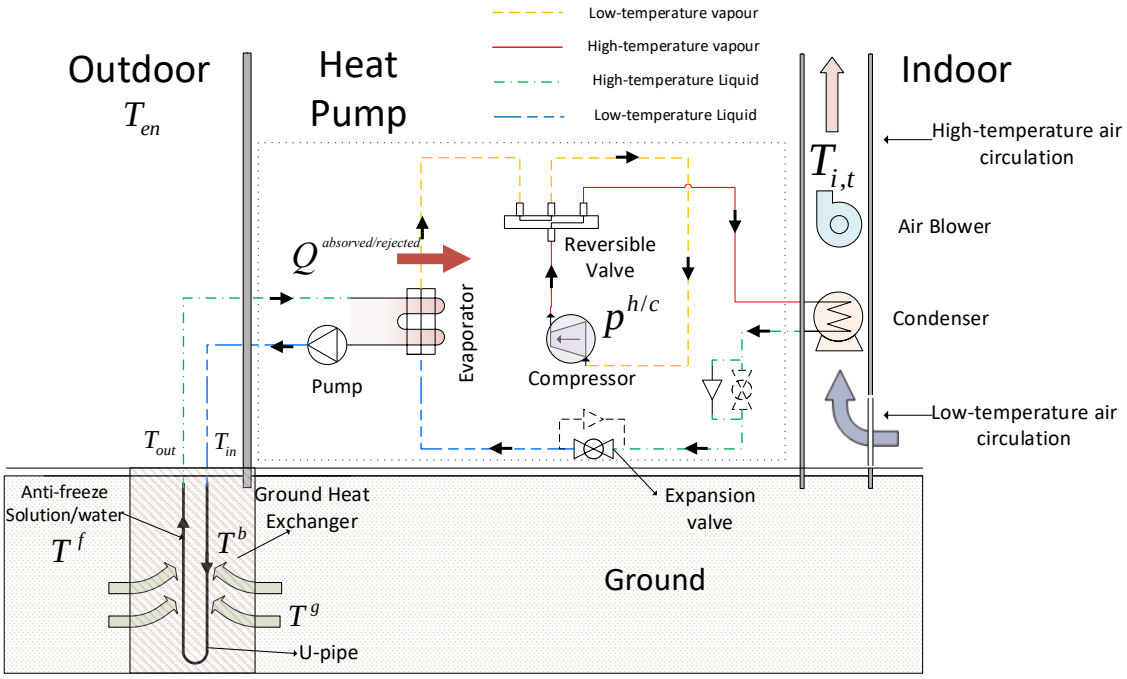

Figure 2.2: Generic configuration of a GSHP system with the arrows depicting the heating cycle [36].

ban areas, mainly because of the high cost of the land and space limitations. For aggregation-based grid service provisions, hundreds of residential GSHP systems would be required, which again is a challenging proposition for urban areas.

- System installation regulations: The installation process for GSHP systems is complex, which include drilling the land, installing the boreholes, etc., and there are no specific regulations related to boreholes in residential areas.

- Determination of thermal properties: The thermal properties of GSHPs might change with time, or even from one location to another. In order to determine these properties, different experimental and ground sampling procedures are necessary.

The performance of a general GSHP unit is identified by the COP and Energy Efficiency

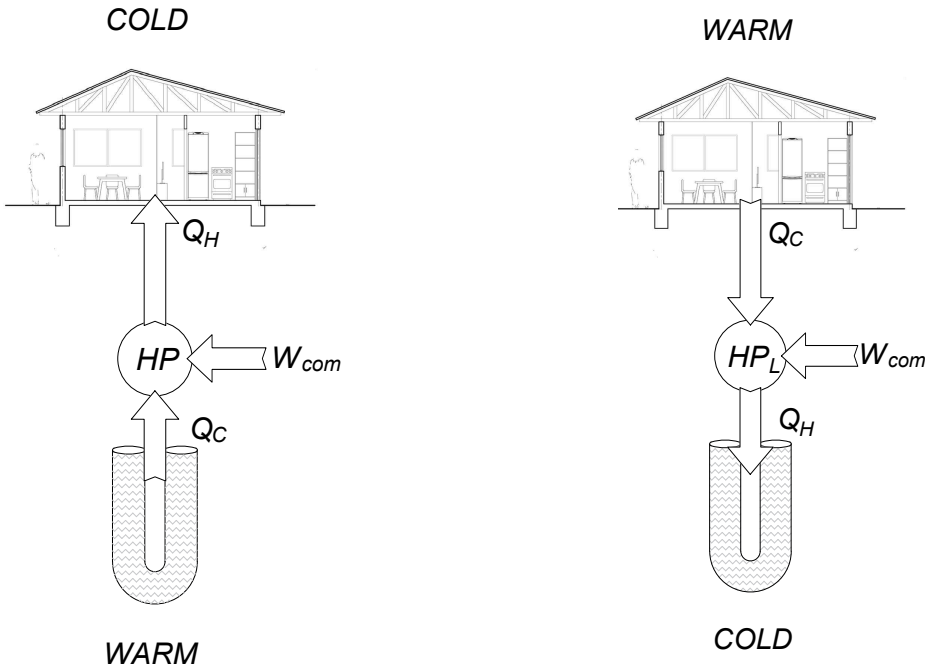

(a) Heating mode

(b) Cooling mode

Figure 2.3: GSHP working principle [15].

Ratio (EER), in both heating and cooling modes, respectively [39], which can be calculated as follows [35]:

$$EER^{HP} = \frac{Q^C}{W_{com}} \tag{2.1}$$

$$COP^{HP} = \frac{Q^H}{W_{com}} \tag{2.2}$$

The variables and parameters can be found in the Nomenclature section. For closed-loop GSHP systems, the COP varies between 3.1 and 4.9, while the EER ranges from 13.4 to 25.8 [36]. In Canada, where air temperatures can go below -30°C, and where winter ground temperatures are generally in the range of –2°C to 4°C, earth-energy systems have a COP between 2.5 and 3.8 [3].

2.1.2 Mathematical Modeling

The thermal model of a GSHP system follows the thermodynamic properties of the typical vapor-compression cooling/heating cycle represented in the T-s diagram, as shown in Figure 2.4. The model considers the mass flow rates from the refrigerant and ground water circulating in the GHX and the heat pump, the power consumption of the compressor, and the heat transfer of the evaporator and condenser [40]. The model presented next, represents the GSHP system operation in heating mode [40, 41].

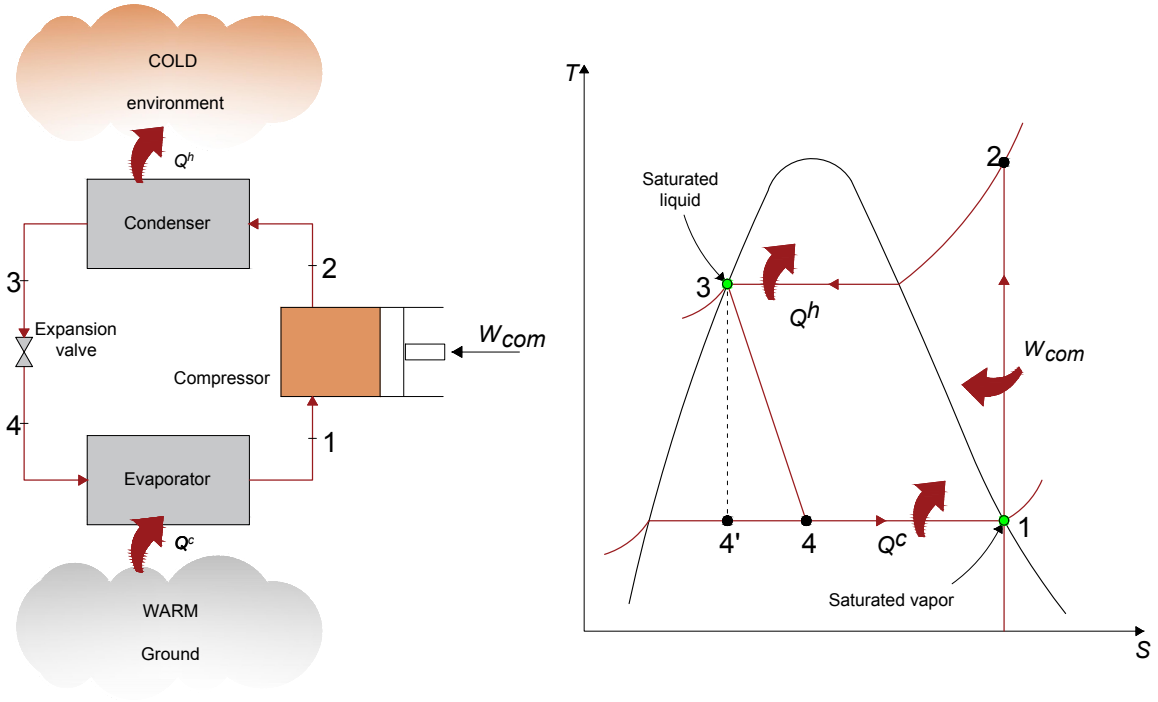

Figure 2.4: T-s diagram of a vapour-compression cycle in heating mode for a heat pump [40].

From the first law of thermodynamics, the heat transfer Q^h between the refrigerant in the GSHP and the indoor air is given by:

$$Q^h = (h_3 - h_2)\dot{m}_{Re} \tag{2.3}$$

Additionally, the heat transfer Q^c between the refrigerant and the underground water in heating mode can be determined as follows:

$$Q^c = c_f(T_{out} - T_{in})\dot{m}_f \tag{2.4}$$

The compressor power consumption W_{com} can be expressed as a product of the mass flow rate and the difference in enthalpy between states 2 and 1, as follows (Figure 2.4):

$$W_{com} = \dot{m}_R(h_2 - h_1) \tag{2.5}$$

The GHX heat transfer Q_{GHX} between the underground fluid and the soil is expressed as follows:

$$Q^{abs/rej} = \frac{\Delta T}{R_{Total}} = \frac{\|T_g - \frac{T_{f1}+T_{f2}}{2}\|}{R_{pp} + R_{bb} + R_g} \tag{2.6}$$

The thermal resistances of the GHX can be calculated as follows:

$$R_{pp} = \frac{S}{2U_{GHX}\pi D_{i,GHX} l_{GHX}} \tag{2.7}$$

$$R_g = \frac{\ln D_{o,GHX}/D_{i,GHX}}{4\pi k_g l_{GHX}} \tag{2.8}$$

$$R_{bb} = \frac{S}{2U_{GHX}\pi D_{o,GHX} l_{GHX}} \tag{2.9}$$

Finally, the overall COP of a GSHP system can be expressed as follows:

$$COP_{system} = COP^{HP} + \frac{Q^{abs/rej}}{W_{com}} = \frac{Q^h + Q^{abs/rej}}{W_{com}} \tag{2.10}$$

$$EER_{system} = EER^{HP} - \frac{Q^{abs/rej}}{W_{com}} = \frac{Q^c - Q^{abs/rej}}{W_{com}} \tag{2.11}$$

2.2 Electricity Market Model and Aggregator Strategies

2.2.1 Ontario's Electricity Market

The IESO, established in 2002, is responsible for the day-to-day operation of the Ontario power system [42]. All participants with direct physical connection must participate in the electricity market; the participants are also allowed to have bilateral contracts. A two-stage market is used, with the pre-dispatch stage or DAM, providing a first estimate of the power dispatch and electricity prices for the next day on an hourly basis. The second stage is the RTM, which is settled every 5 minutes using an MPC approach with 12 fixed intervals, wherein the operating reserves, Market Clearing Prices (MCPs) and dispatch instructions for the next interval are determined.

Ancillary services are provided and managed by the IESO to ensure the reliability of the power system. While some of these services are procured through long-term contracts, some are provided through the markets [42]. The Energy Competition Act of Ontario in 1998 provided authority for the creation of a market in order to provide an efficient and reliable environment to electricity retailers for the sale and purchase of ancillary services in Ontario [43, 44]. Currently, the IESO provides the following four ancillary services to ensure reliable operation of the Ontario's power system [45]:

- Regulation/Automatic Generation Control Service: It matches total system generation to total system load, and helps reduce the frequency deviations in the power system. The IESO contracts with eligible generators to provide regulation service for the period beginning May 1 of each year to April 30 of the following year. This service corrects for short-term changes in electricity use that might affect the stability of the power system. Minimum requirements are calculated by the IESO, and control signals are sent to the generators under contract to raise or lower their output as required. The current regulation service must satisfy the minimum requirement of ± 100 MW of Automatic Generation Control (AGC) to be scheduled at all times; additionally, a minimum overall ramp rate of 50 MW per minute is required.

- Black Start Service: The service is contracted to meet the requirements of restoring the Ontario power system after a major black out. They help the system reliability

with the ability to restart their generation facility with no outside source of power; these facilities have to satisfy specific requirements determined by the IESO.

- Reactive Support and Voltage Control: These are contracted from generators to ensure that the IESO is able to maintain the voltage level of its grid within acceptable limits. Reactive power flow is needed in the ac transmission system to support the transfer of active power over the network. Generation facilities are the major provider of this service in Ontario.

- Reliability Must-Run Resources: Whenever sufficient resources to provide physical services in a reliable way are not available, the IESO may need to call registered facilities in order to maintain the reliability of the grid. The contracts obligate the market participant to offer into the IESO the maximum amount of energy and operating reserve, in accordance with stated performance standards.

- Operating Reserve Markets: Is a stand-by power or demand reserve that can be called on with short notice by the IESO to guarantee available additional resources, such as dispatchable generators or loads, if an unexpected event takes place in the real-time energy market. The three types of operating reserve classes are: 10-minute synchronized (spinning) reserve, 10-minute non-synchronized (non-spinning) reserve and 30-minute non-synchronized reserve.

The IESO launched the Demand Response (DR) auction market in 2016, wherein contracted loads can be called upon by the IESO on short notice for curtailment, in order to maintain the reliability of the grid [46]. However, this pilot market was replaced in December 2019 with the capacity auction program, securing the capacity needed to meet Ontario's short term power needs [47].

2.2.2 Role of Aggregators in the Electricity Market

An aggregator can be defined as an entity which agglomerates a set of retail customers in a power system for the purpose of providing certain services which would otherwise not be feasible by individual agents [48]. These have the resources to provide customer load management and are responsible for the installation of communication and control devices at end-user premises. The main objectives of an aggregator are to (a) provide various

services to the utility and/or (b) reduce the electricity cost of customers. Each aggregator accounts for a significant share of demand in the electricity market, and can negotiate on behalf of the customers directly with the utility. The participating customers in return permit the aggregator to have direct control of their flexible demands such as appliances, smart loads, HVAC loads, etc. [49].

From the utility operator's perspective, the aggregator is seen as a large generator or load, which could provide ancillary services such as spinning and regulating reserve [50]. In addition, the aggregator may also participate in the electricity market with supply offers and/or demand bids. In the case of Ontario, load aggregators act as market participants depending of the service provided, such as capacity reserve or energy storage contributor, or as program participants such as smart metering providers [51].

Load aggregators may be price-taker participants, as illustrated in Figure 2.5, i.e., they do not impact the electricity market prices. In this case, the aggregator only schedules the total load demand of each customer to minimize its total electricity cost considering different factors, such as the electricity prices and customers' load profiles, with the aggregator benefiting from the price difference between the market prices and the customers' fix payments for its services.

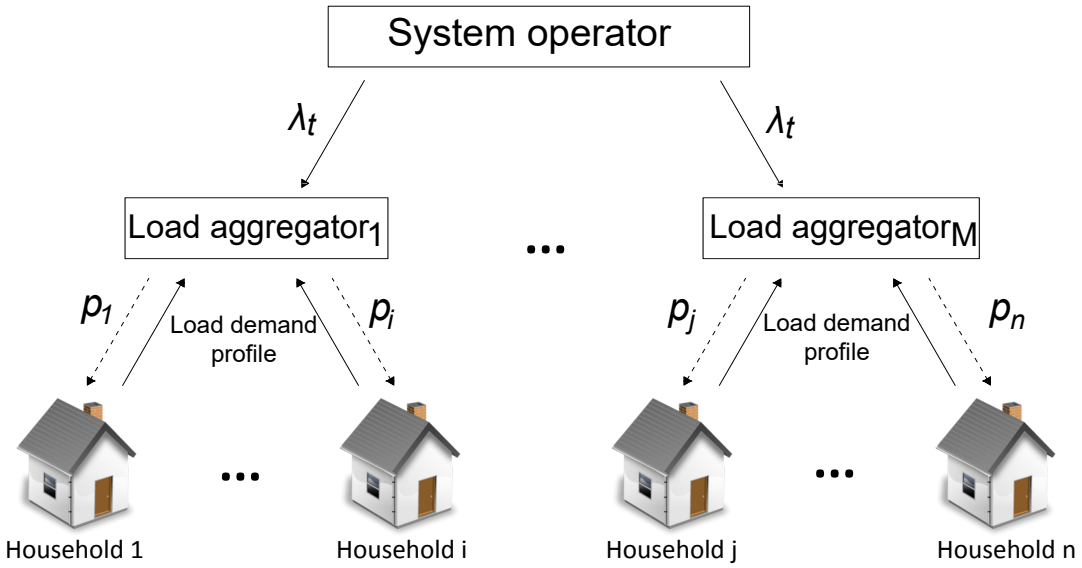

Figure 2.5: Structure of the price-taker load aggregator [49].

In the context of the power system, load aggregators take into account various system and market uncertainties and manage the risks of individual customers by coordinating information exchange between various power system actors. Competition among aggregators can lead to innovative solutions and products and increase participation in electricity markets [52]. Aggregators can be defined and classified according to their responsibilities as follows [53]: production aggregators, commercial aggregators, and load aggregators. Load aggregators can integrate small distributed generation and ESS facilities, and interact with other market players, such as local retailers, microgrids, and RES.

Most aggregator strategies consider their participation in the DAM and RTM with a bi-level or two-stage economic optimization model which aims to maximize the aggregator's profits, or minimize its total operational costs [54]. Other less common objectives include the minimization of system imbalance, or the maximization of social welfare. The aggregator's optimization problem can be formulated as a hierarchical game, where a follower creates optimal decisions to maximize its objective function, which is influenced by the selection of the leader, and upon which the leader maximizes its own objective function [55].

An example for the upper-level problem (leader) is the optimization of the strategic aggregator bidding, which considers the outcome of the lower-level (follower) representing the market clearing process, as discussed in [56].

2.3 Optimization in the Presence of Uncertainties

Optimization modeling can be defined as the process of finding the maximum or minimum of a function, which in an engineering context can represent benefits or costs related to a system [57]. These mathematical models are expressed in terms of objective functions and constraints, which together represent a measure of the system performance, and establish the feasible region for the system variables. An optimization problem can be represented by a set of equations and inequalities, as follows:

$$\min_{x} \quad f(x) \tag{2.12}$$

$$\text{s.t.} \quad g_i(x) = 0 \quad \forall i \tag{2.13}$$

$$h_j(x) \leq 0 \quad \forall j \tag{2.14}$$

where x is the vector of decision variables, $f(x)$ represents the objective function, $g(x)$ the equality constraint functions, and $h(x)$ the inequality constraint functions.

Although the optimization models may have an accurate mathematical representation, the solutions obtained may not necessarily be the optimum in practice due to the uncertainties in model and other system parameters. Depending on the degree of uncertainty, the model optimal solution can lead to different misrepresented outcomes, such as economic losses or under-performing operation, which are highly undesirable. Price uncertainty have always been a challenge for different agent-based participants in the electricity market due to the price volatility [58], and more recently uncertainty of ambient temperature which is becoming relevant due to the increasing integration of thermo-electrical systems. Thus, in order to ensure reliable operational decisions, these uncertainties must be taken into account in optimization models.

A classical approach to deal with uncertainties is through Stochastic Optimization (SO) [59]. There are several SO techniques depending on the problem formulation, with

uncertainties in parameters [60]. In these models, such as in the case of MCS and MPC techniques, uncertainties are represented by Probability Density Functions (PDFs), which are nonlinear, thus making the problems more complex [61]. Despite presenting robust results, adequate PDF representations for the uncertainties considered are only possible if there is a considerable amount of data; hence, the lack of data may lead to assumptions regarding the PDFs, which may yield poor representations with significant errors [62]. Due to these challenges, alternative methods based on range arithmetic, such as RO, have been proposed.

2.3.1 Model Predictive Control (MPC)

MPC can be described as a future behaviour prediction using a system model, based on measurements or estimates of the current state of the system and a hypothetical future input trajectory or feedback control policy [63]. In this context, forecasted inputs are characterized by a finite number of degrees of freedom, which are used to optimize a cost and the first control input of the optimal control sequence is only implemented. The process is repeated at the next time instant using newly available information on the system state. This repetition is instrumental in reducing the gap between the predicted and the actual system response in closed-loop operation. The MPC approach also provides a certain degree of inherent robustness to uncertainties that can arise from unknown variations of the parameters, as well as to model uncertainty in the form of disturbances in the system dynamics [64].

In the MPC approach, the current control action is computed in real-time. A model predictive controller uses, at each sampling instant, the current input and output measurements of the plant, its current state and the plant model, to calculate over a finite horizon, a future control sequence that optimizes a given performance index and satisfies constraints on the control action, using the first control in the sequence as the plant input.

The basic MPC plant structure is illustrated in Figure 2.6, where x_t is the vector of state variables at time t, u_t is the vector of control variables at time t, and y_t is the output of the optimal control problem at time t. The optimization calculates a control sequence for the finite horizon such that a selected objective function is minimized, but only the control action for the next time step is implemented; this process repeats itself every time-step [65].

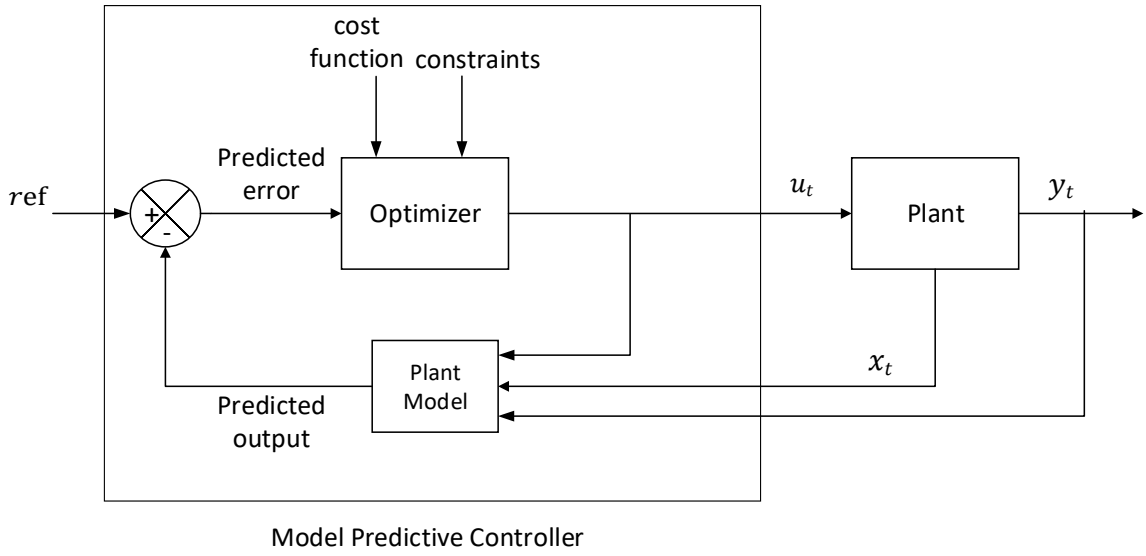

Figure 2.6: MPC structure [66].

2.3.2 Montecarlo Simulations (MCS)

Monte Carlo Simulation (MCS) is a stochastic technique that relies on repeated random sampling and statistical analysis to compute the results [67]. This method of simulation is closely related to random experiments, for which the specific result is not known in advance, and is hence typically used for benchmarking modeling techniques for uncertainty management.

In its most simple form, MCS collects a number of random observations of a population, which is referred to as simple sampling. The number of samples from a random variable x, and are distributed according to its PDF, $f(x)$ [68]. When a random variable is to be obtained from a PDF, it is useful to obtain the variable's Cumulative Distribution Function (CDF) $P(x)$, which denotes the cumulative probability of an event in a given interval (Figure 2.7) and can be obtained by integrating the PDF as follows:

$$P(a < x < b) = \int_a^b f(x)\,dx \tag{2.15}$$

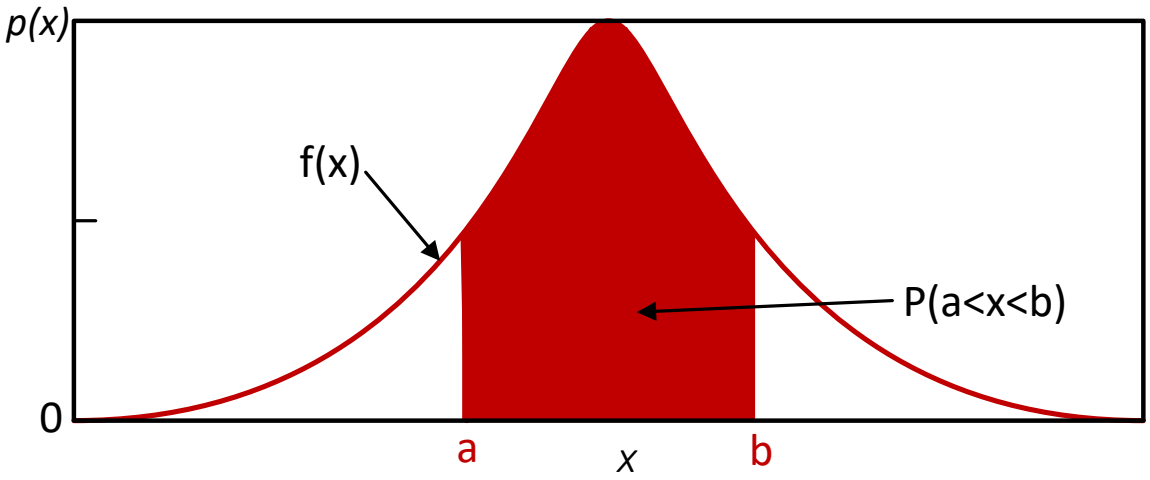

Figure 2.7: PDF and CDF for a normal distribution function [68].

The basic MCS procedure is as follows [69]:

1. Specify a statistical PDF to be used as the source for each of the input parameters.
2. Draw random samples from each PDF, which then represent the values of the input variables. For each set of input parameters, a set of output parameters y_n is obtained.
3. Collect output values y_n from a number of simulation runs.
4. Repeat Steps 2 and 3 for N times, which is the number of trials at which the expected values of the outputs converge.
5. Perform statistical analysis on the values of the output variables to characterize the output variation, from which one can estimate its expected value $E(.)$ and variance σ^2 as follows:

$$E[\mathcal{Y}] = \frac{1}{N}\sum_{n=1}^{N} y_n \tag{2.16}$$

$$\sigma^2[\mathcal{Y}] = \frac{1}{N}\sum_{n=1}^{N}(y_n - E[\mathcal{Y}])^2 \tag{2.17}$$

where $\mathcal{Y} = \{y_1, \ldots, y_N\}$

2.3.3 Robust Optimization (RO)

Robust Optimization (RO) presents an attractive approach to represent random variables through uncertainty sets, rather than probabilistic models, and thus there is no need to assume the intrinsic characteristics of the uncertainties. The method was originally proposed in [70], and employed in a linear optimization problem, seeking to optimize the objective in the worst-case scenario; however, the original model was highly conservative. Several decades later, a method to make the level of conservatism more flexible while maintaining the advantages of the linear model was proposed in [71], where a parameter, the budget of uncertainty Γ, was introduced, which can take any value in [0, M], where M represents the set of coefficients that are subject to uncertainty. Varying Γ from 0 to M allows a trade-off between the level of conservatism and robustness. Thus, for $\Gamma = 0$ the model is deterministic, while for $\Gamma = M$, the most conservative (worst case) scenario is considered, yielding the model proposed in [70].

RO problems seek to optimize an objective function for the worst-case scenario, as follows [72]:

$$\min_{x} \sum_{m=1}^{M} c_m x_m \tag{2.18}$$

$$\text{s.t. } Ax \leq b \tag{2.19}$$

where c, A and b are parameters, x is a variable, and m is an index. Observe that the objective is to minimize the function in terms of the decision variables x_m. By considering uncertainties in the parameters c_m, it is assumed that there is a mismatch of up to $\overline{\Delta c_m}$ in its value. Hence, the values that c_m may assume are in the following interval:

$$c_m \in [c_{m,0}(1 - \overline{\Delta c_m}), c_{m,0}(1 + \overline{\Delta c_m})] \tag{2.20}$$

$$c_m = c_{m,0}(1 + \Delta c_m) \tag{2.21}$$

$$-\overline{\Delta c} \leq \Delta c_m \leq +\overline{\Delta c} \tag{2.22}$$

where $c_{m,0}$ represents the forecast value of c_m, and Δc_m is a variable that represents the mismatch of c_m. Substituting (2.21) in (2.18) and adding several constraints reflecting c_m uncertainty, one has:

$$\min_{X=[x_1,\ldots,x_m]} \max_{\Delta c_m} \sum_{m=1}^{M} \left(c_{m,0}x_m + c_{m,0} \underbrace{\Delta c_m x_m}_{\text{Bi-linear term}} \right) \tag{2.23}$$

$$\text{s.t. } \Delta c_m = \Delta c_m^+ - \Delta c_m^- \qquad \forall m \tag{2.24}$$

$$\Delta c_m^+ \leq \overline{\Delta c} \qquad \forall m \tag{2.25}$$

$$\Delta c_m^- \leq \overline{\Delta c} \qquad \forall m \tag{2.26}$$

$$\sum_{m=1}^{M} \frac{\Delta c_m^+ + \Delta c_m^-}{\overline{\Delta c}} - \Gamma \leq 0 \tag{2.27}$$

$$\Delta c_m^+, \Delta c_m^- \geq 0 \qquad \forall m \tag{2.28}$$

Observe in (2.23) that the problem seeks to minimize the function in terms of x, and maximize it in terms of Δc_m. In (2.24), the variable Δc_m is broken into two positive variables Δc_m^+ and Δc_m^- which represents the upward and downward deviations, respectively, and are limited by $\overline{\Delta c}$ in (2.25) and (2.26). Finally, the level of conservatism is controlled using (2.27), where the budget of uncertainty Γ limits the number of times the value of c_m deviates from the forecast. Note that in the range of values for the budget of uncertainty is $\Gamma \in [0, M]$, $\Gamma = 0$ corresponds to the deterministic model, i.e., no uncertainties considered, and $\Gamma = M$ corresponds to the most conservative scenario, where all values of c_m deviate from the forecast. Hence by choosing different combinations of ($\overline{\Delta c}$, Γ), a set of possible optimum decisions can be obtained, with different degrees of uncertainty.

The modified objective function (2.23) includes a bi-linear term, and thus converts the overall problem into a nonlinear model. Additionally, a min-max structure is a saddle-point

mathematical problem, which may be non-convex. However, the internal maximization problem in (2.23) is linear, and hence it can be replaced by its dual problem using the concept of strong duality [73].

2.4 Summary

This chapter reviewed various background topics, concepts and tools used throughout the thesis. The concept of GSHP was introduced first, providing an overview of its principle of operation and presenting a mathematical model to represent its thermodynamic characteristics. A synopsis of the Ontario's electricity market model and related services was introduced, followed by a comprehensive overview of the role of aggregators in electricity markets. Finally, uncertainty consideration in optimization problems was discussed for different techniques, in particular MPC, MCS and RO.

Chapter 3

Modeling and Operation in Electricity Markets

This chapter presents a novel mathematical model to represent the thermodynamic characteristics of a GSHP system with a vertical U-pipe GHX configuration, and its operation in the electricity market environment via a load aggregator. The developed models allow to determine the GSHP aggregator's optimal load dispatch, considering both HVAC and GSHP systems for residential space heating/cooling, for two different operating strategies: minimizing the aggregator's electricity cost while operating in the electricity market environment, and maximizing the customer's comfort. Simulations and results are presented to illustrate the application and benefits of the proposed models.

3.1 GSHP Thermal Model

As discussed in Section 2.1, systems with vertical U-pipe based GHX are preferred in suburban areas because their installation does not require large spaces [74], and thus these have been considered for the studies presented here. The proposed GSHP model in this thesis considers the mass flow rates of the ground water circulating in the GHX and the heat pump, the power consumption of the compressor, and the heat transfer of the evaporator and condenser, based on [40].

In order to reduce the complexity of the considered heat transfer processes, while maintaining proper accuracy of the thermal load model, the following assumptions are made:

- Seasonal variation of ground temperature is not considered.
- Indoor air temperature is homogeneous, i.e., no heat loss is considered inside the house.
- Temperature of the building envelope is homogeneous.
- Thermal comfort parameters remain within the recommended limits.
- The GSHP system operates either in cooling or heating mode.
- Since the time resolution of the model is one hour, a steady-state heat exchange process is assumed to model thermal systems.

3.1.1 Performance of the GSHP

The COP and EER of the GSHP for each house i at each hour t are calculated as follows [15]:

$$COP_{i,t}^{HP} = COP_{ref}^{HP}\Big[A_h + B_h\Big(\frac{T_{i,t}^{out}}{T_{ref}^{HP}}\Big) + C_h\Big(\frac{T_{ref}^{HP}}{T_{i,t-1}}\Big)\Big] \tag{3.1}$$

$$EER_{i,t}^{HP} = EER_{ref}^{HP}\Big[A_c + B_c\Big(\frac{T_{i,t}^{out}}{T_{ref}^{HP}}\Big) + C_c\Big(\frac{T_{ref}^{HP}}{T_{i,t-1}}\Big)\Big] \tag{3.2}$$

where $COP_{i,t}^{HP}$ and $EER_{i,t}^{HP}$ are the calculated COP and EER of the GSHP, in heating and cooling mode, respectively; $A_{h/c}$, $B_{h/c}$, and $C_{h/c}$ are coefficients shown in Appendix A obtained from a linear data-fitting of the GSHP capacity data-sheets provided also in the Appendix A; $T_{i,t}^{out}$ is the outlet temperature at the GHX terminal; T_{ref}^{HP} is the GSHP's reference temperature of operation (283 °K); $T_{i,t}$ is the indoor air temperature; and COP_{ref}^{HP} and EER_{ref}^{HP} are the rated COP and EER of the GSHP, respectively. All variables and parameters in these and other equations are defined in the Nomenclature section.

3.1.2 House Heat Transfer Balance

The following relations represent the inter-temporal house heat transfer and the GHX contribution that affects the in-house temperature at hour t:

$$Q_{in_{i,t}} = (1-\psi)\phi_t + Q_{G_{i,t}} \tag{3.3}$$

$$Q_{out_{i,t}} = U_A(T_{i,t-1} - T^F_{amb_t}) + U_E(T_{i,t-1} - T_{E_{i,t}}) \tag{3.4}$$

In (3.3), the first term $Q^{h/c}_{GHX}$ corresponds to the heat transfer into the house from the GHX U-pipe based system, the second term represents the solar radiation through the glazed surfaces, with the incidence factor representing the transmittance loss of the solar radiation power, which is effectively reflection [75]; and finally the internal heat gains of the house are given by the third term. In (3.4), the first term denotes the heat transfer from inside the house to the outside environment through the external glazed surfaces, and the second term denotes the heat transfer from inside the house through the external walls and ceiling.

3.1.3 In-house Temperature Relationship

The inside air temperature of house i at hour t, depends on the temperature at time $t-1$, the power consumption of the GSHP unit at time t, and the heat transfers occurring inside the house, as follows:

$$T_{i,t} = T_{i,t-1} + \frac{Q_{in_{i,t}} - Q_{out_{i,t}}}{H_{P_r}} + \frac{Q^h_{i,t}}{H_{P_r}} + \tilde{\alpha}_i \; p^{res}_{i,t} - \frac{Q^c_{i,t}}{H_{P_r}} \qquad \forall i \in \mathcal{I}, t \in \mathcal{T} \tag{3.5}$$

where:

$$Q^h_{i,t} = \underbrace{COP^{HP}_{i,t} \; p^h_{i,t}}_{\text{Bi-linear term}} \tag{3.6}$$

$$Q^{c}_{i,t} = \underbrace{EER^{HP}_{i,t}\ p^{c}_{i,t}}_{\text{Bi-linear term}} \tag{3.7}$$

The first term in (3.5) represents the in-house temperature at $t-1$. The temperature change due to inter-temporal house heat transfers, given in (3.3) and (3.4), are expressed by the second term. The third term denotes the temperature change because of heat transfer from the GSHP system operating in heating mode to the house, the fourth term represents the temperature change due to heat provided by the secondary thermal resistances $p^{res}_{i,t}$ multiplied by the factor $\tilde{\alpha}_i$, which are used occasionally for peak heating in severe weather conditions. The last term represents the temperature change because of heat transfer from the house to the GSHP system operating in cooling mode.

Note that (3.6) and (3.7) are non-linear because of the bi-linear components. However, these can be linearized using the Mccormick envelope approach [76], by replacing the bi-linear terms with a set of linear inequality constraints $\forall\ i\ \in\ \mathcal{I},\ t\ \in\ \mathcal{T}$ as follows:

$$Q^{h/c}_{i,t} \geq W^{h/c}_{i,t}\ \overline{p^{h/c}_{i}} + \overline{W^{h/c}_{i}}\ p^{h/c}_{i,t} - \overline{W^{h/c}_{i}}\ \overline{p^{h/c}_{i}} \tag{3.8}$$

$$Q^{h/c}_{i,t} \leq W^{h/c}_{i,t}\ \overline{p^{h/c}_{i}} + \underline{W^{h/c}_{i}}\ p^{h/c}_{i,t} - \underline{W^{h/c}_{i}}\ \overline{p^{h/c}_{i}} \tag{3.9}$$

$$Q^{h/c}_{i,t} \geq \underline{W^{h/c}_{i}}\ p^{h/c}_{i,t} \tag{3.10}$$

$$Q^{h/c}_{i,t} \leq \overline{W^{h/c}_{i}}\ p^{h/c}_{i,t} \tag{3.11}$$

$$\underline{W^{h/c}_{i}} \leq W^{h/c}_{i,t}\ \leq \overline{W^{h/c}_{i}} \tag{3.12}$$

where $Q^{h}_{i,t}$ denotes the heat injected to the house and $Q^{c}_{i,t}$ the heat extracted from the house, based on the GSHP operation mode.

3.1.4 External Wall Temperature

The temperature of the external walls of the house i at hour t depend on the solar radiation and the heat transfer between the external environment and the external walls of the house, as follows:

$$T_{E_{i,t}} = T_{E_{i,t-1}} + \frac{\psi\phi_t + U_E(T_{E_{i,t-1}} - T^F_{amb_t})}{H_{P_E}} \quad \forall i \in \mathcal{I}, t \in \mathcal{T} \tag{3.13}$$

3.1.5 Comfort Limits

The following constraints ensures that the in-house temperature is within the end-user's comfort range:

$$\underline{T_i} \leq T_{i,t} \leq \overline{T_i} \quad \forall i \in \mathcal{I}, t \in \mathcal{T} \tag{3.14}$$

3.1.6 Cycling Constraint

The following equations guarantee that the temperature inside a house at the end of day is the same as that of the initial temperature T^o_i for the next day:

$$T_{i,\mathcal{T}} = T^o_i \quad \forall i \in \mathcal{I}, t = \mathcal{T} = 24 \tag{3.15}$$

3.1.7 Borehole Thermal Model

The borehole model is built to represent the vertical and radial heat transfer processes along its depth [15, 77]. Based on [78], the U-pipe can be split into 50 equal segments j of height 5 meters each, as seen in Figure 3.1a, to properly represent the vertical temperature variation of the underground fluid. Each segment j yields five different nodes, as per Figure 3.1b, which represent the fluid temperature inside each leg of the U-pipe $T^{f,dn}_{i,t,j}$ and $T^{f,up}_{i,t,j}$ (one leading the fluid up and the other down), the temperatures of the grout regions $T^{b,dn}_{i,t,j}$ and $T^{b,up}_{i,t,j}$, and the temperature of the surrounding ground $T^{g}_{i,t,j}$. Each node has a thermal capacitance and shares a thermal resistance with every adjacent node, which

can be calculated using the following equations based on GHX geometric and thermal properties [79]:

$$R_{bb} = \frac{S}{k_b(d_b - d_{pe})dz} \tag{3.16}$$

$$R_{pp} = \frac{S - d_{pe}}{k_b \ d_{pe} \ dz} \tag{3.17}$$

$$R_b = \frac{1}{\pi \ k_b \ dz} \log\left(\frac{d_x}{d_{pe}\sqrt{\frac{4S}{\pi/d_{pe}} + 1}}\right) \tag{3.18}$$

$$R_g = \frac{1}{\pi \ k_g \ dz} \log\left(\frac{d_g}{d_b}\right) \tag{3.19}$$

Finally, Lax-Wendroff finite difference approximations, as per [80], are applied to the heat-flow equations, considering that v is constant, resulting in the following expressions [81]:

$$\begin{aligned} T_{i,t,j}^{f,dn} = T_{i,t-1,j}^{f,dn} - \frac{v\Delta t}{2\Delta z}\Bigg\{ & [T_{i,t-1,j+1}^{f,dn} - T_{i,t-1,j-1}^{f,dn}] \\ & - \frac{1}{\Delta z}[T_{i,t-1,j+1}^{f,dn} - 2T_{i,t-1,j}^{f,dn} + T_{i,t-1,j-1}^{f,dn}]\Bigg\} \\ & - \frac{\Delta t}{H_{P_f}}\left[\frac{T_{i,t-1,j}^{f,dn} - T_{i,t-1,j}^{f,up}}{R_{pp}} + \frac{T_{i,t-1,j}^{f,dn} - T_{i,t-1,j}^{b,dn}}{R_b}\right] \\ & \forall i \ \in \ \mathcal{I}, t \ \in \ \mathcal{T}, \ j \ \in \ \mathcal{J} \end{aligned} \tag{3.20}$$

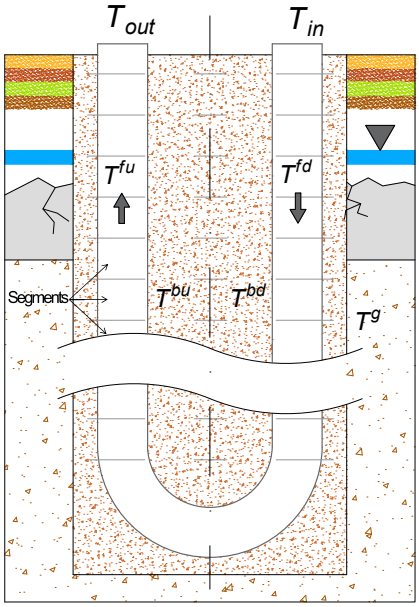

(a) Single U-pipe diagram.

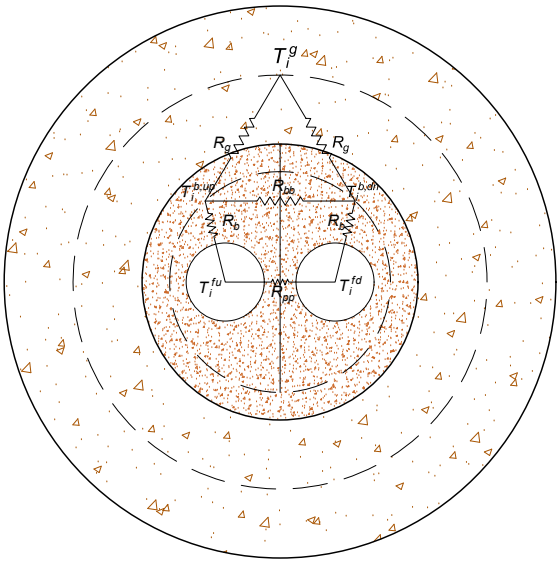

(b) Cross section of a single segment of the U-pipe vertical borehole.

Figure 3.1: Vertical GHX configuration [81].

$$
\begin{aligned}
T_{i,t,j}^{f,up} = T_{i,t-1,j}^{f,up} + \frac{v\Delta t}{2\Delta z}\Bigg\{ & [T_{i,t-1,j+1}^{f,up} - T_{i,t-1,j-1}^{f,up}] \\
& - \frac{1}{\Delta z}[T_{i,t-1,j+1}^{f,up} - 2T_{i,t-1,j}^{f,up} + T_{i,t-1,j-1}^{f,up}]\Bigg\} \\
& - \frac{\Delta t}{H_{P_f}}\left[\frac{T_{i,t-1,j}^{f,up} - T_{i,t-1,j}^{b,up}}{R_b} - \frac{T_{i,t-1,j}^{f,dn} - T_{i,t-1,j}^{f,up}}{R_{pp}}\right] \\
& \forall i \in \mathcal{I}, t \in \mathcal{T},\ j \in \mathcal{J}
\end{aligned}
\tag{3.21}
$$

$$
\begin{aligned}
T_{i,t,j}^{b,dn} = T_{i,t-1,j}^{b,dn} + \frac{\Delta t}{H_{P_b}}\Bigg\{ & \frac{T_{i,t-1,j}^{f,dn} - T_{i,t-1,j}^{b,dn}}{R_b} \\
& + \frac{T_{i,t-1,j}^{b,dn} - T_{i,t-1,j}^{b,up}}{R_{bb}} - \frac{T_{i,t-1,j}^{b,dn} - T_{i,t-1,j}^{g}}{R_g}\Bigg\} \\
& \forall i \in \mathcal{I}, t \in \mathcal{T},\ j \in \mathcal{J}
\end{aligned}
\tag{3.22}
$$

$$T^{b,up}_{i,t,j} = T^{b,up}_{i,t-1,j} + \frac{\Delta t}{H_{P_b}} \Bigg\{ \frac{T^{f,up}_{i,t-1,j} - T^{b,up}_{i,t-1,j}}{R_b} - \frac{T^{b,dn}_{i,t-1,j} - T^{b,up}_{i,t-1,j}}{R_{bb}} - \frac{T^{b,up}_{i,t-1,j} - T^{g}_{i,t-1,j}}{R_g} \Bigg\} \quad \forall i \in \mathcal{I}, t \in \mathcal{T}, j \in \mathcal{J} \tag{3.23}$$

$$T^{g}_{i,t,j} = T^{g}_{i,t-1,j} + \frac{\Delta t}{H_{P_g}} \Bigg\{ \frac{T^{b,dn}_{i,t-1,j} - T^{g}_{i,t-1,j}}{R_g} + \frac{T^{b,up}_{i,t-1,j} - T^{g}_{i,t-1,j}}{R_g} \Bigg\} \quad \forall i \in \mathcal{I}, t \in \mathcal{T}, j \in \mathcal{J} \tag{3.24}$$

The inlet temperature at the terminal of the GHX borehole depends on the GSHP operation mode, cooling and heating respectively, and can be expressed as follows [15]:

$$T^{in}_{i,t} = T^{out}_{i,t-1} + \frac{Q^{rej}_{i,t}}{c_f \dot{m}_f} \tag{3.25}$$

$$T^{in}_{i,t} = T^{out}_{i,t-1} - \frac{Q^{abs}_{i,t}}{c_f \dot{m}_f} \tag{3.26}$$

where $Q^{rej}_{i,t}$ is the heat transferred to the GHX unit, and $Q^{abs}_{i,t}$ is the heat injected by the GHX unit to the household, which can be calculated as follows:

$$Q^{rej}_{i,t} = Q^{c}_{i,t} + p^{c}_{i,t} \tag{3.27}$$

$$Q^{abs}_{i,t} = Q^{h}_{i,t} - p^{h}_{i,t} \tag{3.28}$$

Equation (3.25) and (3.26) can then be written in a composite form to represent the inlet temperature:

$$T_{i,t}^{in} = T_{i,t-1}^{out} + (1 - Z_{a_{i,t}}) \frac{Q_{i,t}^{c} + p_{i,t}^{c}}{c_f \dot{m}_f} - Z_{a_{i,t}} \frac{Q_{i,t}^{h} - p_{i,t}^{h}}{c_f \dot{m}_f} \tag{3.29}$$

where the binary parameter $Z_{a_{i,t}} = \{1, 0\}$ is used to define whether the system is in heating or cooling mode, respectively.

3.2 HVAC Model

The indoor temperature of each house i at hour t is dependent on the temperature at time $t-1$, the power consumption of the HVAC unit at time t, and the heat transfers in the house due to solar radiation, between the room and the environment, and between the room and the external walls of the house, and can be defined as follows [31]:

$$\begin{aligned} T_{i,t} = T_{i,t-1} \ \pm \ \tilde{\alpha}_i p_{i,t}^{h/c} + \frac{(1-\psi)\phi_t + Q_{G_{i,t}}}{H_{P_r}} \\ - \frac{U_A(T_{i,t-1} - T_{amb_t}^{F}) - U_E(T_{i,t-1} - T_{E_{i,t}})}{H_{P_r}} \\ \forall i \ \in \ \mathcal{I}, t \ \in \ \mathcal{T} \end{aligned} \tag{3.30}$$

Equations (3.13) to (3.15) representing the house thermal characteristic for the external wall temperature, the house comfort limits, and the house temperature cycling constraint, respectively, are also included in the HVAC model.

3.3 GSHP/HVAC Load Aggregator Operations Strategies

3.3.1 Proposed Two-Stage Strategy

The objective of the GSHP/HVAC load aggregator is to determine the optimal heating/cooling load dispatch of all houses to minimize its total electricity procurement costs, while maintaining the in-house temperature of all customers within a comfortable range,

considering the physical capacity of the GSHP/HVAC units, the thermal characteristics of each house and the ambient temperature. The load aggregator is assumed to collect information on the uncontrolled loads in the house, the house thermal and heating system characteristics, and the current and forecasted ambient temperature, in order to optimally schedule the GSHP/HVAC load of each house to minimize its cost of total electricity purchase from the electricity market. The following two-stage strategy for the aggregator is proposed, which interacts with the DAM and the RTM, as illustrated in Figure 3.2:

- *Stage 1:* The aggregator schedules the thermal load of each house to minimize its total electricity cost using a forecast of the DAM price $\lambda_t^{DAM_F}$, while satisfying the houses' indoor temperature comfort ranges. The total scheduled load of the aggregator is submitted as a demand bid to the DAM, and it is assumed that the entire bid quantity $P_t^{DAM^*}$ is cleared, which is then an input to the aggregator's real-time operation model.
- *Stage 2:* The load aggregator updates the forecast of local ambient temperature, RTM price forecast, and energy consumption by uncontrolled loads, and uses $P_t^{DAM^*}$ from the DAM. The aggregator then solves the real-time operation model to determine the final thermal load dispatch and other associated decision variables, assuming here that the RTM operation takes place one hour ahead.

GSHP Load Aggregator Model for Participation in DAM

- *Objective Function:* The GSHP load aggregator seeks to minimize the total cost of purchasing electricity from the DAM, as follows:

$$\min_{P_t^{DAM},\ P_t^{DAMres}} \ J_1 = \sum_{t}^{24} \left[\lambda_t^{DAM_F} P_t^{DAM} + \widehat{\lambda}^{DAM_F} P_t^{DAMres} \right] \tag{3.31}$$

where the first term represents the energy procurement cost at hour t at DAM price, and the second term denotes the total cost of serving the aggregated electrical load of secondary thermal resistances, assuming that it is procured at the maximum forecasted DAM price [3]. The GSHP system capacity is typically designed to provide majority of the household's annual heating energy requirement, with the occasional

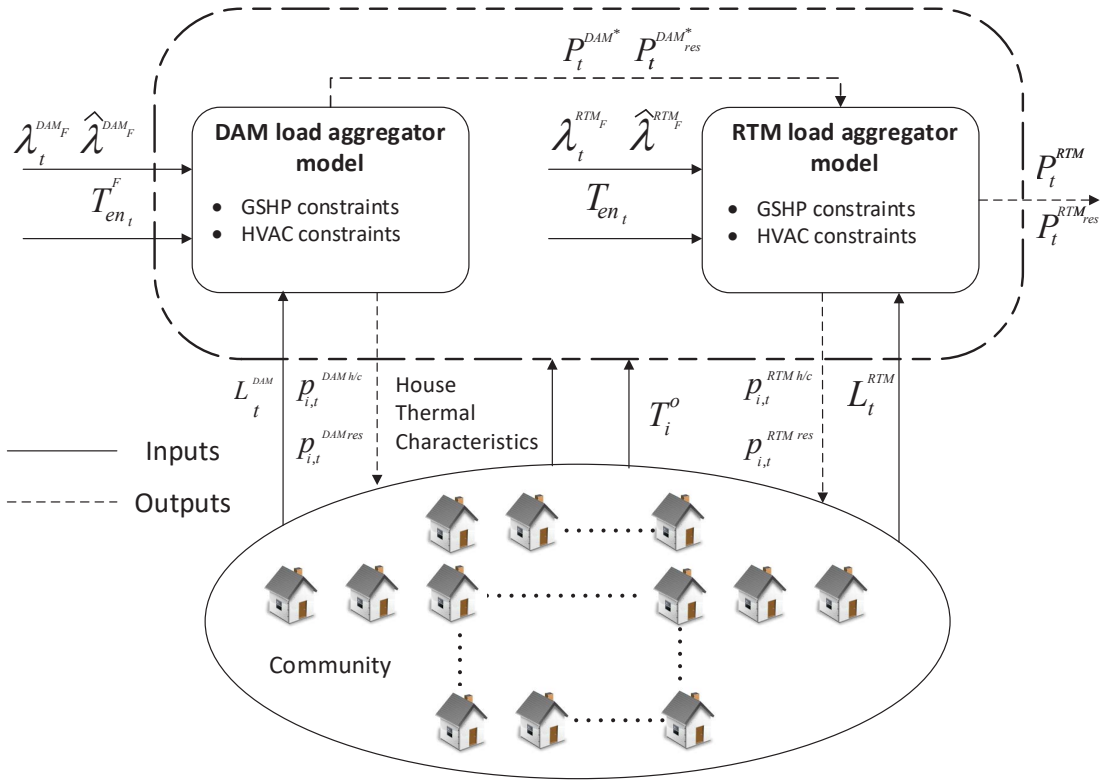

Figure 3.2: Framework of the GSHP load aggregator participating in the electricity market.

peak heating load that occurs during severe weather conditions being met by a supplementary heating system, i.e., secondary thermal resistances [9]. Therefore, to minimize the use of these resistances, their operation is penalized in the model by costing them at the maximum forecasted DAM electricity price.

- *Total Aggregated Load:* The total load procured by the aggregator at hour t is given by:

$$P_t^{DAM} = L_t^{DAM} + \sum_i p_{i,t}^{DAMh} + \sum_i p_{i,t}^{DAMc} \quad \forall i \in \mathcal{I}, t \in \mathcal{T} \tag{3.32}$$

$$P_t^{DAMres} = \sum_i p_{i,t}^{DAMres} \quad \forall i \in \mathcal{I}, t \in \mathcal{T} \tag{3.33}$$

The first term in (3.32) corresponds to the aggregated uncontrolled load in the community, and the second and third terms, which are mutually exclusive decision variables, represent the aggregated GSHP/HVAC load during heating and cooling operation, respectively. Equation (3.33) defines the aggregated load from the secondary thermal resistances of houses, represented by the decision variable $p_{i,t}^{DAMres}$.

- *Capacity Limits:* These ensure that the thermal system power consumption are within their capacity limits, as follows:

$$0 \leq p_{i,t}^{DAMh/c} \leq \overline{P_i^{h/c}} \quad \forall i \in \mathcal{I}, t \in \mathcal{T} \tag{3.34}$$

$$0 \leq p_{i,t}^{DAMres} \leq \overline{P_i^{res}} \quad \forall i \in \mathcal{I}, t \in \mathcal{T} \tag{3.35}$$

- *Operation Coordination:* The following constraints guarantee that the GSHP/HVAC unit operates either in heating or cooling mode:

$$p_{i,t}^{DAMc} \leq (1 - Z_{a_{i,t}})M \quad \forall i \in \mathcal{I}, t \in \mathcal{T} \tag{3.36}$$

$$p_{i,t}^{DAMh} \ , \ p_{i,t}^{DAMres} \leq Z_{a_{i,t}} M \quad \forall i \in \mathcal{I}, t \in \mathcal{T} \tag{3.37}$$

where M is a large number.

- *Thermal Load Modeling:* Includes the HVAC or GSHP operational constraints (3.3)-(3.30) as appropriate, formulated for DAM operation.

GSHP Load Aggregator Model for Participation in RTM

- *Objective Function:* The aggregator seeks to minimize its total penalties payable for any deviations in the real-time load dispatch from the DAM dispatch, at the RTM

price, as follows:

$$\min_{\Delta P_t\ ,\ \Delta P_t^{res}} \ J_2 = \ \sum_{t}^{24} \left[\lambda_t^{RTM_F} \Delta P_t + \widehat{\lambda}^{RTM_F} \Delta P_t^{res} \right] \tag{3.38}$$

where

$$\Delta P_t = \left| P_t^{DAM^*} - P_t^{RTM} \right| \quad \forall t \ \in \ \mathcal{T} \tag{3.39}$$

$$\Delta P_t^{res} = \left| P_t^{DAM*res} - P_t^{RTMres} \right| \quad \forall t \ \in \ \mathcal{T} \tag{3.40}$$

In (3.38), the first term denotes the penalties paid by the aggregator for any deviation in the total aggregated load from DAM dispatch at the forecasted RTM price, and the second term denotes the total penalties for deviation of the aggregated electrical load of the secondary resistances at the maximum forecasted RTM price, as previously argued. The model is subject to constraints (3.32) to (3.36) and the thermal load model relations (3.3)-(3.30) for either GSHP or HVAC systems, as appropriate, formulated for RTM operation.

The RTM load aggregator model presented above is nonlinear because of (3.39) and (3.40), which are linearized using mutually exclusive non-negative auxiliary variables ΔP_t^+ and ΔP_t^- that represent the deviations of the aggregator's demand in RTM as compared to DAM operation, as follows [82]:

$$\Delta P_t = \Delta P_t^+ + \Delta P_t^- \quad \forall t \ \in \ \mathcal{T} \tag{3.41}$$

$$\Delta P_t^+ = P_t^{RTM} - P_t^{DAM^*} \quad \forall t \ \in \ \mathcal{T} \tag{3.42}$$

$$\Delta P_t^- = P_t^{DAM^*} - P_t^{RTM} \quad \forall t \ \in \ \mathcal{T} \tag{3.43}$$

And similarly for ΔP_t^{res}.

3.3.2 Base Case Strategy

The Base Case strategy correspond to the worst case scenario for space heating and cooling, i.e., the set point of the thermostat is kept fixed, and it is assumed that the community is only equipped with electric HVAC systems. The Base Case is where the total power consumption of the GSHP/HVAC system is determined by maximizing the customer comfort, i.e., minimizing the deviation of the in-house temperature from a reference set point, given as follows:

$$J_3 = \sum_{i}^{\mathcal{I}} \sum_{t}^{24} |T_{i,t}^{Ref} - T_{i,t}| \tag{3.44}$$

This objective function is nonlinear, but can be readily linearized applying the same principle as in (3.41)-(3.43), i.e., considering mutually exclusive non-negative variables $\Delta T_{i,t}^{+}$ and $\Delta T_{i,t}^{-}$, as follows:

$$\Delta T_{i,t} = \Delta T_{i,t}^{+} + \Delta T_{i,t}^{-} \quad \forall t \in \mathcal{T}, \forall i \in \mathcal{I} \tag{3.45}$$

$$\Delta T_{t}^{+} = T_{i,t}^{Ref} - T_{i,t} \quad \forall t \in \mathcal{T}, \forall i \in \mathcal{I} \tag{3.46}$$

$$\Delta P_{t}^{-} = T_{i,t} - T_{i,t}^{Ref} \quad \forall t \in T, \forall i \in \mathcal{I} \tag{3.47}$$

and subject to (3.32)-(3.36), and the GSHP/HVAC system constraints as appropriate.

3.4 Results and Discussions

3.4.1 Test System

The present study considers a GSHP/HVAC load aggregator in Ontario, Canada, that submits demand bids to the IESO and purchases electricity for its clients. The weather data is from 2019 [83], The solar irradiation, shown in Figure 3.3, and the internal heat

gains in a typical house, presented in Figure 3.4, are taken from [84] and [85], respectively. The load aggregator is assumed to provide electricity to 800 houses, as in [86], with each house assumed to have the same thermal characteristic, and all customers assumed to stay at home from 6 PM to 8 AM, for simplicity and without loss of generality. The latter assumptions are relaxed in Chapter 4, so that uncertainty can be better represented in the proposed techniques.

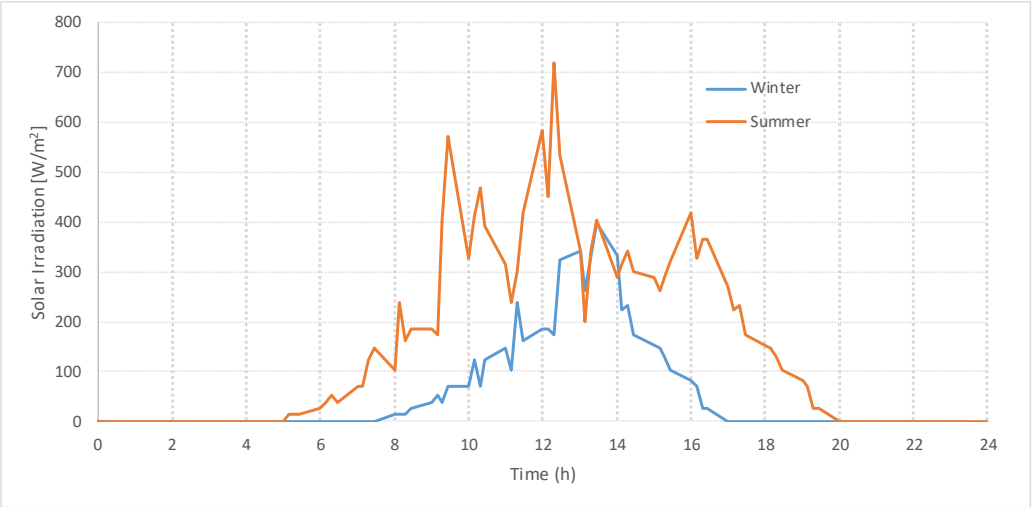

Figure 3.3: Solar irradiation profile of a typical winter and summer day [84].

All model parameters are presented in the following tables: Table 3.1 illustrates all the thermal parameters of the GHX model; the recommended thermal comfort ranges are presented in Table 3.2; the parameters for the house geometric and thermal characteristics are given in Table 3.3 and the characteristics of conventional HVAC system and detailed GSHP system, obtained from [15, 31, 87], are presented in Table 3.4.

The electricity prices were obtained from [88], considering the 3h pre-dispatch price of Ontario as the DAM price forecast $\lambda_t^{DAM_F}$, and the Hourly Ontario Energy Prices (HOEPs) as the RTM price forecast $\lambda_t^{RTM_F}$. The uncontrolled loads, i.e., loads other than HVAC/GSHPs, were obtained from [89] for day-ahead profiles of operation, and the RTM load profiles for the uncontrolled loads were obtained assuming, for each hour, a normal distribution with L_t^{DAM} as mean and a 25% standard deviation, as per [90], to model a

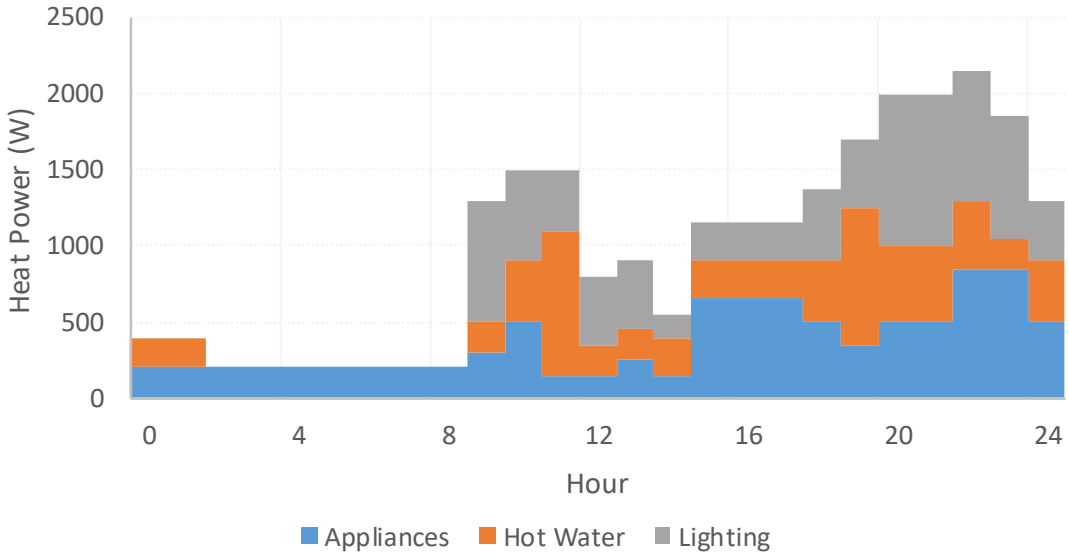

Figure 3.4: Internal heat gain in a typical household [85].

Table 3.1: Geometric-thermal Characteristics of the GHX [79]

Item	Value
Number of segments	50
Borehole depth [m]	250
Grout thermal capacitance H_{P_b} [J/°C]	537.3
Ground thermal capacitance H_{P_g} [J/°C]	2110.5
Fluid thermal capacitance H_{P_f} [J/°C]	365.7
Pipe to pipe thermal resistance R_{pp} [°C/W]	0.291
Borehole conductive thermal resistance R_b [°C/W]	0.061
Grout-to-Grout thermal resistance R_{bb} [°C/W]	0.239
Grout-to-ground thermal resistance R_g [°C/W]	0.051
Fluid specific heat c_f [J/kg °C]	4361
Fluid mass flow rate $\dot{m}_f$ [kg/s]	0.53
Velocity of the underground fluid v [m/s]	0.032

reasonable variation with respect to the DAM uncontrolled load profile.

It is assumed in this work that customers are not equipped with any Home Energy Management System (HEMS) with which they could optimize their GSHP/HVAC oper-

Table 3.2: Household Indoor Temperature Ranges for Thermal Comfort

Time	Temperature range [°C]	
	Minimum	Maximum
6 PM to 9 AM	20	22
9 AM to 6 PM	17	25

Table 3.3: Household Geometric and Thermal Characteristics [15]

Item	Value
Area [m^2]	325
Volume [m^3]	225
Glazed surface portion [%]	9.5
R ceiling [m^2 °C /W]	7.67
R external walls [m^2 °C /W]	4.67

Table 3.4: GSHP and HVAC Characteristics [31, 87]

GSHP	
Model	BP030
Cooling Capacity [Btu/hr]	28500
Heating Capacity [Btu/hr]	20500
EER_{ref}^{HP}	19.4
COP_{ref}^{HP}	4.3
HVAC	
Power capacity [kW]	7
Heating/cooling capability	0.4

ation and minimize costs. Furthermore, for the case of customers with programmable thermostats, is assumed that these are not programmed, prioritizing comfort over saving. In this context, the worst case scenario is considered here for the Base Case, or business as usual, to better highlight the advantages of aggregating GSHP/HVAC flexibility, which does not require direct customer involvement and presents multiple advantages for electricity markets [91].

3.4.2 Study Cases

Simulations were carried out for the whole of 2019, and the following four sample days were specifically selected to analyze the daily operation of the GSHP/HVAC units: January 31, February 4, July 20 and September 9, since these are the coldest day in winter, the warmest day in winter, the warmest day in summer, and the coldest day in summer, respectively. Also, a comparative analysis was performed on the performance of the GSHP model for optimal heating/cooling power dispatch as a viable alternative to existing HVAC systems from a load aggregator's perspective. Note that the GSHP optimization model is a linear programming (LP) problem; thus, the mathematical models were implemented in GAMS, and solved using the CPLEX solver.

The load schedules for 2019 are shown in Figure 3.5 for DAM operations in the Proposed two-stage Strategy (the results for RTM operation yield similar conclusions) and the Base Case, for both the aggregated GSHP and HVAC technologies. Observe that in both technologies, the total power scheduled for the Base Case is slightly higher as compared to the Proposed Strategy. Additionally, note in Figure 3.5a that the GSHP loads scheduled in the winter months are considerable higher as compared to those scheduled in the summer, since the secondary thermal resistances are required on some days within the first two months of the year during severe cold weather conditions. On the other hand, observe that the power consumption during the summer months are higher as compared to winter months with the aggregated HVAC annual dispatch, as shown in Figure 3.5b. The power demand is higher in the Base Case as compared to the Proposed Strategy, as expected.

In Figure 3.6, the aggregator's total daily electricity cost for the proposed two-stage strategy and the Base Case, for both the aggregated GSHP and HVAC technologies, is presented. Note that in both cases the Base Case daily total electricity cost is higher than the daily cost in the Proposed Strategy, with the peak costs being high in some winter days due to the use of secondary resistances, which are charged at the maximum forecasted DAM/RTM price. Observe in Figure 3.6b that the daily electricity price in the summer months is higher for the HVAC technology in both strategies, compared to the daily costs with GSHP technologies, shown in Figure 3.6a. This is because the considerable lower GSHP power dispatch on those months, due to a significant higher EER of the GSHP units in cooling mode, compared to HVAC systems.

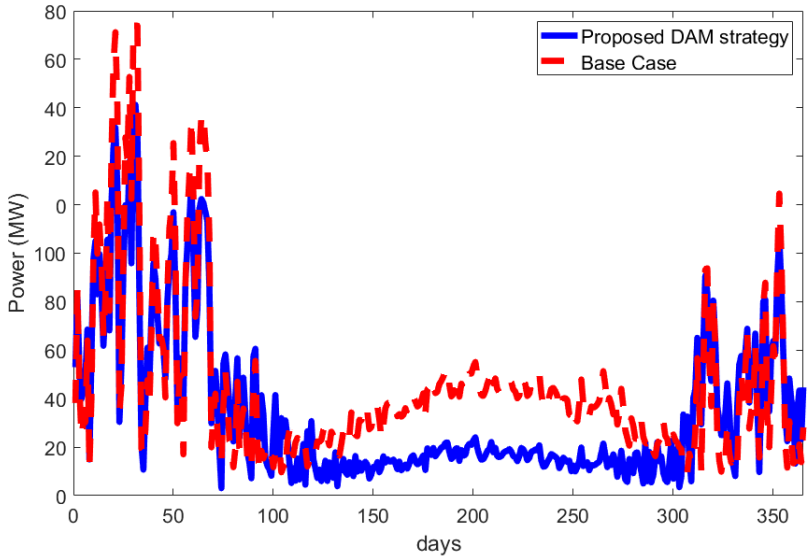

(a) GSHP.

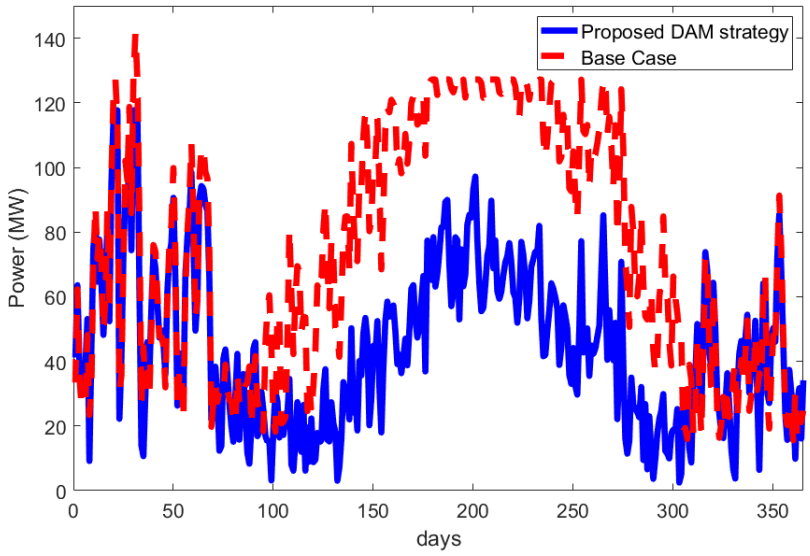

(b) HVAC.

Figure 3.5: Annual schedule of the aggregated GSHP/HVAC load.

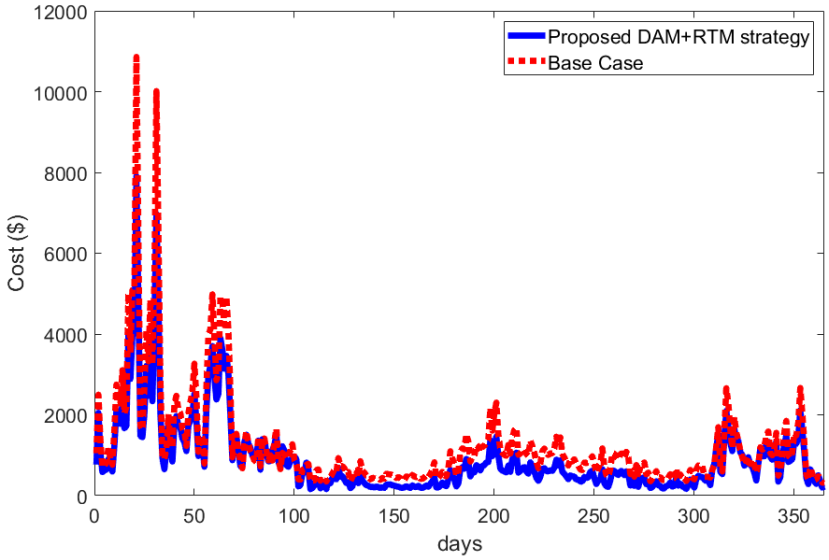

(a) GSHP.

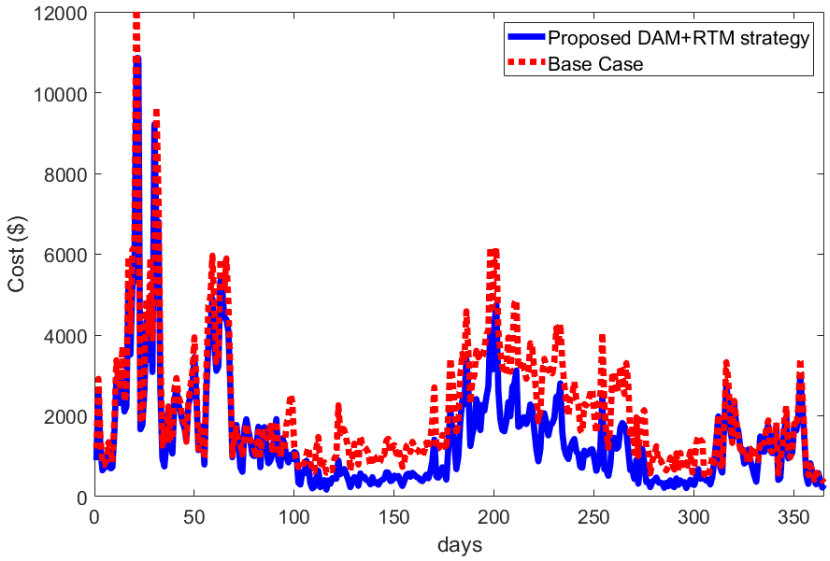

(b) HVAC.

Figure 3.6: Aggregator total annual cost.

The borehole inlet and outlet temperature profiles at the terminals of the U-pipe, the borehole grout temperature, and the ground temperature are shown for the year 2019 in Figure 3.7. Note that when the GSHP operates in heating mode during the first few months of the year (typically January to March), the outlet temperature is higher than the inlet temperature, and both profiles are lower than the grout and ground temperature. This is because, as the fluid flows through the U-pipe, heat is absorved from the surrounding ground and the borehole grout, thus increasing the difference between inlet and outlet temperatures, while the inlet and outlet temperatures decrease; note also that the grout temperature decreases, following the behavior of the fluid temperature. The ground temperature increases because it has the lowest initial temperature, but its change rate starts to decrease when all other temperatures are lower in comparison, due to their different thermal characteristics, such as thermal conductance (resistances). When the GSHP operates in cooling mode in the second part of the year (April to September), the temperature difference decreases until the inlet temperature surpasses the outlet temperature, and both profiles are higher than the grout and ground temperature. This is because heat is transferred to the surrounding ground, and thus the temperature difference between inlet and outlet temperatures begins to increase; additionally, the grout temperature starts to decrease, along with the ground temperature, but at a lower rate of change, due to its different thermal characteristics than the other GHX thermal components. Finally, near the end of year (October to December), i.e., at the start of the winter season, the GSHP returns to operate mostly in heating mode, as it was the case during the first few months of the year.

Observe that the ground temperature presents the smallest variations among all temperature profiles, as expected, and the grout temperature profile is in accordance with the physical and anticipated system behavior, being lower than the ground temperature in the first half of the year, i.e., heat flowing from the ground to the grout, and vice-versa during the last 6 months. Note that the ground temperature at the end of the year is higher with respect to its initial temperature, which means that the ground is heating up and thus this could affect on the long term the efficiency of the GSHP unit in cooling mode.

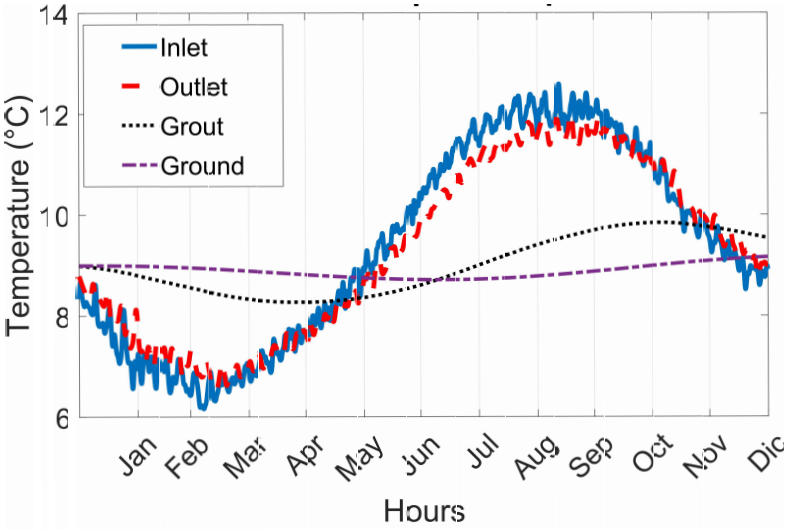

Figure 3.7: Annual temperature profile of the borehole for 2019.

The daily aggregated GSHP load dispatch profiles and electricity prices for the days analyzed are shown in Figures 3.8, for DAM operations in the Proposed two-stage Strategy (the RTM operation yield similar results) and the Base Case. For the GSHP, the units operate at full capacity for the entire day (see Figure 3.8a) on the coldest day of the year for both strategies, and thus there is less flexibility to provide load shifting and peak power reduction. In Figure 3.8b, note that the effects on load shifting for the Proposed Strategy, compared to the Base Case, are considerable; thus, the peak dispatch occurs early in the day when the electricity price is low, and then there is no power dispatched until late in the afternoon, unlike for the Base Case, where the peak load occurs at noon when the prices are high. A similar load shifting effect is observed in Figure 3.8d. Note also that there is a noticeable load reduction in summer days as observed in Figures 3.8c and 3.8d, where the hourly power dispatch is considerable lower compared with the power dispatch values for the Base Case scenario.

Figure 3.9 presents the dispatch of secondary thermal resistances in the GSHP unit to provide additional heating during the coldest period of the day. Observe that there is a significant load reduction for the secondary resistances in the Proposed Strategy, which decreases the daily total aggregator cost.

The heating/cooling demand profiles for the daily power dispatch with HVAC is shown

in Figure 3.10. Note that the HVAC units operate at full capacity on the coldest and warmest days of the year for the Base Case, as depicted in Figures 3.10a and 3.10c, respectively. On the other hand, in the Proposed Strategy, the aggregator reduces the power dispatch when the electricity price is high, keeping the customer temperatures within the given constraints. Observe also, note that there are significant changes on the other analyzed days with respect to the time of the peak loads; for example, the peak load occurs late at night, as shown in Figure 3.10b, or late in the afternoon, as illustrated in Figure 3.10d, when the electricity prices are low. The load reduction and peak load shifting of controlled loads is clearly reflected in the variation of in-house temperature and the aggregator total cost.

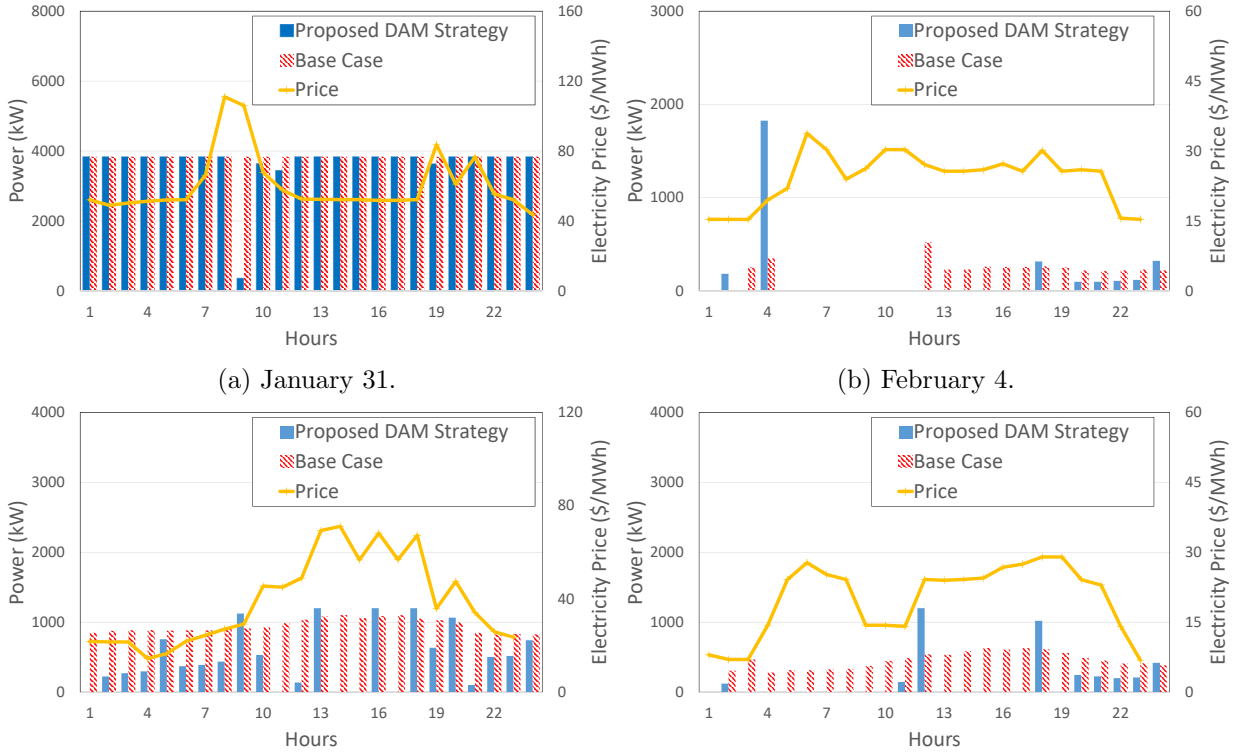

(a) January 31.

(b) February 4.

(c) July 20.

(d) September 9.

Figure 3.8: Aggregated GSHP electrical load dispatch.

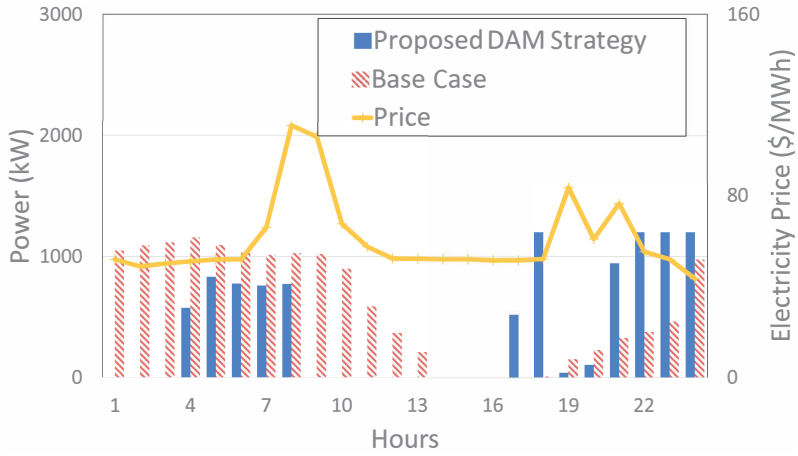

Figure 3.9: GSHP secondary thermal resistance dispatch for January 31.

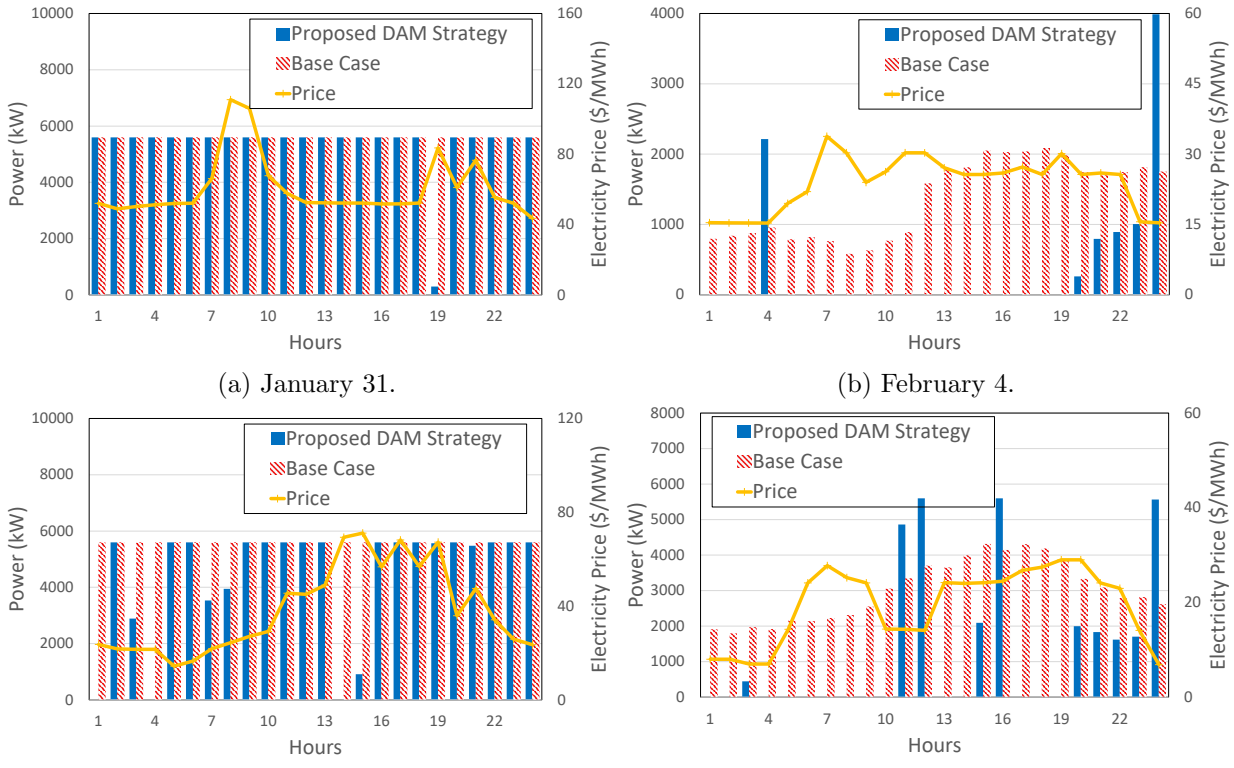

(a) January 31.

(b) February 4.

(c) July 20.

(d) September 9.

Figure 3.10: Aggregated HVAC electrical load dispatch.

The GSHP operating modes are depicted in Figure 3.11. Thus, during winter, the GSHP is predominantly operating in heating mode, as shown in Figure 3.11a, and a similar operation behaviour is noticed during the warmest days in summer when the GSHP is predominantly operating in cooling mode, as observed in Figure 3.11c. Although the GSHP operation is predominantly in heating mode in winter, and in cooling mode in summer, it may switch its operation mode for a few hours within the same day; this can be attributed to atypical temperatures on such days for the season, as observed in Figure 3.11b, which was the warmest day in that winter, and in Figure 3.11d, which was the coldest day in that summer.

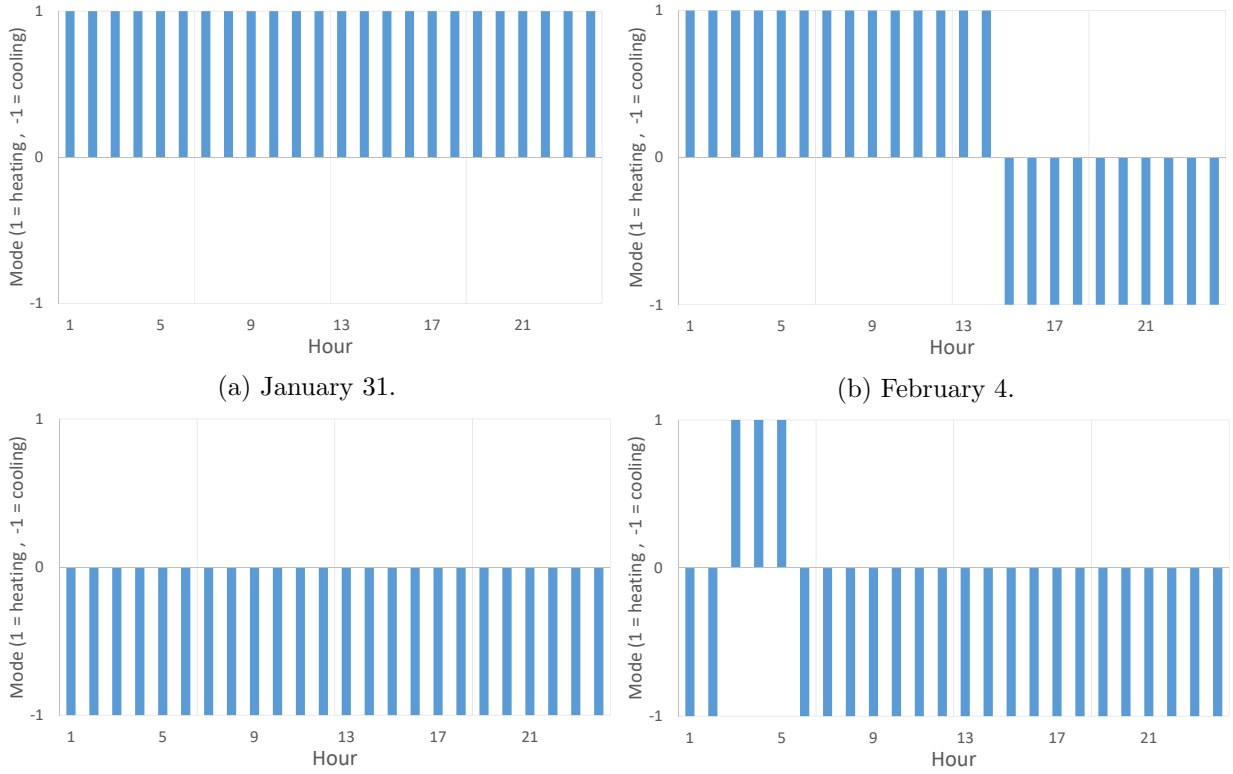

(a) January 31.

(b) February 4.

(c) July 20.

(d) September 9.

Figure 3.11: GSHP operation mode, with 1 representing heating and -1 cooling.

The house temperature profiles, and the ambient temperature for each typical day (referenced with the right y-axis) are presented in Figure 3.12. Observe that the temperature profiles with the Proposed Strategy vary considerably on all these days, within the specified

limits. Thus, the house temperature profile is at the lower comfort limit for the coldest day of the year, as shown in Figure 3.12a, due to the reduction in the power dispatch of the secondary resistances on that day, as shown in Figure 3.9; on this day, the highest temperature deviation with respect to the Base Case takes place. On other days, the temperature profile deviation on the Proposed Strategy are smaller and fluctuates from the Base Case temperature profile.

For the Base Case, the temperature remains at the set point on all days, except on July 20 (Figure 3.12c) when there is a small deviation from the set point because of the warm temperatures registered on that day. The small deviation in temperature from the set point, noted in summer months, is a consequence of the limited power capacity of the GSHP. On the other hand, in winter, such small temperature deviations from the set point in the Base Case are not observed (Figure 3.12a), because of the dispatch of secondary thermal resistances.

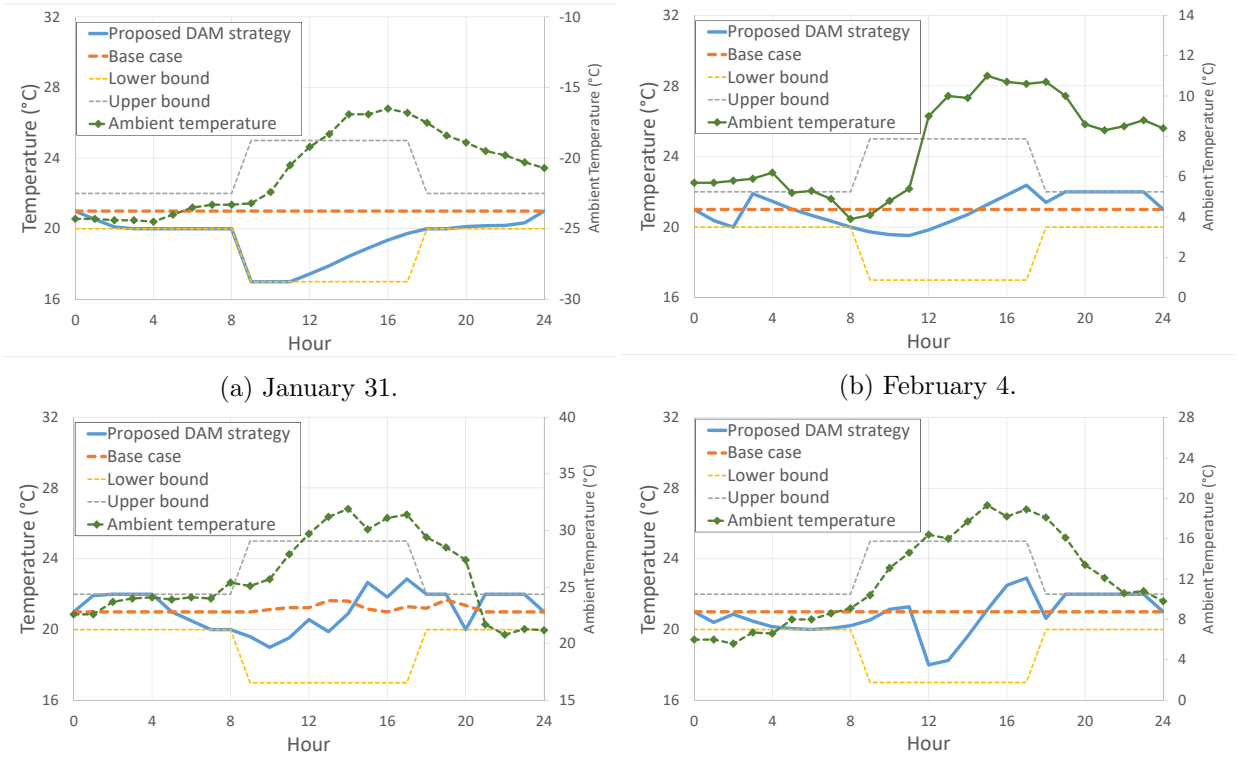

(a) January 31.

(b) February 4.

(c) July 20.

(d) September 9.

Figure 3.12: Comparison of house temperature profiles.

3.4.3 Economic Analysis

The aforementioned models were solved for all days in 2019, yielding the results illustrated in Table 3.5, where the load aggregator's total electricity cost for the year decreases by 15% and 11% with the GSHP and HVAC systems, respectively, using the Proposed Strategy, as compared to their respective Base Cases. Furthermore, the GSHP system requires 66% less heating/cooling energy in the Base Case as compared to the HVAC, while, with the Proposed Strategy, the GSHP system requires 63% less heating/cooling energy than with HVAC.

Table 3.5: Comparison of GSHP Versus HVAC Operations for 2019

Item	GSHP		HVAC	
	Base Case	Proposed Strategy	Base Case	Proposed Strategy
Aggregator total operating cost ($)	$425,137 (-27%**)	$371,157 (-15%*, -30%**)	$585,204	$525,881 (-11%*)
Annual heating/cooling dispatch (GWh)	6.6 (-66%**)	6.4 (-1%*, -63%**)	19.3	18.6 (-4%*)

* With respect to Base Case
** With respect to HVAC

An economic impact analysis for the aggregator is carried out here for a 25 year span, to examine the feasibility and long-term profitability of the Proposed Strategy with GSHP systems, while comparing it to existing conventional HVAC systems in the Base Case. The parameters in Table 3.6 were obtained using the historic electricity price and power demand data obtained from [88] and [92], which yield the price inflation and demand growth rate; the annual capital and operational costs of the GSHP and HVAC systems were extracted from [9]. The analysis was carried out considering the initial cost of switching the current HVAC system to the GSHP system in each community household, which is borne by the aggregator. The cost savings of the project comparison analysis, shown in Table 3.5, are considered as the cost savings for the first year, which forms the basis for annual simulations considering the price inflation and demand growth rate to determine the potential cost savings on each year thereafter, which are illustrated in the incremental net cash-flow diagram in Figure 3.13, with the accrue savings showing a considerable increase in year 13 due to the avoided cost of HVAC replacement in that year.

With the information from the incremental cash flow, an incremental Internal Rate of Return (IRR) of 7.33% can be calculated, which is higher than a typical Minimum Acceptable Rate of Return (MARR) of 5% to 6% for public utility projects like this one [93], making it suitable for investment. The cost and energy savings achieved from applying the Proposed Strategy on GSHP systems demonstrate that these systems are effective and economic alternatives for residential space heating/cooling applications.

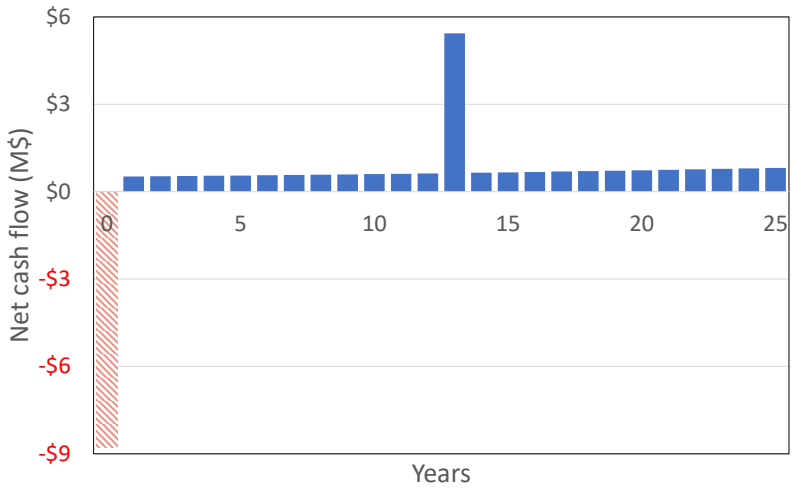

Figure 3.13: Incremental net cash flow diagram of GSHP compared with HVAC.

Table 3.6: Economic Parameters of GSHP/HVAC Systems [9, 88, 92]

Item	GSHP	HVAC
Capital cost ($/unit)	$11,000	$6,000
O&M cost ($/unit)	$120	$500
Lifetime (years)	25	13
DAM/RTM price inflation	3.50%/year	
Market demand growth	0.15%/year	
Incremental IRR (ΔIRR)	7.33%	

3.5 Summary

In this Chapter, detailed mathematical model of a deterministic GSHP system with vertical U-pipe GHX configuration and a two-stage strategy for a load aggregator's have been developed. Thus, the thermal modeling of the GSHP system, considering its thermodynamic characteristics for more realistic modeling, and a conventional HVAC model were described first. Then, the Proposed two-stage Strategy for a load aggregator models to participate in the DAM and RTM, to minimize the total electricity cost, and a Base Case strategy, considering minimization of the differential temperature were presented and discussed. A description of a test system for optimal load dispatch by an aggregator were then provided. Finally, results for different case studies were presented, analyzed, and compared in detail, demonstrating the effectiveness of the proposed two-stage strategy for optimal aggregator load dispatch of HVAC and GSHP systems, and the advantages of GSHP compared to HVAC.

Chapter 4

Uncertainty Modeling

This chapter presents three mathematical formulations to represent uncertainties for the dispatch of aggregated GSHP. Thus, typical MPC and MCS approaches are first discussed, based on an existing deterministic model that represents the operation and participation of the aggregator in electricity markets, to account for uncertainties on the electricity prices and ambient temperatures on the dispatch of aggregated GSHP systems. A novel RO approach is then proposed and developed, and all methods are finally validated, analyzed, and compared using a benchmark test system. Simulations and results are presented to illustrate the benefits of the proposed RO technique for GSHP dispatch by aggregators in terms of computational burden and proper representation of uncertainties.

4.1 Model Predictive Control (MPC)

As explained in Section 2.3.1, in order to capture the uncertainties in electricity prices and ambient temperature forecasts, an MPC approach is typically used, in which the optimization problem is solved representing the forecast uncertainties on electricity prices $\lambda_t^{Y_F}$ and ambient temperature $T_{amb_t}^F \; \forall \; t \; \in \; \mathcal{T}$, as follows for the DAM and RTM:

$$\lambda_t^{Y_F} = \lambda_{0,t}^{Y_F} + \epsilon_t^{\lambda} \tag{4.1}$$

$$T_{amb_t}^F = T_{amb_{0,t}}^F + \epsilon_t^T \tag{4.2}$$

where ϵ_t^{λ} and ϵ_t^{T} are the electricity price and ambient temperature forecasting errors, which are assumed here to increase with forecast lead time [64].

The obtained optimal solutions from the DAM and RTM are implemented only for the next time step; thus, for a time horizon of 24 hours, only the solution for the first hour is used for the GSHP power dispatch $p_{i,t}^{h}$ in heating mode and $p_{i,t}^{c}$ in cooling mode, respectively. The process is then repeated for the next iteration and so on. The procedure is illustrated in Figure 4.1.

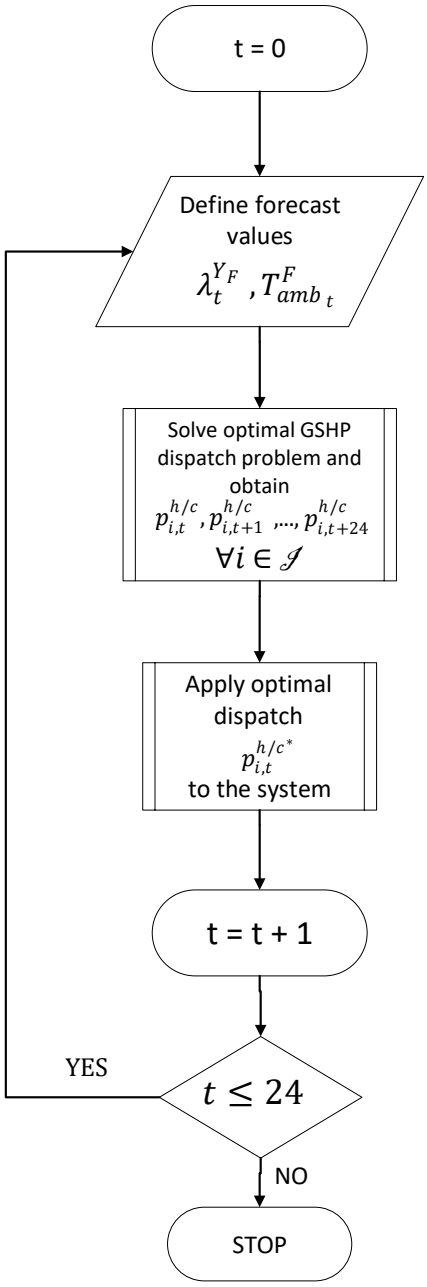

Figure 4.1: MPC approach for GSHP daily dispatch.

4.2 Montecarlo Simulations (MCS)

As explained in Section 2.3.2, the MCS approach is widely used to obtain stochastic solutions to problems involving uncertainties by using random values for the uncertain parameters. The resulting outcome is commonly expressed as a probability distribution instead of a single optimal solution. In this study, random number generation is used to sample the CDFs of the forecasted electricity prices and the ambient temperature, for the DAM and RTM $\forall\ t\ \in\ \mathcal{T}$, as follows:

$$\lambda_t^{Y_F} = \lambda_{0,t}^{Y_F}(1 + \xi_t^{\lambda^{Y_F}}) \tag{4.3}$$

$$T_{amb_t}^F = T_{amb_{0,t}}^F(1 + \xi_t^{T_{amb}^F}) \tag{4.4}$$

where $\xi_t^{\lambda^{Y_F}}$ and $\xi_t^{T_{amb}^F}$ are random scalars obtained from standard normal distribution, with mean μ and standard deviation ρ obtained from historical data.

In the MCS procedure, each iteration is simulated as a deterministic problem, with (4.3) and (4.4) defining the uncertain parameters, and the output variables are collected to perform statistical analyses and estimate their expected values. The iterations stop when the latter converge to fixed values.

4.3 Robust Optimization (RO)

In the RO formulation, the optimization model seeks to minimize the aggregator's total electricity procurement costs considering the uncertainty in electricity prices, and the ambient temperatures, as illustrated in Figure 4.2. As explained in Section 2.3.3, the uncertainty in electricity prices are formulated for the DAM and RTM in terms of their center values, i.e., forecast price, and its deviation from it, as follows:

$$\lambda_t^{Y_F} = \lambda_{0,t}^{Y_F}(1 + \Delta\lambda_t^{Y_F}) \qquad \forall t\ \in\ \mathcal{T} \tag{4.5}$$

The RO formulation minimizes the total procurement cost of electricity under worst case

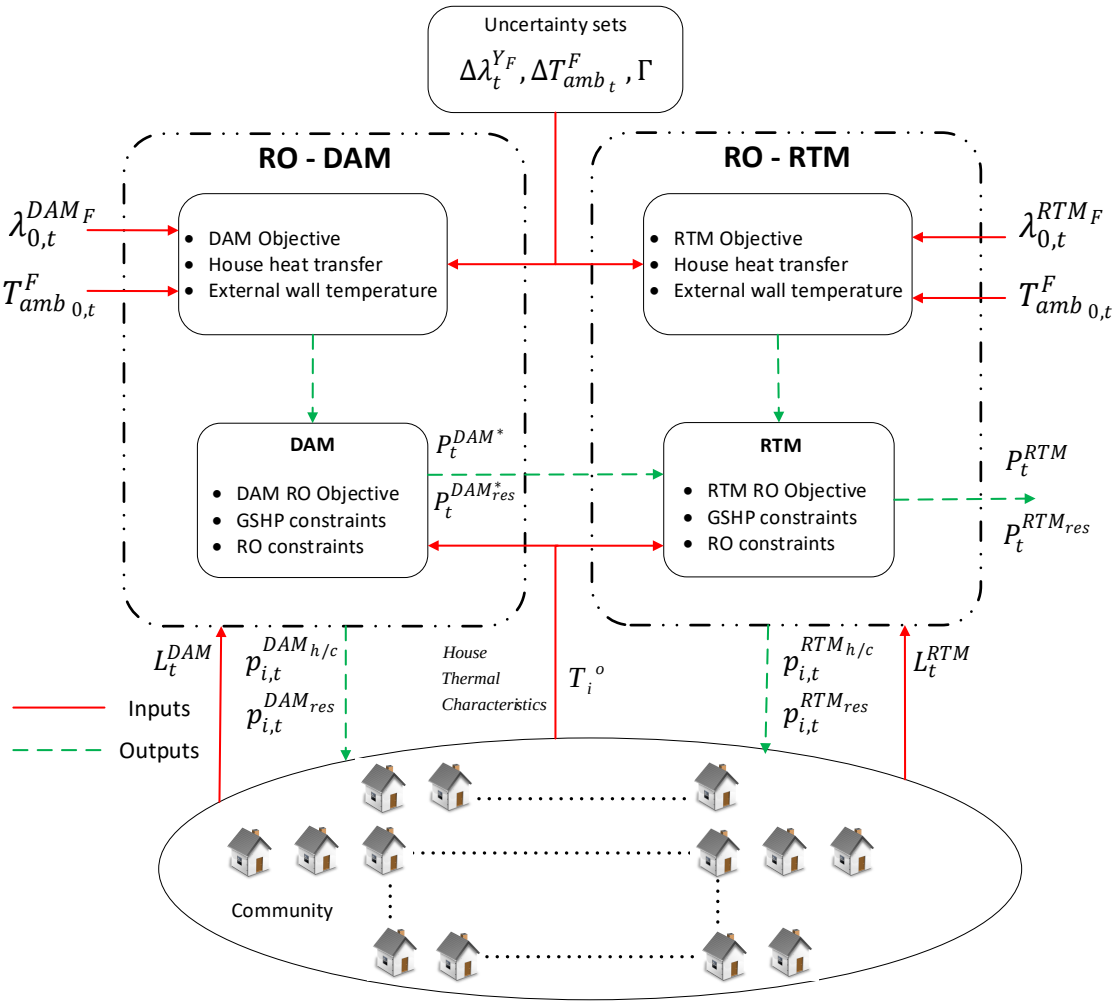

Figure 4.2: RO based framework of the load aggregator participating in the electricity market

scenarios. Thus, substituting (4.5) in (3.31) for the DAM, and in (3.38) for RTM, the following objective functions are obtained:

$$\min_{\substack{P_t^{DAM},\\ P_t^{DAMres}}} \max_{\Delta\lambda_t^{DAM_F}} J_1 = \sum_t^{24} \Bigg[\lambda_t^{DAM_F} P_t^{DAM} + \widehat{\lambda}^{DAM_F} P_t^{DAMres} + \underbrace{\Delta\lambda_t^{DAM_F} P_t^{DAM}}_{\text{Bi-linear term}} \lambda_{0,t}^{DAM_F} + \underbrace{\widehat{\Delta\lambda}_t^{DAM_F} P_t^{DAMres}}_{\text{Bi-linear term}} \widehat{\lambda}^{DAM_F} \Bigg] \tag{4.6}$$

$$\min_{\substack{\Delta P_t,\\ \Delta P_t^{res}}} \max_{\Delta\lambda_t^{RTM_F}} J_2 = \sum_t^{24} \Bigg[\lambda_t^{RTM_F} \Delta P_t + \widehat{\lambda}^{RTM_F} \Delta P_t^{res} + \underbrace{\Delta\lambda_t^{RTM_F} \Delta P_t}_{\text{Bi-linear term}} \lambda_{0,t}^{RTM_F} + \underbrace{\widehat{\Delta\lambda}_t^{RTM_F} \Delta P_t^{res}}_{\text{Bi-linear term}} \widehat{\lambda}^{RTM_F} \Bigg] \tag{4.7}$$

where, for the DAM and RTM:

$$\Delta\lambda_t^{Y_F} = \Delta\lambda_t^{Y_F+} - \Delta\lambda_t^{Y_F-} \ \forall t \ \in \ \mathcal{T} \tag{4.8}$$

$$\Delta\lambda_t^{Y_F+} - \overline{\Delta\lambda} \leq 0 \ \forall t \ \in \ \mathcal{T} \tag{4.9}$$

$$\Delta\lambda_t^{Y_F-} - \overline{\Delta\lambda} \leq 0 \ \forall t \ \in \ \mathcal{T} \tag{4.10}$$

$$\sum_t^{24} \frac{\Delta\lambda_t^{Y_F+} + \Delta\lambda_t^{Y_F-}}{\overline{\Delta\lambda}} - \Gamma \leq 0 \tag{4.11}$$

$$\Delta\lambda_t^{Y_F+}, \Delta\lambda_t^{Y_F-} \geq 0 \ \forall t \ \in \ \mathcal{T} \tag{4.12}$$

The modified objective functions (4.6) and (4.7) represent a min-max problem, where the total electricity cost is minimized in terms of the aggregated GSHP power variables and maximized in terms of electricity price deviations. Equation (4.8) defines the DAM and RTM price deviations, and (4.9) and (4.10) limit the positive and negative deviations to the maximum allowed deviation based on historical data analyses and chosen confidence levels. Finally, (4.11) presents the flexibility of conservatism assumed through the budget of uncertainty Γ, which determines the maximum number of times prices may deviate

from the forecasted values. Note that higher allowed deviations $\overline{\Delta\lambda}$ provide more financial protection against larger price uncertainties.

Equations (4.6) and (4.7) have a saddle-node and nonlinear problem structure due to the new set of bi-linear terms. Hence, based on the dual of the maximization problem, the following set of objective functions represented in linear form can be obtained [94]:

$$\min_{\substack{P_t^{DAM},P_t^{DAMres},\\ \beta_{1,t}^{DAM},\beta_{2,t}^{DAM},\\ \beta_{3,t}^{DAM},\beta_4^{DAM}}} J_1 = \sum_t^{24} \Bigg[\lambda_t^{DAM_F} P_t^{DAM} + \widehat{\lambda}^{DAM_F} P_t^{DAMres} + \overline{\Delta\lambda}(\beta_{2,t}^{DAM} + \beta_{2,t}^{DAMres} + \beta_{3,t}^{DAM} + \beta_{3,t}^{DAMres} \Bigg] + \Gamma(\beta_4^{DAM} + \beta_4^{DAMres}) \tag{4.13}$$

$$\min_{\substack{\Delta P_t,\Delta P_t^{res},\\ \beta_{1,t}^{RTM},\beta_{2,t}^{RTM},\\ \beta_{3,t}^{RTM},\beta_4^{RTM}}} J_2 = \sum_t^{24} \Bigg[\lambda_t^{RTM_F} \Delta P_t + \widehat{\lambda}^{RTM_F} \Delta P_t^{res} + \overline{\Delta\lambda}(\beta_{2,t}^{RTM} + \beta_{2,t}^{RTMres} + \beta_{3,t}^{RTM} + \beta_{3,t}^{RTMres} \Bigg] + \Gamma(\beta_4^{RTM} + \beta_4^{RTMres}) \tag{4.14}$$

where:

$$\beta_{1,t}^{DAM} = P_t^{DAM} \lambda_{0,t}^{DAM_F} \qquad \forall t \in \mathcal{T} \tag{4.15}$$

$$\beta_{1,t}^{RTM} = \Delta P_t \lambda_{0,t}^{RTM_F} \qquad \forall t \in \mathcal{T} \tag{4.16}$$

$$\beta_{1,t}^{DAMres} = P_t^{DAMres} \widehat{\lambda}^{DAM_F} \qquad \forall t \in \mathcal{T} \tag{4.17}$$

$$\beta_{1,t}^{DAMres} = P_t^{DAMres} \widehat{\lambda}^{DAM_F} \qquad \forall t \in \mathcal{T} \tag{4.18}$$

$$-\beta^Y_{1,t} + \beta^Y_{2,t} + \frac{\beta^Y_4}{\overline{\Delta\lambda}} \geq 0 \qquad \forall t \in \mathcal{T} \tag{4.19}$$

$$\beta^Y_{1,t} + \beta^Y_{3,t} + \frac{\beta^Y_4}{\overline{\Delta\lambda}} \geq 0 \qquad \forall t \in \mathcal{T} \tag{4.20}$$

$$\beta^Y_{2,t}, \beta^Y_{3,t}, \beta^Y_4 \geq 0 \qquad \forall t \in \mathcal{T} \tag{4.21}$$

The objective functions are thus converted into minimization problems without bi-linear terms.

The second source of uncertainty are the forecasted ambient temperatures. As with the price, the ambient temperature can be expressed in terms of their center values and deviation, as follows:

$$T^F_{amb_t} = T^F_{amb_{0,t}}(1 + \Delta T^F_{amb_t}) \qquad \forall t \tag{4.22}$$

Substituting (4.22) in (3.4) and (3.13) for the house heat transfer balance and external wall temperature calculations, respectively, results in the following set of linear constraints:

$$Q_{out_{i,t}} = Q_{out_{0,i,t}} - U_A \Delta T^F_{amb_t} T^F_{amb_{0,t}} \tag{4.23}$$

$$T_{E_{i,t}} = T_{E_{0,i,t}} - \frac{U_E \Delta T^F_{amb_t} T^F_{amb_{0,t}}}{H_{P_E}} \qquad \forall i \in \mathcal{I}, t \in \mathcal{T} \tag{4.24}$$

where:

$$\Delta T^F_{amb_t} = \Delta T^{F+}_{amb_t} - \Delta T^{F-}_{amb_t} \qquad \forall t \in \mathcal{T} \tag{4.25}$$

$$\Delta T^{F+}_{amb_t} - \overline{\Delta T^F_{amb_t}} \leq 0 \qquad \forall t \in \mathcal{T} \tag{4.26}$$

$$\Delta T^{F-}_{amb_t} - \overline{\Delta T^{F}_{amb_t}} \leq 0 \qquad \forall t \in \mathcal{T} \tag{4.27}$$

$$\sum_{t}^{T} \frac{\Delta T^{F+}_{amb_t} + \Delta T^{F-}_{amb_t}}{\overline{\Delta T^{F}_{amb_t}}} - \Gamma \leq 0 \tag{4.28}$$

$$\Delta T^{F+}_{amb_t}, \Delta T^{F-}_{amb_t} \geq 0 \qquad \forall t \in \mathcal{T} \tag{4.29}$$

The complete RO DAM model comprises (4.13), (4.15), (4.17), (4.19)-(4.21), (4.23)-(4.29), the GSHP thermal constraints discussed in Section 3.1, (3.1)-(3.3), (3.5)-(3.12) and (3.14)-(3.29), and the operational constraints (3.32)-(3.37). Similarly for the RO RTM model, it comprises (4.14), (4.16), (4.18), (4.19)-(4.21), (4.23)-(4.29), the same GSHP thermal constraints as the RO DAM model formulated for the RTM operation. Finally, observe that these RO models are linear optimization problems, and hence they can be solved using LP techniques.

4.4 Results and Discussion

4.4.1 Test System

As discussed in Section 3.4.1, this work considers a GSHP load aggregator in Ontario, Canada, that submits demand bids to the IESO and purchases electricity for its clients. The load aggregator is assumed to provide electricity to 800 houses, as in [86], but unlike Chapter 3 that assumed only one type of house and GSHP unit, two different house thermal characteristics and four different GSHP units are used here, which result in 8 different types of homes that are then equally distributed among the 800 houses. Finally, as in Chapter 3, all customers are assumed to be at home from 6 PM to 8 AM, for simplicity and without loss of generality.

The recommended thermal comfort ranges are presented in Table 3.2, the parameters for the two house's geometric and thermal characteristics are given in Table 4.1, and the characteristics of the four GSHP system units, obtained from [15,95] and [87], are presented in Table 4.2. The electricity prices, uncontrolled DAM loads L_t^{DAM}, the weather data, solar

irradiation for that year and internal heat gains in a typical house are considered to be the same as discussed in Chapter 3.

Table 4.1: Household Geometric and Thermal Characteristics

Item	House 1 [15]	House 2 [95]
Area [m^2]	325	260
Volume [m^3]	225	174
Glazed surface portion [%]	9.5	7.2
R ceiling [m^2 °C /W]	7.67	6.92
R external walls [m^2 °C /W]	4.67	3.37

Table 4.2: GSHP Characteristics [87]

Model	BP018	BP024	BP030	BP036
Cooling Capacity [Btu/hr]	20,500	26,000	28,500	37,500
Heating Capacity [Btu/hr]	14,800	18,000	20,500	26,000
EER_{ref}^{HP}	19.0	21.1	19.4	19.7
COP_{ref}^{HP}	3.8	4.0	4.3	4.1

Simulations were carried out for the following four sample days specifically selected to analyze the daily operation of the GSHP units: January 31, February 4, July 20, and September 9, 2019, since these are the coldest day in winter, the warmest day in winter, the warmest day in summer, and the coldest day in summer, respectively. Since all GSHP optimization models are LP problems, they were implemented in GAMS and solved using the CPLEX solver.

4.4.2 Results

A fixed one-hour recalculation time is considered for the MPC approach implementation of the optimal power dispatch, with a typical 24-hour moving prediction horizon and a forecasting error increasing over time as in [96] for the estimated electricity price error, and in [97] for the estimated outdoor temperature error, as depicted in Figure 4.3. The estimated forecast errors were obtained using the Root Mean Square Error (RMSE) standard metric.

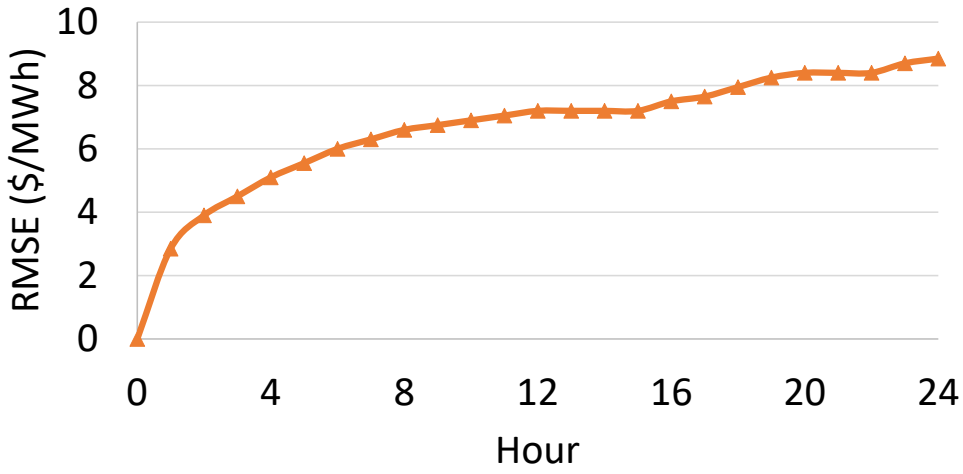

(a)

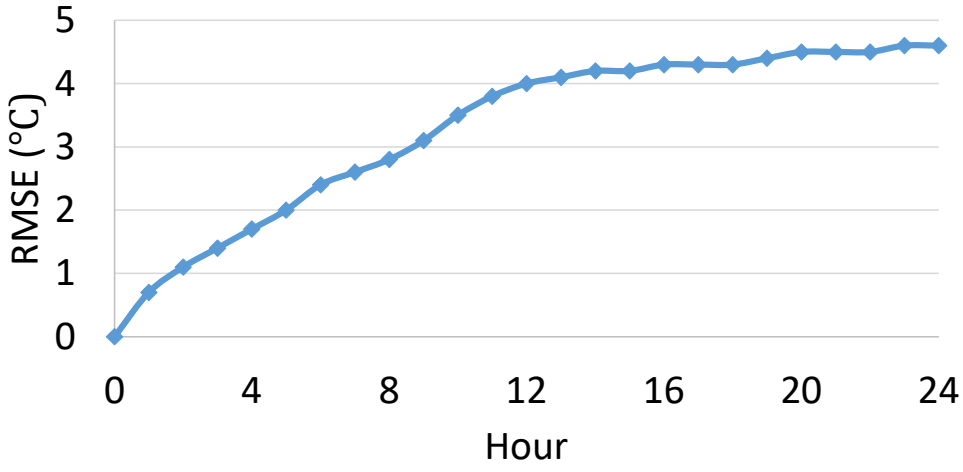

(b)

Figure 4.3: RMSEs for (a) electricity price [96], and (b) ambient temperature [97]

For the MCS technique, the deterministic optimization problem is repeatedly solved considering uncertainties in electricity prices and ambient temperature, assuming the deviations to be normally distributed, with mean 0 and hourly standard deviations for the electricity price SD_t^{λ} and ambient temperature SD_t^{T}, obtained from historical data and illustrated in Figure 4.4. Observe in Figure 4.5 and Figure 4.6 that increasing the number of iterations beyond 2000 does not provide any significant change in the results for the

total electricity costs and aggregated GSHP load, respectively; hence, the MCS studies presented consider 2000 iterations.

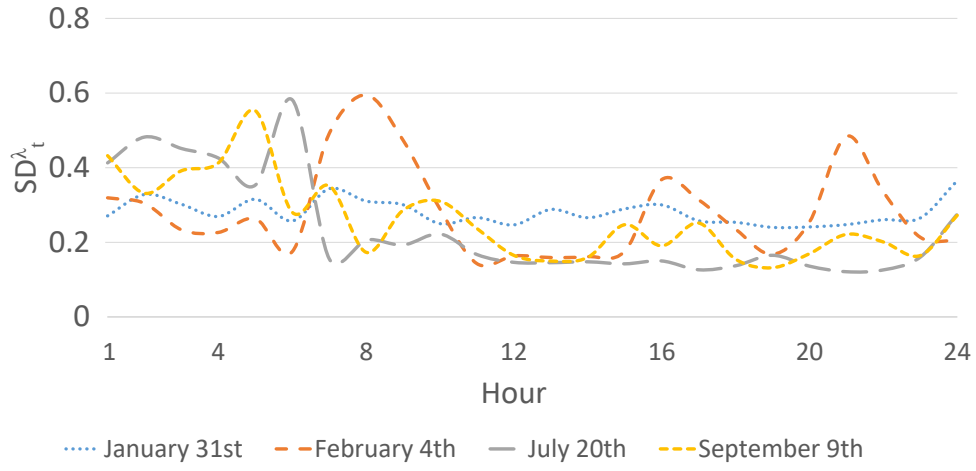

(a)

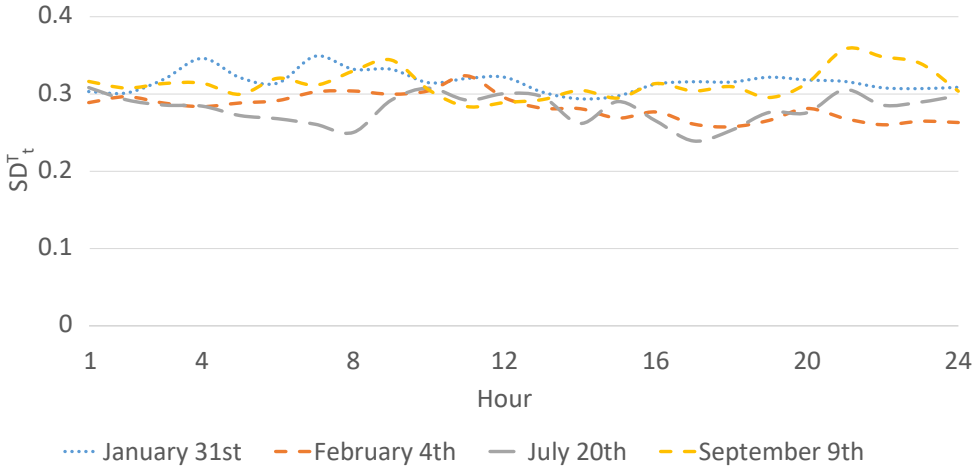

(b)

Figure 4.4: Hourly standard deviations for (a) electricity price and (b) ambient temperature, obtained from 10-year historical data for the given day.

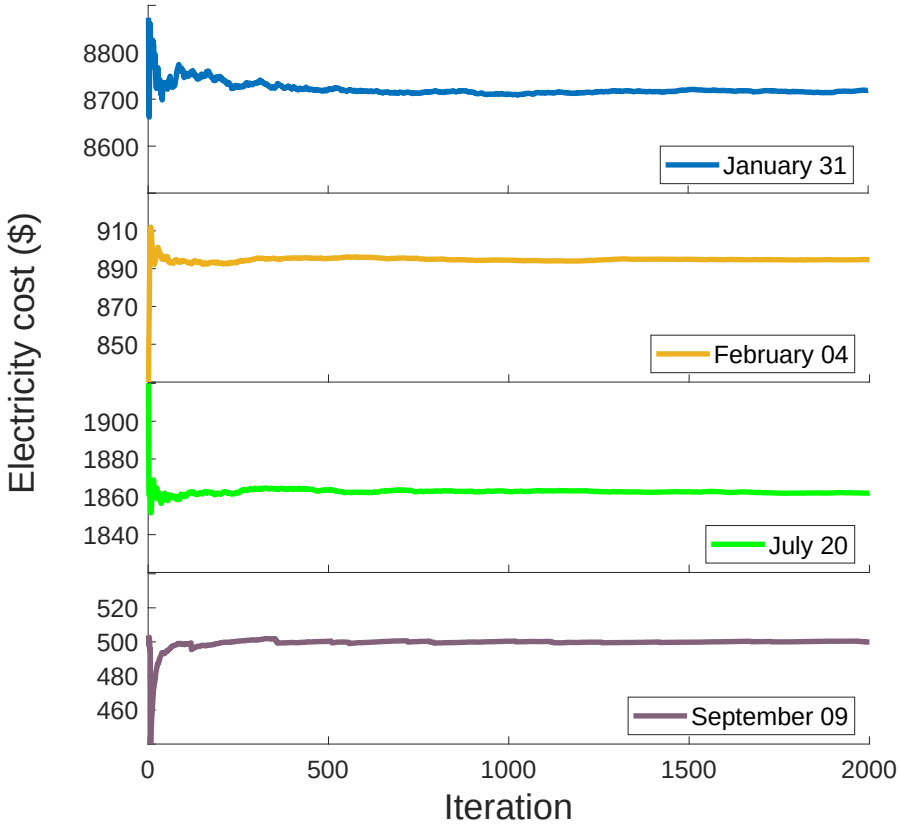

Figure 4.5: MCS convergence for the aggregator total costs.

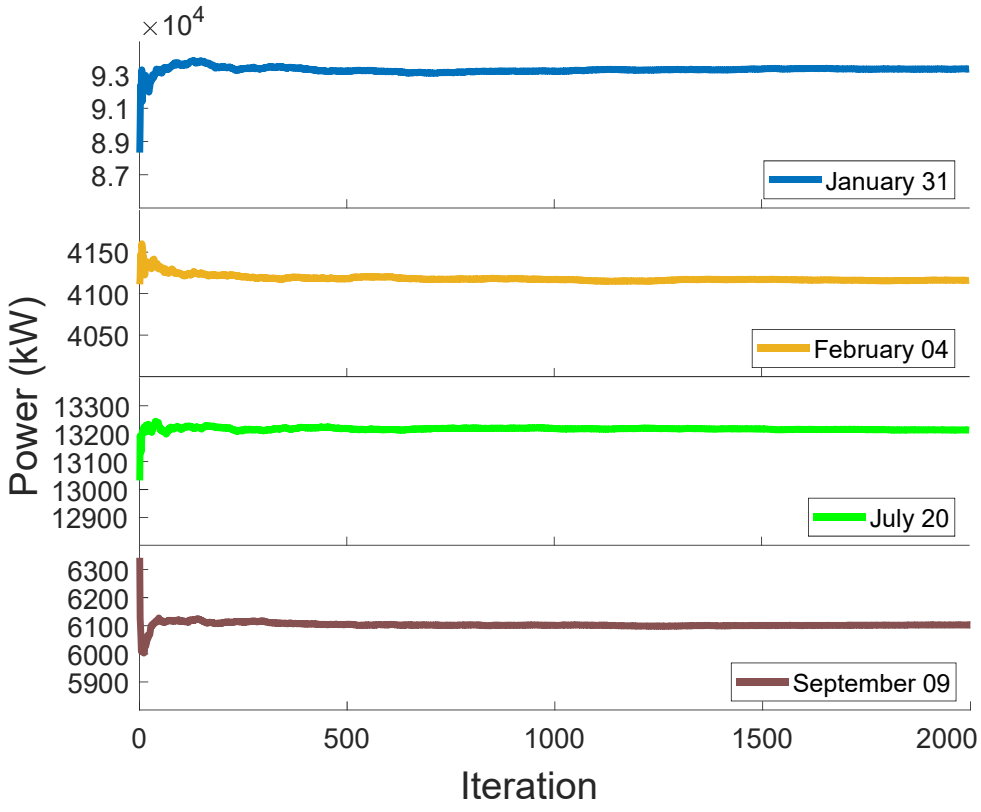

Figure 4.6: MCS convergence for the aggregator power dispatch.

The RO simulations were carried out for different values of $\overline{\Delta\lambda}$, $\overline{\Delta T}$, and Γ, as follows: $\overline{\Delta\lambda} \in [0.5SD_t^{\lambda}, SD_t^{\lambda}, 1.5SD_t^{\lambda}, 2SD_t^{\lambda}]$; $\overline{\Delta T} \in [0.5SD_t^{T}, SD_t^{T}, 1.5SD_t^{T}, 2SD_t^{T}]$; and $\Gamma \in [0, 6, 12, 18, 24]$. Therefore, 20 different scenarios were simulated for each day. Figure 4.7 presents the total electricity costs for the load aggregator for each day and for different combinations of $\overline{\Delta\lambda}$, $\overline{\Delta T}$, and Γ. Note that $\Gamma = 0$ corresponds to the deterministic case, as the electricity cost does not change with different combinations of $\overline{\Delta\lambda}$ and $\overline{\Delta T}$. Furthermore, as Γ increases, the electricity prices and ambient temperature forecast deviate from their original values, resulting in total electricity cost increases. The same occurs with the increase in $\overline{\Delta\lambda}$ and $\overline{\Delta T}$ deviations for a specific Γ, with larger prices and temperature deviations leading to higher electricity costs, as expected.

The aggregated GSHP optimal power dispatch for all RO combinations is shown in Figure 4.8, where it can be observed that the total GSHP power dispatched is less sensitive to changes in $\overline{\Delta\lambda}$, $\overline{\Delta T}$, and Γ as compared to the sensitivity of the electricity costs. This can be attributed to the lower SD_t^T values for the in-house temperature changes, which result in lower variations on the GSHP overall power dispatch. Furthermore, note that the total GSHP power dispatch sensitivity to uncertainties is even less on extreme cold days, as shown in Figure 4.8a, because the GSHP units operate at its maximum capacity almost at every hour, thus reducing the power dispatch flexibility with respect to the changes in the uncertainty parameters. Finally, observe that the power dispatch is more sensitive to uncertainty changes on days with low GSHP demand, for the warmest day in the winter and coldest day in the summer, respectively, as illustrated in Figures 4.8b and 4.8d.

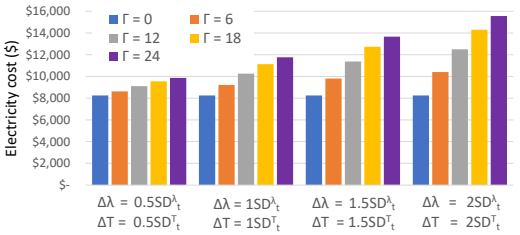

(a) January 31.

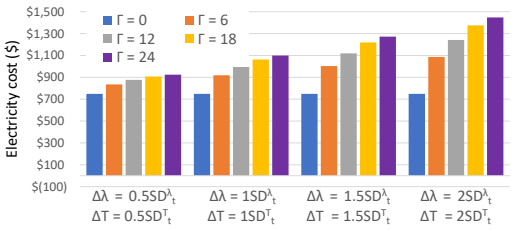

(b) February 4.

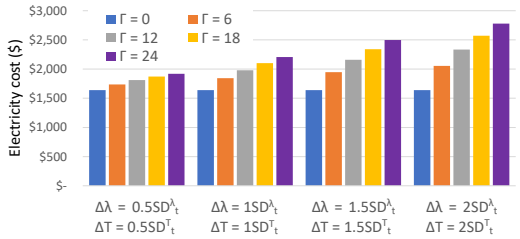

(c) July 20.

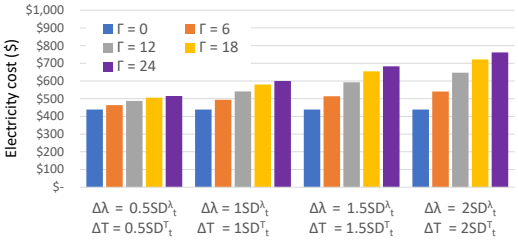

(d) September 9.

Figure 4.7: Aggregator electricity costs for the RO model.

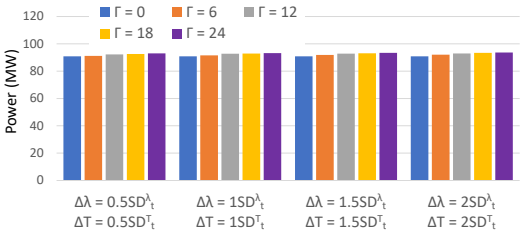

(a) January 31.

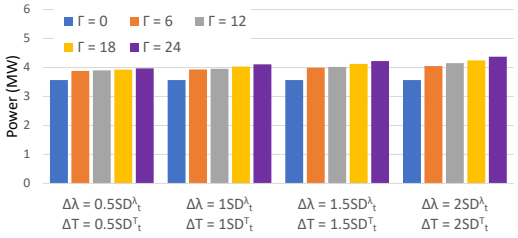

(b) February 4.

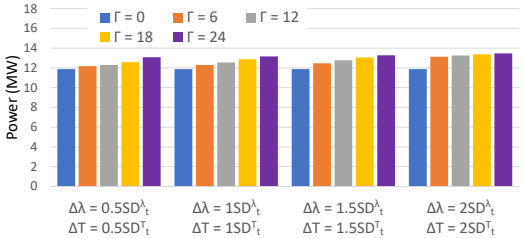

(c) July 20.

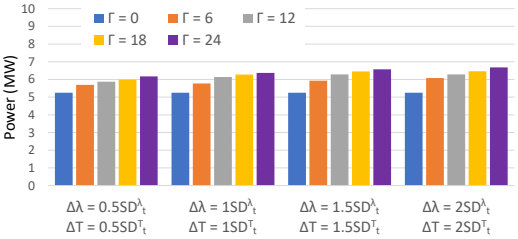

(d) September 9.

Figure 4.8: Aggregated GSHP power dispatch for the RO model.

4.4.3 Comparison and Discussions

To validate the proposed RO model in this work, a comparison is performed with respect to the obtained results from the MCS and MPC approaches, along with the results from the deterministic scenario of the Proposed Strategy, in terms of the GSHP power dispatch and in-house temperatures. Thus, the aggregated GSHP power dispatch is presented in Figure 4.9 for the MCS, MPC, and RO approaches, for different combinations of $\overline{\Delta\lambda_t}$, $\overline{\Delta T_t}$, and Γ, and the deterministic scenario. Note that the dispatch profiles are similar in all cases with peak demands occurring at similar times; this is due to the relatively low SD_t^T values, as previously explained. Observe also that the demand profile in winter days are in general similar in all cases, with relatively small deviations for each scenario, as shown in Figures 4.9a and 4.9b; however, there are higher variations in the power dispatch profiles during summer days, due to the higher EER of the GSHP units in cooling mode.

The indoor temperature profiles for the MCS, MPC, and RO approaches for different combinations of $\overline{\Delta\lambda_t}$, $\overline{\Delta T_t}$, and Γ are shown in Figure 4.10 for House 20 and in Figure 4.11 for House 344, as these have different thermal characteristics and are equipped with different GSHP units. Note that, in general, they present a similar behaviour with small temperature profile variations, due mainly to the different house and GSHP geometric and thermal characteristics between each house type; this is again due to low values of SD_t^T. Observe for House 20 that the temperature profiles differ slightly on different scenarios, specially on extreme cold and warm days, as observed in Figures 4.10a and 4.10c, as this house is equipped with the smallest GSHP capacity unit (BP018). This is not the case for House 344, in which the temperature profiles follow a similar behaviour with minimal deviations with respect to each scenario, even in extreme temperatures, as observed in Figure 4.11a, due to the higher capacity of the GSHP unit (BP030).

A detailed comparison with respect to the obtained results from the MCS and MPC approaches is presented in Table 4.3, where the results of all three approaches in terms of total electricity cost, aggregated GSHP power dispatch, and computational burden are presented. Observe that in all cases, the deterministic scenario presents the lowest total electricity cost, followed by the MPC, and then the MCS scenarios, with the RO model resulting in the highest costs as Γ increases, i.e., as the uncertainty increases; a similar behaviour can be observed in terms of the aggregated GSHP power dispatch. This is expected since the larger the price and temperature deviations are, the larger the cost and power deviations become, to account for the increase uncertainty; furthermore, the

RO approach is the most conservative, as it considers the worst case scenario. Note that the proposed RO approach can be solved within 4 minutes in all scenarios, while the computational burden of solving the MPC and MCS simulations is considerably higher.

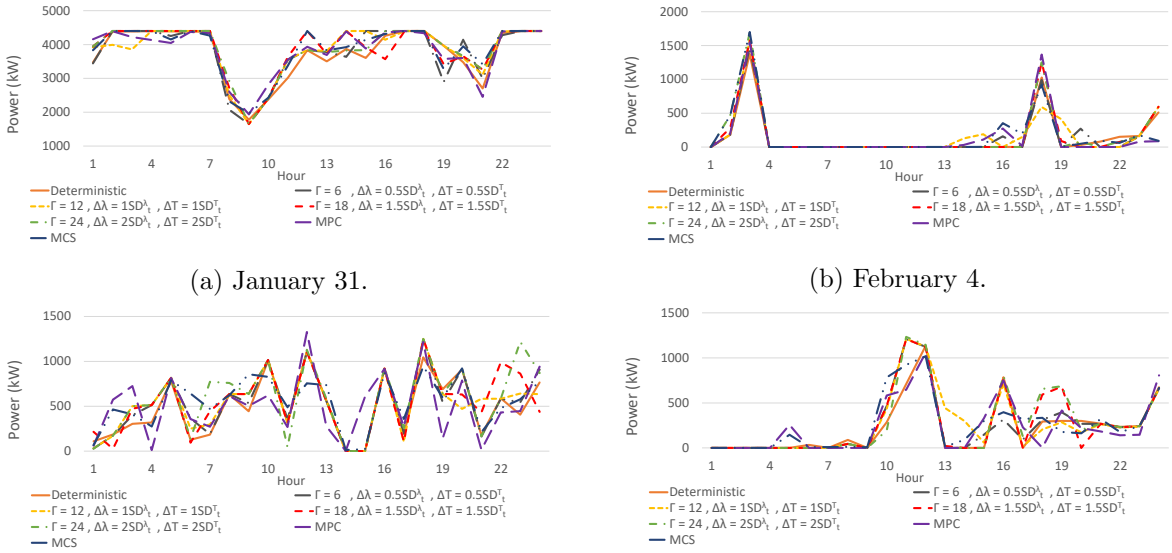

(a) January 31.

(b) February 4.

(c) July 20.

(d) September 9.

Figure 4.9: Comparison of aggregated GSHP power dispatched.

Table 4.3: Summary Comparison of Uncertainty Methods

Day	RO					MPC	MCS
		$\overline{\Delta\lambda} = 0.5SD_t^{\lambda}$ $\overline{\Delta T} = 0.5SD_t^{T}$	$\overline{\Delta\lambda} = SD_t^{\lambda}$ $\overline{\Delta T} = SD_t^{T}$	$\overline{\Delta\lambda} = 1.5SD_t^{\lambda}$ $\overline{\Delta T} = 1.5SD_t^{T}$	$\overline{\Delta\lambda} = 2SD_t^{\lambda}$ $\overline{\Delta T} = 2SD_t^{T}$		
	$\Gamma = 0$	$\Gamma = 6$	$\Gamma = 12$	$\Gamma = 18$	$\Gamma = 24$		
Total electricity cost ($)							
31-Jan	8,247	8,619	10,258	12,730	15,567	8,529	8,719
04-Feb	749	835	997	1,219	1,447	842	893
20-Jul	1,638	1,736	1,980	2,340	2,779	1,770	1,862
04-Sep	438	464	541	683	761	475	500
Power dispatch (MW)							
31-Jan	90.9	91.1	92.8	93.1	93.7	91.6	93.2
04-Feb	3.6	3.9	4.0	4.1	4.4	3.8	4.1
20-Jul	11.9	12.2	12.5	13.1	13.5	12.4	13.2
04-Sep	5.1	5.7	6.1	6.4	6.7	5.6	6.1
Computational burden (minutes)							
31-Jan	3.1	3.2	3.3	3.3	3.4	85	6105
04-Feb	2.5	2.9	3.1	3.0	3.1	80	4914
20-Jul	2.6	2.6	2.7	2.7	2.9	83	5251
04-Sep	2.9	2.9	3.0	3.0	3.1	83	5382

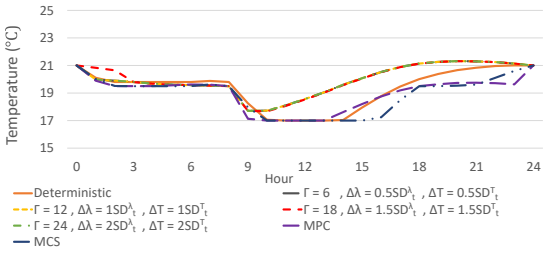

(a) January 31.

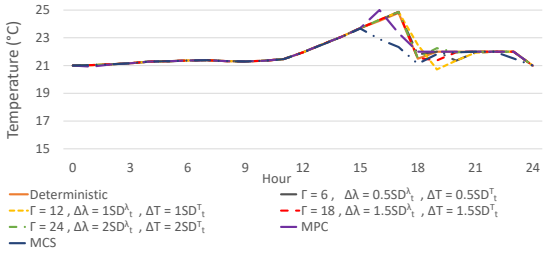

(b) February 4.

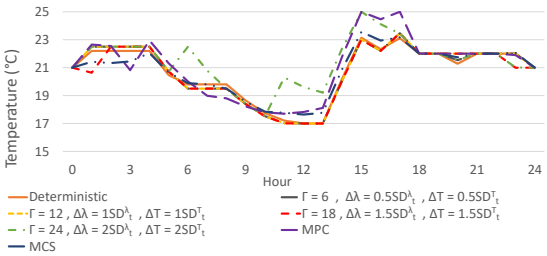

(c) July 20.

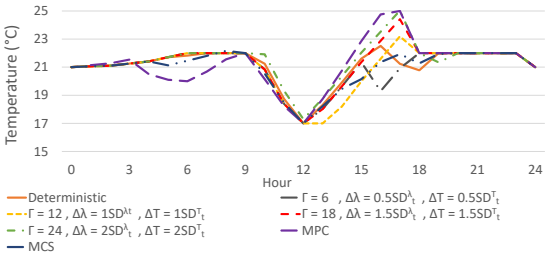

(d) September 9.

Figure 4.10: Comparison of indoor temperature profiles for House 20.

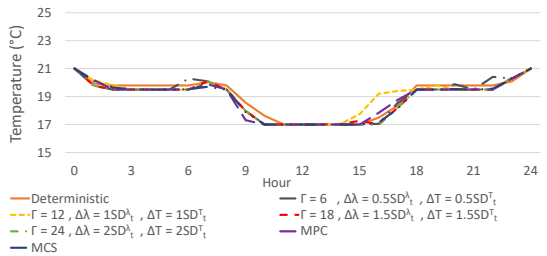

(a) January 31.

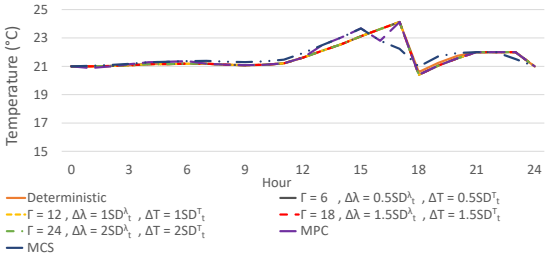

(b) February 4.

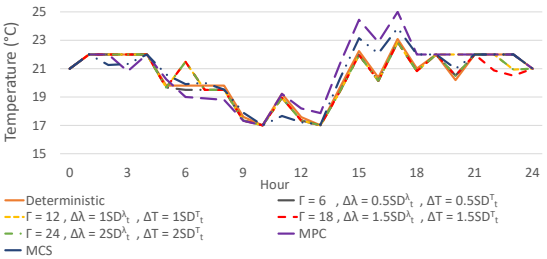

(c) July 20.

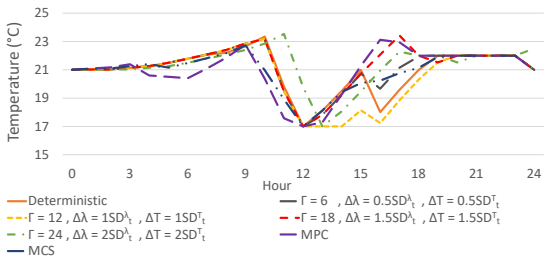

(d) September 9.

Figure 4.11: Comparison of indoor temperature profiles for House 344.

4.5 Summary

The GSHP load aggregator model presented in Chapter 3 to minimize the total electricity cost for a GSHP load aggregator was further extended in this chapter considering electricity price and ambient temperature uncertainties, based on range arithmetic techniques. For this purpose, electricity price and ambient temperature uncertainties MPC, MCS, and RO approaches to account for were presented. The implementation of each technique were discussed, including the development of a linear RO mathematical model. It was shown that the RO model yields multiple scenarios for the operator to choose based on the desired level of protection against uncertainties. For validation and comparison purposes, the RO model results were discussed vis-a-vis the ones obtained with the MPC and MCS techniques, showing that the proposed RO approach was computationally more efficient, while properly representing the considered uncertainties. This demonstrated the advantages of the RO approach for GSHP power dispatch by load aggregators.

Chapter 5

Conclusions, Contributions and Future Work

5.1 Summary and Conclusions

In this thesis, a novel detailed mathematical model of a GSHP system with vertical U-pipe GHX configuration has been proposed, considering the thermal modeling of residential homes and a GSHP system. These detailed thermodynamic models were included in a two-stage strategy for a load aggregator participating as price-taker in the DAM and RTM, to determine the optimal power dispatch of the aggregated GSHP load. However, since the electricity prices and ambient temperatures are subject to uncertainties, an RO uncertainty model was developed based on range arithmetic, to determine the operational decisions for a GSHP load aggregator.

In the first part of the thesis, a deterministic optimal scheduling model for a GSHP aggregator was presented. Detailed Non-linear functions were used to represent the thermodynamic characteristics of the in-house temperature, absolute deviation in the total aggregated load from DAM dispatch at the RTM price, and the objective function for the Base-Case strategy. These nonlinear representations were linearized using McCormick Envelopes and mutually exclusive non-negative auxiliary variables, eliminating bi-linear terms and non-linearities from the absolute variables in the model. The proposed novel linear formulation was implemented to simulate the operation for the GSHP aggregator,

comparing it with a base-case strategy that seeks to maximize the customer's comfort by minimizing the deviation of the in-house temperature from a reference set point. Additionally, the thermodynamic model of a conventional HVAC system was considered to compare it with the performance of the GSHP system. Both models were studied using corresponding DAM and RTM prices from the IESO for 2019, demonstrating that the proposed linear GSHP aggregator model yielded better results, with a significantly lower total procurement cost, as compared to the Base-Case and the conventional HVAC model.

In the second part of the thesis, range arithmetic techniques to represent electricity price uncertainties were introduced in the model. To this effect, an RO model was developed to optimize the GSHP's load aggregator power dispatch for the worst-case scenario for a given budget of uncertainty, which allowed studying a range of scenarios from the deterministic to the most conservative case. For validation purposes, the RO model results were compared with those obtained with MPC and MCS techniques considering fixed intervals of uncertainty. Simulations were carried out for specific days of the year for the above considered uncertainty techniques, considering their corresponding uncertainties in the DAM and RTM electricity prices, and ambient temperature forecasts. Studies revealed that the proposed RO approach was computationally more efficient to represent uncertainties for GSHP power dispatch by load aggregators.

The following conclusions can be drawn from this work:

- The proposed detailed mathematical model of a GSHP system, with vertical U-pipe GHX configuration and a two-stage strategy for a load aggregator, demonstrate that these systems are more effective and economic alternatives for residential space heating/cooling applications than the conventional HVAC system and the typical maximization of the customers' thermal comfort.

- The proposed linear thermodynamic representation of the GSHP aggregator significantly reduces the computational burden of the mathematical model, without loss of accuracy, making it simpler to implement uncertainty techniques, such as MPC, MCS and RO.

- The RO model yields optimum schedules that are protected against the worst-case scenario, for a given budget of uncertainty. The model can be efficiently varied from deterministic to the most conservative while properly representing the considered uncertainties, thus demonstrating the advantages of the RO approach.

5.2 Contributions

The main contributions of this thesis can be summarized as follows:

- A novel linear mathematical model for residential space heating/cooling of a GSHP system with vertical U-pipe GHX closed-loop configuration was proposed and validated, accounting for its thermal and geometric characteristics, as well as the switching between heating and cooling modes based on the average ambient temperature.
- A GSHP load aggregator model was developed for its participation in wholesale electricity markets as a price-taker, to provide peak load reduction and load shifting services by optimally dispatching the aggregated GSHP loads with two different operating strategies: a base-case that seeks to maximize the house comfort and a two-stage operation in DAM and RTM to minimize the aggregator's total electricity cost. The model was implemented and validated with respect to a mathematical model of an existing conventional HVAC system, comparing its operational performance with that of the GSHP system.
- Carried out simulations for a whole year considering the integration of several GSHPs / HVACs by the load aggregator and determining their respective optimal operation strategies in the DAM and RTM. These were coupled together with a techno-economic analysis, to determine the feasibility and long-term profitability for a load aggregator to invest in GSHP systems operating with the proposed strategy.
- An RO mathematical model was proposed that considers uncertainties in the electricity prices and ambient temperature to optimize the aggregated GSHP load dispatch, controlling their in-house temperatures to minimize overall costs under the worst-case scenario.
- A realistic test system, with multiple and different house thermal and geometric characteristics, along with different GSHP unit characteristics, was used to compare and analyze the results of the proposed RO approach with respect to MPC and MCS techniques, demonstrating the feasibility and advantages of the proposed RO mathematical model in practical applications.

The proposed GSHP thermodynamic model, and load aggregator strategies, presented in Chapter 3 were published in [86] and [98]. The uncertainty models and related approaches detailed in Chapter 4 have been submitted for publication in [99].

5.3 Future Work

Based on the work presented in this thesis, the following issues could be addressed in the future:

- Consider the GSHP load aggregator participating as a price-maker in the market. For this purpose, a bi-level model could be developed for a load aggregator that seeks to maximize profits by providing energy and ancillary services, while minimizing its total electricity costs.
- Study the potential of the GSHP unit to operate as an ESS by considering the thermal characteristics of the soil to store energy during the GSHP operation.
- Apply the proposed techniques to model uncertainties in other system parameters such as customer willingness to participate in the program and customer's time at home.

References

[1] NRCAN, "Secondary energy use and GHG emissions by end-use." http://oee.nrcan.gc.ca/corporate/statistics/neud/dpa/home.cfm, August 2018.

[2] NRCAN, "Comprehensive energy use database." http://oee.nrcan.gc.ca/corporate/statistics/neud/dpa/menus/trends/comprehensive_tables/list.cfm, August 2018.

[3] NRCAN, "Ground-source heat pumps (earth-energy systems)." https://www.nrcan.gc.ca/energy/publications/efficiency/heating-heat-pump/6833, March 2017.

[4] P. Healy and V. Ugursal, "Performance and economic feasibility of ground source heat pumps in cold climate," *International Journal of Energy Research*, vol. 21, no. 10, pp. 857–870, 1997.

[5] T. Sivasakthivel, K. Murugesan, and H. Thomas, "Optimization of operating parameters of ground source heat pump system for space heating and cooling by taguchi method and utility concept," *Applied Energy*, vol. 116, pp. 76 – 85, 2014.

[6] H. Esen, M. Esen, and O. Ozsolak, "Modelling and experimental performance analysis of solar-assisted ground source heat pump system," *Journal of Experimental & Theoretical Artificial Intelligence*, vol. 29, no. 1, pp. 1–17, 2017.

[7] A. H. Kidder and J. H. Neher, "Residential heat pump experiments in Philadelphia - earth as a heat source," *Transactions of the American Institute of Electrical Engineers, Part II: Applications and Industry*, vol. 71, pp. 343–350, Nov 1952.

[8] W. Wong, J. McClung, A. Snijders, J. Kokko, D. McClenahan, and J. Thornton, "First large-scale solar seasonal borehole thermal energy storage in Canada," in *Proceedings of Ecostock Conference, Stockton*, Citeseer, 2006.

[9] NRCAN, "Heating and Cooling With a Heat Pump." `https://www.nrcan.gc.ca/energy-efficiency/energy-star-canada/about/energy-star-announcements/publications/heating-and-cooling-heat-pump/6817#t`, 2009.

[10] E. Hirst and B. Kirby, *Retail-load participation in competitive wholesale electricity markets*. Citeseer, 2001.

[11] IESO, "Demand Response Auction." `https://www.ieso.ca/en/Sector-Participants/Market-Operations/Markets-and-Related-Programs/Demand-Response-Auction`, July 2022.

[12] B. Wong, A. Snijders, and L. McClung, "Recent inter-seasonal underground thermal energy storage applications in Canada," in *2006 IEEE EIC Climate Change Conference*, pp. 1–7, May 2006.

[13] K. Gamage, M. Yousefzadeh, E. Uzgoren, and Y. Merzifonluoglu, "Optimization of a ground source heat pump system using monte-carlo simulation," in *7th International Ege Energy Symposium & Exhibition*, 06 2014.

[14] J. Alvarez Vargas, K. Ponnambalam, and V. Quintana, "Electricity markets under uncertainty," *2007 IEEE Lausanne POWERTECH, Proceedings*, pp. 966 – 970, 08 2007.

[15] W. Mendieta and C. A. Cañizares, "Primary frequency control in isolated microgrids using thermostatically controllable loads," *IEEE Transactions on Smart Grid*, vol. 12, pp. 93–105, Jan 2021.

[16] R. Halvgaard, N. Poulsen, H. Madsen, and J. Jørgensen, "Economic model predictive control for building climate control in a smart grid," in *2012 IEEE PES Innovative Smart Grid Technologies (ISGT)*, pp. 1–6, Jan 2012.

[17] O. Zogou and A. Stamatelos, "Optimization of thermal performance of a building with ground source heat pump system," *Energy conversion and management*, vol. 48, no. 11, pp. 2853–2863, 2007.

[18] S. Self, B. Reddy, and M. Rosen, "Geothermal heat pump systems: Status review and comparison with other heating options," *Applied Energy*, vol. 101, pp. 341–348, 2013.

[19] W. Retkowski and J. Thöming, "Thermoeconomic optimization of vertical ground-source heat pump systems through nonlinear integer programming," *Applied Energy*, vol. 114, pp. 492–503, 2014.

[20] A. Capozza, A. Zarrella, and M. De Carli, "Long-term analysis of two GSHP systems using validated numerical models and proposals to optimize the operating parameters," *Energy and Buildings*, vol. 93, pp. 50–64, 2015.

[21] M. Song and M. Amelin, "Purchase bidding strategy for a retailer with flexible demands in day-ahead electricity market," *IEEE Transactions on Power Systems*, vol. 32, pp. 1839–1850, May 2017.

[22] K. Dehghanpour, M. Nehrir, J. Sheppard, and N. Kelly, "Agent-based modeling of retail electrical energy markets with demand response," *IEEE Transactions on Smart Grid*, vol. 9, pp. 3465–3475, July 2018.

[23] R. Henríquez, G. Wenzel, D. E. Olivares, and M. Negrete-Pincetic, "Participation of demand response aggregators in electricity markets: Optimal portfolio management," *IEEE Transactions on Smart Grid*, vol. 9, no. 5, pp. 4861–4871, 2018.

[24] X. Ayón, J. Gruber, B. Hayes, J. Usaola, and M. Prodanović, "An optimal day-ahead load scheduling approach based on the flexibility of aggregate demands," *Applied Energy*, vol. 198, pp. 1–11, 2017.

[25] M. Di Somma, G. Graditi, and P. Siano, "Optimal bidding strategy for a der aggregator in the day-ahead market in the presence of demand flexibility," *IEEE Transactions on Industrial Electronics*, vol. 66, no. 2, pp. 1509–1519, 2019.

[26] M. Parvania, M. Fotuhi-Firuzabad, and M. Shahidehpour, "Optimal demand response aggregation in wholesale electricity markets," *IEEE Transactions on Smart Grid*, vol. 4, no. 4, pp. 1957–1965, 2013.

[27] A. Najafi, A. Tavakoli, M. Pourakbari-Kasmaei, and M. Lehtonen, "A risk-based optimal self-scheduling of smart energy hub in the day-ahead and regulation markets," *Journal of Cleaner Production*, vol. 279, p. 123631, 2021.

[28] M. González Vayá and G. Andersson, "Optimal bidding strategy of a plug-in electric vehicle aggregator in day-ahead electricity markets under uncertainty," *IEEE Transactions on Power Systems*, vol. 30, no. 5, pp. 2375–2385, 2015.

[29] J. Yi, P. F. Lyons, P. J. Davison, P. Wang, and P. C. Taylor, "Robust scheduling scheme for energy storage to facilitate high penetration of renewables," *IEEE Transactions on Sustainable Energy*, vol. 7, no. 2, pp. 797–807, 2016.

[30] Y. Xu, L. Xie, and C. Singh, "Optimal scheduling and operation of load aggregators with electric energy storage facing price and demand uncertainties," in *2011 North American Power Symposium*, pp. 1–7, 2011.

[31] S. Chen, Q. Chen, and Y. Xu, "Strategic bidding and compensation mechanism for a load aggregator with direct thermostat control capabilities," *IEEE Transactions on Smart Grid*, vol. 9, pp. 2327–2336, May 2018.

[32] G. Liu, Y. Xu, and K. Tomsovic, "Bidding strategy for microgrid in day-ahead market based on hybrid stochastic/robust optimization," *IEEE Transactions on Smart Grid*, vol. 7, no. 1, pp. 227–237, 2016.

[33] P. Emrani-Rahaghi and H. Hashemi-Dezaki, "Optimal scenario-based operation and scheduling of residential energy hubs including plug-in hybrid electric vehicle and heat storage system considering the uncertainties of electricity price and renewable distributed generations," *Journal of Energy Storage*, vol. 33, p. 102038, 2021.

[34] Z. Song, J. Shi, S. Li, Z. Chen, W. Yang, and Z. Zhang, "Day ahead bidding of a load aggregator considering residential consumers demand response uncertainty modeling," *Applied Sciences*, vol. 10, no. 20, 2020.

[35] A. Al-Haq, "Technical and economic assessment of ground source heat pump systems in Ontario," Master's thesis, University of Waterloo, 2017.

[36] S. Keeling, *Ground Source Heat Pumps*. CIBSE, 2013.

[37] L. Ming, G. Qing, J. Yan, and G. Qin, "The big challenge of ground source heat pumps application in china," in *2010 IEEE International Conference on Intelligent System Design and Engineering Application*, vol. 2, pp. 594–597, 2010.

[38] L. Rybach and B. Sanner, "Ground source heat pump systems, the European experience," *Geo-Heat Center Quarterly Bulletin*, vol. 21, no. 1, pp. 16–26, 2000.

[39] N. Aste, R. Adhikari, and M. Manfren, "Cost optimal analysis of heat pump technology adoption in residential reference buildings," *Renewable Energy*, vol. 60, pp. 615 – 624, 2013.

[40] S. Rees, *Advances in Ground-source Heat Pump Systems*. Woodhead Publishing, 2016.

[41] S. Sanaye and B. Niroomand, "Thermal-economic modeling and optimization of vertical ground-coupled heat pump," *Energy Conversion and Management*, vol. 50, no. 4, pp. 1136 – 1147, 2009.

[42] H. Zareipour, C. Cañizares, and K. Bhattacharya, "The operation of ontario's competitive electricity market: Overview, experiences, and lessons," *IEEE Transactions on Power Systems*, vol. 22, pp. 1782–1793, Nov 2007.

[43] Minister of Energy, Science and Technology, "Bill 35, energy competition act, 199." `https://www.ola.org/en/legislative-business/bills/parliament-36/session-2/bill-35`, 1998.

[44] B. Danai, Jong Kim, A. I. Cohen, V. Brandwajn, and Show-Kang Chang, "Scheduling energy and ancillary service in the new ontario electricity market," in *PICA 2001. Innovative Computing for Power - Electric Energy Meets the Market. 22nd IEEE Power Engineering Society. International Conference on Power Industry Computer Applications (Cat. No.01CH37195)*, pp. 161–165, May 2001.

[45] IESO, "Ancillary services market." `http://www.ieso.ca/ancillary-services`, April 2016.

[46] IESO, "Demand response pilot." `http://www.ieso.ca/en/Sector-Participants/Market-Operations/Markets-and-Related-Programs/Demand-Response-Pilot`, May 2015.

[47] IESO, "Capacity Auction." `https://www.ieso.ca/en/Sector-Participants/Market-Operations/Markets-and-Related-Programs/Capacity-Auction`, July 2022.

[48] Z. Pei, Y. Ma, M. Wu, and J. Yang, "Study on load-participated demand response model based on load aggregator," *Frontiers in Energy Research*, vol. 9, 2021.

[49] L. Gkatzikis, I. Koutsopoulos, and T. Salonidis, "The role of aggregators in smart grid demand response markets," *IEEE Journal on Selected Areas in Communications*, vol. 31, pp. 1247–1257, July 2013.

[50] M. A. Ortega-Vazquez, F. Bouffard, and V. Silva, "Electric vehicle aggregator/system operator coordination for charging scheduling and services procurement," *IEEE Transactions on Power Systems*, vol. 28, pp. 1806–1815, May 2013.

[51] IESO, "Registered Participants." `https://www.ieso.ca/en/Sector-Participants/Registered-Participants`, July 2022.

[52] S. Burger, J. P. Chaves-Ávila, C. Batlle, and I. J. Pérez-Arriaga, "A review of the value of aggregators in electricity systems," *Renewable and Sustainable Energy Reviews*, vol. 77, pp. 395 – 405, 2017.

[53] S. Kerscher and P. Arboleya, "The key role of aggregators in the energy transition under the latest european regulatory framework," *International Journal of Electrical Power & Energy Systems*, vol. 134, p. 107361, 2022.

[54] Q. Tang, X. Wu, S. Dong, and R. Ma, "Framework design of load aggregators participating in electricity market," in *2018 2nd IEEE Conference on Energy Internet and Energy System Integration (EI2)*, pp. 1–6, 2018.

[55] S. Dempe, V. Kalashnikov, G. A. Pérez-Valdés, and N. Kalashnykova, *Bilevel Programming Problems: Theory, Algorithms and Applications to Energy Networks*. Berlin, Heidelberg: Springer Berlin Heidelberg, 2015.

[56] X. Xiao, J. Wang, R. Lin, D. J. Hill, and C. Kang, "Large-scale aggregation of prosumers toward strategic bidding in joint energy and regulation markets," *Applied Energy*, vol. 271, p. 115159, 2020.

[57] S. S. Rao, *Engineering Optimization: Theory and Practice*. John Wiley & Sons, Ltd, 2009.

[58] A. R. Jordehi, "How to deal with uncertainties in electric power systems? A review," *Renewable and Sustainable Energy Reviews*, vol. 96, pp. 145–155, 2018.

[59] A. Shapiro, D. Dentcheva, and A. Ruszczynski, *Lectures in Stochastic Programming: Modeling and Theory*. SIAM, 2009.

[60] D. E. Olivares, J. D. Lara, C. A. Canizares, and M. Kazerani, "Stochastic-predictive energy management system for isolated microgrids," *IEEE Transactions on Smart Grid*, vol. 6, pp. 2681–2693, Nov. 2015.

[61] B. Fanzeres, A. Street, and L. A. Barroso, "Contracting strategies for renewable generators: A hybrid stochastic and robust optimization approach," *IEEE Transactions on Power Systems*, vol. 30, no. 4, pp. 1825–1837, 2015.

[62] J. D. Lara, D. E. Olivares, and C. A. Cañizares, "Robust energy management of isolated microgrids," *IEEE Systems Journal*, vol. 13, no. 1, pp. 680–691, 2019.

[63] E. F. Camacho and C. B. Alba, *Model predictive control*. Springer, London, UK, 2013.

[64] B. Kouvaritakis and M. Cannon, "Model predictive control," *Switzerland: Springer International Publishing*, vol. 38, 2016.

[65] D. Olivares, *An energy management system for isolated microgrids considering uncertainty*. PhD thesis, University of Waterloo, 2014.

[66] S. H. Zak, *Systems and control*, vol. 198. Oxford University Press New York, 2003.

[67] C. Z. Mooney, *Monte carlo simulation*. Sage, 1997.

[68] M. Amelin, *On Monte Carlo simulation and analysis of electricity markets*. PhD thesis, KTH, 2004.

[69] P. Glasserman, *Monte Carlo methods in financial engineering*. Applications of mathematics ; 53, New York: Springer, 2004.

[70] A. L. Soyster, "Convex programming with set-inclusive constraints and applications to inexact linear programming," *Operations Research*, vol. 21, no. 5, pp. 1154–1157, 1973.

[71] D. Bertsimas and M. Sim, "The price of robustness," *Operations Research*, vol. 52, no. 1, pp. 35–53, 2004.

[72] A. Ben-Tal, *Robust optimization*. Princeton series in applied mathematics, Princeton: Princeton University Press, 2009.

[73] F. S. Hillier, *Introduction to operations research*. New York, NY: McGraw-Hill, tenth edition. ed., 2015 - 2015.

[74] C. Zhang, S. Hu, Y. Liu, and Q. Wang, "Optimal design of borehole heat exchangers based on hourly load simulation," *Energy*, vol. 116, pp. 1180–1190, 2016.

[75] W. Shurcliff, "Transmittance and reflection loss of multi-plate planar window of a solar-radiation collector: Formulas and tabulations of results for the case n = 1-5," *Solar Energy*, vol. 16, no. 3, pp. 149–154, 1974.

[76] P. M. Castro, "Tightening piecewise mccormick relaxations for bilinear problems," *Computers & Chemical Engineering*, vol. 72, pp. 300–311, 2015. A Tribute to Ignacio E. Grossmann.

[77] A. Pan, L. Lu, P. Cui, and L. Jia, "A new analytical heat transfer model for deep borehole heat exchangers with coaxial tubes," *International Journal of Heat and Mass Transfer*, vol. 141, pp. 1056–1065, 2019.

[78] Y. Luo, H. Guo, F. Meggers, and L. Zhang, "Deep coaxial borehole heat exchanger: Analytical modeling and thermal analysis," *Energy*, vol. 185, pp. 1298–1313, 2019.

[79] F. Ruiz-Calvo and M. De Rosa and J. Acuña and J.M. Corberán and C. Montagud, "Experimental validation of a short-term Borehole-to-Ground (B2G) dynamic model," *Applied Energy*, vol. 140, pp. 210–223, 2015.

[80] S. Chapra and R. Canale, *Numerical Methods for Engineers*. McGraw-Hill Inc., New York, 1988.

[81] T. Śliwa and A. Gonet, "Theoretical Model of Borehole Heat Exchanger," *Journal of Energy Resources Technology*, vol. 127, pp. 142–148, 12 2004.

[82] D. Bertsimas and J. N. Tsitsiklis, *Introduction to Linear Optimization*, vol. 6. Athena Scientific, Belmont, MA, 1997.

[83] Government of Canada, "Weather information." `https://weather.gc.ca/city/pages/on-82_metric_e.html`, August 2019.

[84] Government of Canada, "Photovoltaic and solar resource maps." https://www.nrcan.gc.ca/18366, August 2019.

[85] B. Johnson, "Patterns of residential occupancy." http://web.mit.edu/parmstr/Public/NRCan/ir464.pdf, 1981.

[86] D. Peralta, C. Cañizares, and K. Bhattacharya, "Ground Source Heat Pump Modeling and aggregation for services provision in electricity markets," in *IEEE Power Energy Society General Meeting (PESGM)*, pp. 1–5, 2020.

[87] BOSCH, "Engineering Submittal Sheet." https://www.bosch-climate.us/files/Greensource_BP_engineering_submittal_sheet_11.2018_US.pdf, 2019.

[88] IESO, "Yearly HOEP and Predispatch Report." http://reports.ieso.ca/public/PriceHOEPPredispOR/, 2019.

[89] Waterloo North Hydro, "2019 residential historical usage." https://www.wnhwebpresentment.com/app/capricorn?para=index, February 2020.

[90] J. Xie and T. Hong and T. Laing and C. Kang, "On Normality Assumption in Residual Simulation for Probabilistic Load Forecasting," *IEEE Transactions on Smart Grid*, vol. 8, no. 3, pp. 1046–1053, 2017.

[91] S. Burger and J. P. Chaves-Ávila and C. Batlle and I. J. Pérez-Arriaga, "A review of the value of aggregators in electricity systems," *Renewable and Sustainable Energy Reviews*, vol. 77, pp. 395–405, 2017.

[92] IESO, "Historical Demand Report." http://reports.ieso.ca/public/Demand/, 2019.

[93] B. Erdogmus, M. Toksoy, B. Ozerdem, and N. Aksoy, "Economic assessment of geothermal district heating systems: A case study of Balcova–Narlidere, Turkey," *Energy and Buildings*, vol. 38, no. 9, pp. 1053–1059, 2006.

[94] D. Bertsimas and M. Sim, "The price of robustness," *Operations research*, vol. 52, no. 1, pp. 35–53, 2004.

[95] E. Ibrahim, H. Aglan, M. Khan, M. Bhuyan, R. Wendt, and S. Livengood, "Thermal performance characteristics of an energy-efficient, healthy house," *ASHRAE Transactions*, vol. 110, pp. 432–442, 01 2004.

[96] D. Kontogiannis, D. Bargiotas, A. Daskalopulu, A. Arvanitidis, and L. Tsoukalas, "Error compensation enhanced day-ahead electricity price forecasting," *Energies*, vol. 15, p. 1466, 02 2022.

[97] J. Hou, H. Li, N. Nord, and G. Huang, "Model predictive control under weather forecast uncertainty for hvac systems in university buildings," *Energy and Buildings*, vol. 257, p. 111793, 2022.

[98] D. Peralta, C. A. Cañizares, and K. Bhattacharya, "Ground Source Heat Pump modeling, operation, and participation in electricity markets," *IEEE Transactions on Smart Grid*, vol. 13, no. 2, pp. 1126–1138, 2022.

[99] D. Peralta, C. A. Cañizares, and K. Bhattacharya, "Modeling of Ground Source Heat Pump systems and their operation under uncertainties," *Applied Energy*, 2022.

Appendix A

GSHP Capacity Data-sheets

Tables A.1 to A.4 depict the GSHP capacities for the different units considered in the thesis with respect to the in-house and borehole fluid temperatures; and Table A.5 presents the linear data-fitting coefficients for the performance of the GSHP in heating or cooling mode.

Table A.1: Bosch BP018

GHX fluid temperature (°F)	In-house temperature (°F)	Total capacity (BTUH)	EER	GHX fluid temperature (°F)	In-house temperature (°F)	Total capacity (BTUH)	COP
50	60	21000	21.9	30	60	14200	3.9
50	70	22400	24.2	30	70	13900	3.7
50	80	23800	26.8	30	80	13400	3.3
60	60	20100	21	40	60	16300	4.3
60	70	21400	23	40	70	15900	4
60	80	22800	25.2	40	80	15400	3.6
70	60	19200	19.3	50	60	18500	4.8
70	70	20500	21	50	70	18000	4.3
70	80	21700	22.6	50	80	17500	3.9
80	60	18200	17	60	60	20800	5.3
80	70	19400	18.3	60	70	20300	4.8
80	80	20700	19.7	60	80	19800	4.3
90	60	17300	14.8	70	60	23200	4.9
90	70	18400	15.7	70	70	22600	5.2
90	80	19600	16.8	70	80	22000	4.6
100	60	16300	12.6	80	60	25600	6.4
100	70	17400	13.4	80	70	25000	5.6
100	80	18500	14.2	80	80	24400	4.9

Table A.2: Bosch BP024

GHX fluid temperature (°F)	In-house temperature (°F)	Total capacity (BTUH)	EER	GHX fluid temperature (°F)	In-house temperature (°F)	Total capacity (BTUH)	COP
50	60	28100	30.8	30	60	19300	4.1
50	70	30000	33.1	30	70	18900	3.6
50	80	31900	35.5	30	80	18600	3.2
60	60	26800	24.9	40	60	22100	4.5
60	70	28700	26.7	40	70	21700	4
60	80	30500	28.5	40	80	21300	3.5
70	60	25600	20.7	50	60	25200	5
70	70	27300	22.1	50	70	24700	4.4
70	80	29000	23.3	50	80	24200	3.9
80	60	24200	17.2	60	60	28500	5.5
80	70	25900	18.4	60	70	27900	4.8
80	80	27600	19.5	60	80	27300	4.2
90	60	22900	14.5	70	60	32000	6
90	70	24400	15.3	70	70	31300	5.2
90	80	26000	16.2	70	80	30600	4.6
100	60	21500	12.1	80	60	35500	6.3
100	70	23000	12.9	80	70	34800	5.6
100	80	24500	13.6	80	80	34000	4.9

Table A.3: Bosch BP030

GHX fluid temperature (°F)	In-house temperature (°F)	Total capacity (BTUH)	EER	GHX fluid temperature (°F)	In-house temperature (°F)	Total capacity (BTUH)	COP
50	60	30900	27.2	30	60	20500	4.2
50	70	32800	28.1	30	70	20000	3.7
50	80	34800	28.7	30	80	19600	3.2
60	60	29500	22.9	40	60	23400	4.8
60	70	31400	23.7	40	70	22800	4.2
60	80	33200	24.3	40	80	22300	3.6
70	60	28000	19.3	50	60	26500	5.4
70	70	29900	20.1	50	70	26000	4.7
70	80	31700	20.7	50	80	25600	4.1
80	60	26600	16.3	60	60	30100	5.9
80	70	28300	17	60	70	29300	5.2
80	80	30200	17.7	60	80	28800	4.5
90	60	25200	13.8	70	60	33700	6.4
90	70	26800	14.4	70	70	33200	5.6
90	80	28500	15	70	80	32200	4.9
100	60	23600	11.6	80	60	37700	6.6
100	70	25300	12.2	80	70	36900	5.8
100	80	26900	12.7	80	80	36100	5.1

Table A.4: Bosch BP036

GHX fluid temperature (°F)	In-house temperature (°F)	Total capacity (BTUH)	EER	GHX fluid temperature (°F)	In-house temperature (°F)	Total capacity (BTUH)	COP
50	60	37800	24.2	30	60	27000	4.2
50	70	40300	25.6	30	70	26700	3.7
50	80	42900	27	30	80	26000	3.3
60	60	36200	20.8	40	60	30800	4.6
60	70	38500	22	40	70	30600	4.2
60	80	41000	23.2	40	80	29700	3.7
70	60	34500	18	50	60	35000	5.1
70	70	36800	19	50	70	34400	4.6
70	80	39200	20.1	50	80	33800	4.1
80	60	32700	15.4	60	60	39600	5.6
80	70	35000	16.4	60	70	38700	5
80	80	37300	17.3	60	80	37800	4.5
90	60	31000	13.3	70	60	44400	6.1
90	70	33100	14.1	70	70	43300	5.5
90	80	35200	14.8	70	80	42400	4.9
100	60	29200	11.3	80	60	49100	6.6
100	70	31200	12	80	70	48100	5.9
100	80	33400	12.8	80	80	47100	5.2

Table A.5: GSHP Data-fitting Coefficients

Model	BP018	BP024	BP030	BP036
A_c	11.22	13.35	13.5	10.37
B_c	-6.076	-8.833	-7.71	-6.592
C_c	-3.983	-3.18	-4.562	-2.62
A_h	-9.737	-11.84	-12.25	-11.3
B_h	5.081	5.106	5.224	5.419
C_h	6.028	8.146	8.43	7.273